Gas profiling in Quasi-Closed Pressure Regulated Anaerobic Fermentation Systems.

A thesis submitted in fulfilment of the requirements for the degree of

Doctor of Philosophy

Asaf Rotbart

BEng – Technion, Haifa, Israel, 2005.

MEng – Tel-Aviv University, Tel-Aviv, Israel, 2011.

School of Engineering

College of Science, Engineering and Health

RMIT University

September 2017

Declaration

I certify that except where due acknowledgement has been made, the work is that of the author alone; the work has not been submitted previously, in whole or in part, to qualify for any other academic award; the content of the thesis is the result of work which has been carried out since the official commencement date of the approved research program; any editorial work, paid or unpaid, carried out by a third party is acknowledged; and, ethics procedures and guidelines have been followed.

Asaf Rotbart

September 2017

Acknowledgements

I wish to acknowledge and thank the following people who contributed to the research and whose help has ensured the completion of this thesis:

First and foremost, I would like to thank my senior supervisor, Prof. Kourosh Kalantar-zadeh, for his mentoring, endless support and his encouragement during my PhD candidature. Your vision and commitment for this research were of great help and your passion for research and innovation was great inspiration for me.

I would also like to thank my second supervisor, Dr Jianzhen Ou for his valuable ideas, his patience and his commitment throughout my entire PhD degree. Your calmness and dedication to excellence during this PhD degree had taught and helped me tremendously.

Prof. Peter Gibson and his team at The Department of Gastroenterology, Monash University whose enabled incorporation of the new gas profiling technologies in *in-vitro* systems for human fecal incubation. With his wide knowledge and patience, Prof. Gibson provided outstanding guidance to this research and kindly addressed any question I had.

Dr CK Yao who collaborated with me in the application of the new gas-sensing technology in fecal incubation *in-vitro*. CK was dedicated to enabling the technology and its medical application. Together with her vast experience and knowledge, CK assisted me in producing unique and invaluable results. Thanks, CK for your kind support and for expanding my knowledge in gastroenterology. Look what we achieved today!

Mr Nam Ha for his assistance in the initial days of developing the intestinal gas sensing technology for *in-vitro* systems. His contribution to the design, manufacturing and testing together with his unique skill of assembling electronic systems helped significantly in accelerating the completion of the system and assured its reliability throughout my PhD research.

Mr Alex Zylewicz and his colleagues of the School of Engineering, RMIT University, for assisting in the fabrication of the gas profiling systems.

Dr Kyle Berean for his friendly support during the research, his valuable advice and his rich experience in the field of gas sensing. Special thanks to Kyle who manufactured PDMS membranes which were critical components in the fourth chapter of this thesis.

Mr Michael Chrisp for his assistance in the fabrication of the anaerobic digestion sensing arrays. Your professional work in both hardware and software assisted significantly in this study.

Dr Maazuza Othman for providing the vision, knowledge and guidance in the study of gas profiling in anaerobic digestion processes. Your assistance enabled the experiment to be performed smoothly and you addressed any of my concerns.

Mrs Zubayeda Zahan who assisted me with conducting anaerobic digestion experiments. Your professional skills, dedication and knowledge helped greatly in the success of this study. Thank you for being always available for my questions and queries.

Mr Lachlan Greve for his useful contributions to the study of gas profiling in anaerobic digestion processes.

Dr Peter Moate for his useful comments and contribution to the study of calculation methods for profiling gas in fermentation systems.

Associate supervisor, Prof. Gary Rosengarten, for his support along this PhD degree.

Current and former researchers and students within the School of Engineering at RMIT University: Dr Eric Adetutu, Dr Adam Chrimes, Dr Torben Daeneke, Dr Yichao Wang, Dr Emily Nguyen, Ben Carey, Chris Harrison, Naresh Pillali, Rhiannon Clark, Paul Atkin, Nripen Dhar Hareen Khan, Nitu Syed, Baoyue Zhang and Ali Zavabeti for your assistance and for providing a productive environment to conduct my research.

The technical staff who work hard to keep these facilities operational and helped me conducting lab work and calibration. Specifically, Mr Paul Jones, Mr Zeyad Nasa, Mr Dru Morrish, Ms Peg Gee Chang and their teams in RMIT University.

The technical staff Alex Bogatyrev and Elizabeth Ly of The Department of Gastroenterology, Monash University, for their assistance with the set-up of the fecal incubation experiments *in-vitro*.

My research would not have been possible without the financial support from the Australian government in the form of the Australian Postgraduate Award (APA). I would also like to acknowledge the additional financial support from the School of Engineering

Finally, special thanks to all of my friends and family for putting up with me and providing the support I needed. Especially those that selflessly gave their time to proof-read sections of this thesis, Jacob Rothfield, Jacklyn Yowell, Simon Rose and Jessica Lee.

Dedication

To my loved family:

my parents, Orly and Avi, and my siblings, Yael, Zvika and Michal,

who stuck by me, supported and comforted me throughout the entire process.

I couldn't have done this without your unconditional support, commitment and love.

ABSTRACT

Fermentation of organic materials by microorganisms is an essential component in a variety of medical, industrial and agricultural applications. Many of these fermentations take place in quasi-closed pressure regulated anaerobic fermentation systems and involve the production of different gases. These gases are highly indicative as they are identifiable with biological processes and different bacteria species. Profiling gas components in such systems can assist with their microbial activities analysis, diagnosis and monitoring. However, methods for gas profiling in such fermentation systems lack real-time, accurate, simple, portable and cost-effective gas profiling technologies for continuously measuring gases in both anaerobic headspaces and in liquid media.

The aim of this PhD research is to enhance the understanding, diagnosis and monitoring of these systems and their associated applications using gas components. This was specifically achieved by resolving the limitations and inadequacies of gas profiling in quasi-closed pressure regulated anaerobic fermentation systems.

Firstly, the author of this thesis thoroughly reviewed the methods utilized for accurate profiling of gas components. Specifically, he focused on profiling intestinal gases produced *in-vitro* during fecal incubation. Secondly, the author investigated the calculation methods for profiling the production of these gases and their kinetics. Finally, the author explored gas profiling in both liquid and gas phases for *in-situ* monitoring of anaerobic digestion fermentation systems.

The first stage involved addressing limitations of profiling intestinal gases produced by incubation of fecal matters *in-vitro*. The past available technologies for sensing colonic gases *in-vitro* were either bulky, expensive, offline or included only limited

number of gas types. In addition, the gut environment *in-vitro* is generally simulated with N_2 as an inert gas where the supplementation of important fermentation gases, such as CO_2 and H_2, was not understood.

As such, the author developed a low-cost, portable and real-time gas sensing technology for monitoring CO_2, CH_4, H_2, H_2S and NO*x* simultaneously in the anaerobic headspace of fecal fermentation systems *in-vitro*. The author demonstrated the performance of the new technology on healthy human fecal samples and validated the new technology for both accuracy and reproducibility.

The author also explored the impact of the initial headspace environment composition on the fermentation gas profiles. It was found that supplying the reactor with CO_2 enhanced CH_4 and H_2 production and inhibited H_2S production. Furthermore, it was shown that fecal incubation together with high fermentable fibre could suppress H_2S production. Finally, the author found that healthy human fecal samples did not produce NO*x* spontaneously.

In the second stage, the author investigated the calculation methods for profiling the production of gases and their kinetics in quasi-closed pressure regulated anaerobic fermentation systems. Surprisingly, the author discovered that there was no existing standardized or comprehensive method for such calculations. Therefore, the author developed a rigorous gas fermentation model and a novel mass-flow equation for accurately profiling the produced gases and introduced these into the literature. This new model was designed to match the commonly used commercial fermentation systems, making the new technology readily available for many applications and studies. The author demonstrated the performance of the new model for human fecal sample incubation using the *in-vitro* technology developed in the first stage and validated its accuracy. Moreover, the author found that the contribution of newly

introduced components in the mass-flow equation exceeded 9.1% of the overall gas profile.

In the final stage, the author researched the monitoring capability of anaerobic digestion processes using *in-situ* measurements of gas components in both liquid and gas phases. As an integral part of the microbial activity of anaerobic digestion processes, gas components have the potential of providing the necessary information for monitoring such processes effectively. However, current technologies for gas sensing in liquid-phase have been inadequate. Previously, Real-time profiling of gas components in both phases simultaneously has not been thoroughly studied due to lack of the required technology. This has possibly hindered important insights about the system's health.

In order to conduct this research, the author developed a novel, relatively simple, low-cost technique for measuring gas components in both phases simultaneously. Using this technique, dissolved gases were measured *in-situ* using membrane protected gas sensors which, in comparison to other approaches, eliminated many complications, delays or sample contamination. The author demonstrated the performances of the new technology on a series of anaerobic digestion batch experiments and confirmed its accuracy, longevity and reproducibly.

Utilizing the new technique, the author identified patterns and signatures that were associated with process imbalances but not clearly observed in commonly used indicators such as volatile acids and pH. The author also explored the impact of inoculum age on the process and showed that, relative to freshly collected inoculum, processes using aged inoculum had a higher potential to enter imbalanced states and failure.

It is the position of this author that the insights and technological advances achieved in this PhD research have contributed significantly to the advancement of the field of anaerobic fermentation. In particular, this was achieved by creating new, simple, accurate and reliable technologies, while adding significantly to the knowledge of quasi-closed, pressure regulated anaerobic fermentation systems and their applications.

List of symbols

$\tilde{C}_{\mathrm{i}} = (\tilde{C}_i^1, \tilde{C}_i^2, \dots, \tilde{C}_i^K)$	Gas composition array of ΔV_i at the *i*th interval comprised of *K* different gas species
$C_F^i = (C_F^{i,1}, C_F^{i,2}, \dots, C_F^{i,K})$	Vented volume composition array and headspace mixing ratio array at venting event at time t_F comprised of *K* different gas species
$C_i = (C_i^1, C_i^2, \dots, C_i^K)$	Headspace gas mixing ratio at time t_i ,comprised of *K* different gas species
C^k	Headspace concentration of gas species *k*
$CP_i\ [psi]$	Cumulative pressure by the end of the *i*th interval
$CGP_i = (CGP_i^1, CGP_i^2, \dots, CGP_i^K)$	Cumulative gas production array by the end of the *i*th interval comprised of *K* different gas species
$DG_i = (DG_i^1, DG_i^2, \dots, DG_i^K)[mL]$	Dissolved gas array at the *i*th interval comprised of *K* different gas species
$DG_i^k\ [mL]$	Dissolved gas of type *k* during the *i*th interval
$GP^k(t_j)$ [mL]	Cumulative gas production of gas species *k* at time t_j
$H_{cp}^k\ [psi^{-1}]$	Solubility constant for the *k*th gas species during the *i*th interval
n^+ [mol]	Gas produced due to fermentation [mol]

P^+ [kPa]	Transient headspace pressure increment
P_h [kPa]	Headspace's pressure
P_{atm} $[psi]$	Atmospheric pressure
P_{cal} [psi]	Calibration pressure conditions
P_i [psi]	Headspace pressure at time t_i
P^k [kPa]	Gas species *k* partial pressure
P_{th} [psi]	Headspace pressure regulation threshold
PCF_i	Pressure compensation factor at time t_i
R	Gas constant
$S_i = (S_i^1, S_i^2, \dots, S_i^K)$	Headspace gas sensors reading at time t_i
T_0	Temperature at zero-degree Celsius (0° C)
T_{10}	10-min length normalized triangular window filter
t_F^i $[h]$	*i*th interval venting event time
T_{cal} $[K]$	Calibration temperature
t_i $[h]$	*i*th sample time
T_i [K]	Headspace temperature at time t_i
T_h [K]	Headspace's temperature
TCF_i	Temperature compensation factor at time t_i

$TCGP_{\mathrm{i}}$ [mL]	Total cumulative gas produced by the end of the *i*th interval
$\gamma_i \left[\frac{\mathrm{mL}}{\mathrm{psi}}\right]$	Pressure to volume of gas produced at STP conversion factor
$\tau_v[h]$	Venting event duration
V^+ [mL]	Gas produced due to fermentation [mL]
$V_F^i\ [mL]$	Vented gas during the *i*th interval
$V_e^i\ [mL]$	Effective headspace volume
V_h [mL]	Headspace volume
$V_s\ [mL]$	Slurry volume
$\Delta_i'\ [mL]$	Gas produced due to fermentation by the *i*th interval's venting event
Δ_t [h]	Sampling interval
ΔGC (%vol)	Difference between GC measurement and the gas sensors readings
$\Delta \mathrm{n}_i$ [mmol]	Gas production due to fermentation at time t_i
$\Delta P_i\ [psi]$	Headspace internal pressure variation for the *i*th interval
ΔV_i [mL]	Gas produced due to fermentation during the *i*th interval

List of abbreviations

2D	Two dimensional
ABS	Acrylonitrile-butadiene-styrene
AD	Anaerobic digestion
ADC	Analogue to digital converter
AGW	Australian Gastroenterology Week
AMP	Amplifier
Ar	Argon
BMP	Biochemical methane potential
BSG	British Society of Gastroenterology
CGP	Cumulative gas production
CH_4	Methane
CO_2	Carbon dioxide
COD	Chemical oxygen demand
CP	Cumulative pressure
CV	Coefficient of variation
DG	Dissolved gas
EC	Electrochemical
FOS	Fructooligosaccharides
GC	Gas chromatography

GC-MS	Gas chromatographers coupled with mass spectrometry
GESA	Gastroenterological Society of Australia
GI	Gastrointestinal
GPP	Gas production profile
H_2	Hydrogen
H_2S	Hydrogen sulfide
HDPE	High-density polyethylene
HPLC	High pressure liquid chromatography
IBD	Inflammatory bowel disease
IMS	Ion mobility spectroscopy
IR	Infra red
LS	Laser spectrometry
MP	Micro processor
MS	Mass spectrometry
N_2	Nitrogen
NDIR	Non-dispersive infrared
NIRS	Near infra-red spectroscopy
NO*x*	Nitrogen oxides
OFMSW	Organic fraction of municipal solid waste

PC	Personal computer
PCF	Pressure compensation factor
PCT	Physisorption-based charge-transfer
PDMS	Polydimethylsiloxane
PTR-MS	Proton transfer reaction mass spectroscopy
RS	Resistant starch
SIFT-MS	Selected ion flow tube mass spectroscopy
SnS_2	Tin sulfide
SPME	Solid phase micro-extraction
SRB	Sulfide reducing bacteria
STP	Standard temperature and pressure conditions
TC	Thermal conductivity
TCF	Temperature compensation factor
TCGP	Total cumulative gas production
TS	Total solids
UC	Ulcerative colitis
VA	Volatile acids
VS	Volatile solids

List of Tables

List of Figures

Table of Contents

Chapter 1. INTRODUCTION

1.1 Background

Fermentation processes are important parts of many farming, medical and industrial procedures and their advances have gone through a long and rich history [1]. Measurement of gas constituents in such fermentation systems is of utmost importance as the gas molecules play critical roles in the incorporated metabolic pathways.

Fermentation environments or reactors, with no gas inlet, can be closed (and allow the pressure to build up) or operate under constant pressure conditions (by releasing gases when the pressure goes above a certain threshold). Many near constant-pressure fermentation systems occur at the sludge located at the bottom of wastewater ponds [2-5] in which organic matter is fermented *in-situ* to produce methane, hydrogen and sulfide containing compounds. Additionally, near constant-pressure reactors show up in nature in gastrointestinal tracts of ruminants *in-vivo* [6] and appear in the intestines of most animal species [7,8]. Such fermentation systems are also regularly used in food production processes *in-situ* including in closed-chamber bakeries [9] and closed or constant-pressure containers for long term fermentation of foods such as Korean Kim-Chi dishes [10]. Closed fermentation is used in some cheese processes [11,12] and are also the base for many beverage industries [13-15]. *In-vitro* units have been frequently applied for simulating the fermentation of ruminant feedstuffs [16,17], food products [18,19] and human fecal samples [20-23]. *In-vitro* approaches were also used for assessing the health of samples from waste water treatment facilities [24] and substrates from bio-gas plants [25,26].

In some occasions, these *in-vitro*, *in-situ* and *in-vivo* fermentation systems, with no gas inlets, utilize gas production profile (GPP) consisting of the quantity, composition and kinetics of gas production, to monitor and assess the health of the procedure. *In-vitro* fermentation

systems have generally been employed to quantify, understand, predict GPPs [16-26] and eventually for extrapolating such data to real systems. *In-situ* units, on the other side, have been frequently employed for screening whole waste water system in plants [27-34] and food processing units [9,15,35,36]. Some recent breakthroughs also show the importance of such gas measurements *in-vivo* using the ingestible gas sensing capsule technologies [37-40].

In this PhD research, the author introduces a novel work with regard to gas profiling in quasi-closed, pressure regulated anaerobic fermentation systems. In particular, the author targets profiling intestinal gases which are produced during incubation of human feces *in-vitro*. Additionally, the author targets the calculations of GPP in such fermentation systems and, finally, demonstrates gas profiling *in-situ* for monitoring anaerobic digestion (AD) systems for wastewater treatment and biogas production. The aspects developed and presented in this PhD research have not been implemented on any fermentation systems previously.

1.1.1 Intestinal gases

Human intestine hosts trillions of microorganisms that play significant roles in digestive processes [7]. By breaking down food intake as a part of their metabolic activities, these microorganisms satisfy their energy needs [41] and, as a result, produce short-chain fatty acids and specific gases such as carbon dioxide (CO_2), hydrogen (H_2), methane (CH_4), hydrogen sulfide (H_2S) and nitrogen oxide (NO_x) [42].

1.1.1.1 Production pathways for intestinal gases

CO_2 is the common fermentation gas for most colonic microorganisms [7]. H_2 is partially generated during the fermentation process by hydrogen-producing bacteria, which are mainly members of the *Firmicutes* phyla including *Roseburia spp*., *Ruminococcus spp*., *Clostridium spp.* and *Bacteroides spp*. [42]. Through the activities of these bacteria with ferredoxin

oxidoreductase, H_2 is generated from pyruvate or by the reoxidation of reduced pyridine and flavin nucleotides [42]. The majority of intestinal H_2 is oxidized by three groups of hydrogenotrophic microbes to maintain balance of the fermentation process: sulfate-reducing bacteria (SRB; mainly *Desulfovibrio spp*., *Desulfobacter spp*., *Desulfobulbus spp*. and *Desulfotomaculum spp*. [7]), methanogenic archaea (mainly *methanobrevibacter smithii* and *methanosphaerastadtmanae* [43]) and acetogens (mainly genera *Ruminococcus, Clostridium* and *Streptococcus* [42]). SRB produce H_2S using sulfate as the electron acceptor and H_2 or organic compounds as the electron donor [44]. Methanogenic archaea reduces CO_2 or methanol to produce CH_4 using H_2 as the electron donor [45]. Acetogens use the acetyl-CoA pathway to synthesize acetates from CO_2 and H_2 [42]. Some demonstrations suggest the possibility of NO*x* exogenous production although the bacterial origin is still unclear [46,47]. An illustration of major intestinal gas production pathways is presented in

Figure 1.1.

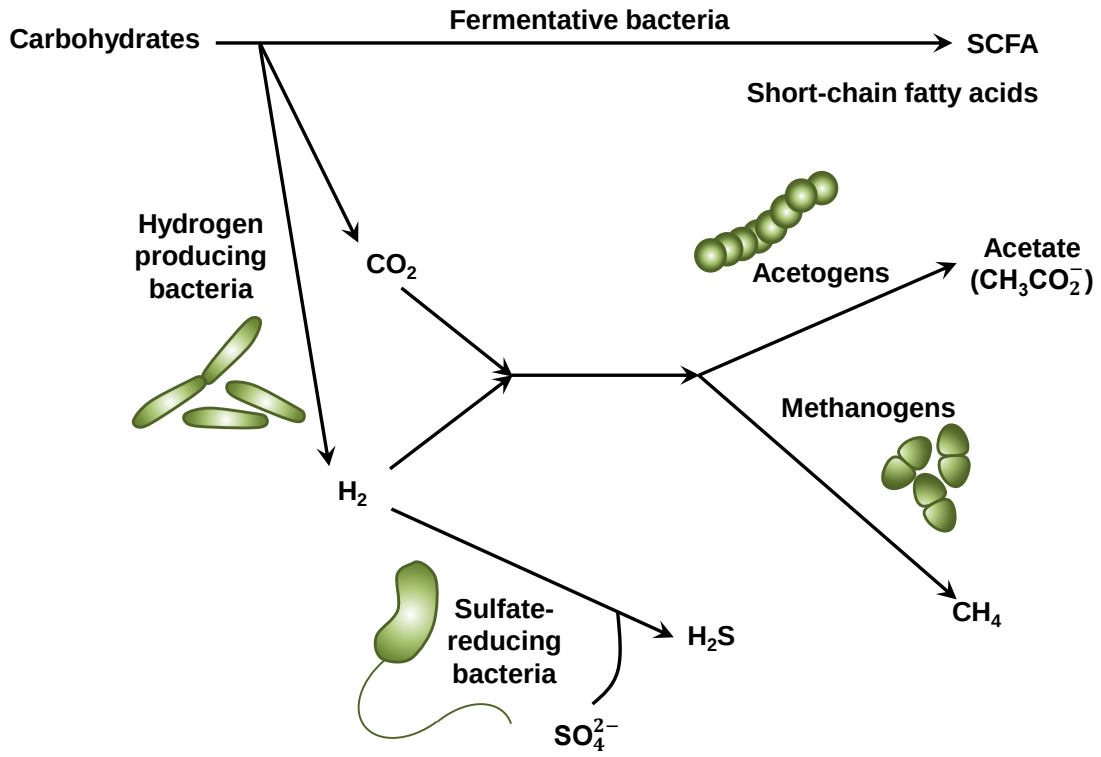

Figure 1.1. Illustration of major intestinal gas production pathways.

1.1.1.2 Intestinal gas and gastrointestinal disorders

Luminal distension from intestinal gas formation may cause unpleasant symptoms such as bloating and pain particularly in patients with irritable bowel syndrome [48]. From a clinical point of view, intestinal gases may affect health both directly and indirectly, and can be potentially used as biomarkers to assess gastrointestinal function and diseases [42,49]. Gases formed are potentially evacuated *via* the anus and such events may be associated with little to quite an unpleasant odor, depending upon the content of the gas. Any gas formation that occupies a volume distends the lumen of the intestine. In patients with irritable bowel syndrome, stimulation of mechanoreceptors can lead to symptoms of bloating and pain [50,51]. Specific gases may have direct physiological or pathophysiological effects. CH_4 can interact with the neuromuscular function of the intestinal tract and has been associated with the slowing down of intestinal motility with subsequent constipation [52]. H_2S is a gasotransmitter that affects chloride secretion and inhibits gastrointestinal (GI) smooth muscle contractility [53]. In addition, its accumulation in the colonic lumen, due to defective detoxification mechanisms and/or excessive production, may be pathogenically related to inflammatory bowel diseases (IBD), especially ulcerative colitis (UC) [54] and in colon cancers [45]. NO*x* is another gasotransmitter that contributes to the regulation of intestinal motility, mucosal blood flow and secretory functions [55]. NO*x* is also a co-factor to H_2S in driving the inflammatory process in UC [56,57]. In view of these associations, sensing and profiling intestinal gases may reveal valuable insight into gastrointestinal functionalities, and may enable a more accurate and personalized treatment of gut-related syndromes or illnesses and help in their prevention [42].

1.1.1.3 Intestinal gas sensing methods and limitations

From studies that took place several decades ago, direct gas sensing methods based on insertion of tubes into the oral cavity and anus have shown the value of assessing gases of the

gut [8]. However, the invasive nature of these methods has led to their limited application. Indirect approaches have included H_2/CH_4 breath tests [58,59] and room calorimetry [60,61]. These methods rely on measuring intestinal gases that are first absorbed across the gut mucosa, then recirculated to the lung *via* the blood stream and eventually excreted by respiration. However, significant inaccuracies occur due to interfering gases produced by other parts of the human body and activities [8]. Another facile indirect method is based on measuring the gases produced *via in-vitro* culturing of fecal samples. Advantageously, fecal samples are easy to obtain and examine. The microbiota found in the feces also represent a good reflection of the microbial community of the distal colon [21,62-65].

Usually in the *in-vitro* culturing process, fresh fecal samples are collected and immediately placed in sealed containers with an inert gas (commonly nitrogen) headspace and kept at 37°C. Generally, within 1.5 h, the samples are mixed with phosphate buffer and supporting substratum, which depends on the purpose of the measurement, to produce a fecal slurry [20] that is subsequently incubated in a sealed oxygen-free container kept at 37–40 ºC to mimic anaerobic human colonic conditions [8]. As a result of the fermentation, aliquots of gas are released into the headspace.

Traditionally, these gases are captured either by solid phase microextraction (SPME) fibers or pumped into gas sample holders. The captured headspace gas is then commonly analyzed by gas chromatographers coupled with mass spectrometry (GC-MS) [21,62-65]. However, GC-MS is an offline analytical tool that is unable to perform real-time and continuous measurements to reveal the gas production kinetics [66]. Understanding the gas production kinetics is vital for evaluating the metabolic activities of intestinal microbiota [22]. In order to implement real-time gas investigations, gas analysis instruments utilized in the latest breath test approaches can be applied. These include proton transfer reaction mass spectroscopy (PTR-MS), selected ion flow tube mass spectroscopy (SIFT-MS), ion mobility

spectroscopy (IMS) and laser spectrometry (LS) systems. However, these methods are rather expensive, the equipment is bulky, they involve high level operative skills and, hence, their application and access are limited [67,68]. Alternatively, low-cost and portable gas sensor technologies can be implemented for retrieving clinical insight from intestinal gases with adequate accuracy and much smaller costs, even enabling viable point-of-care systems [67,69,70]. Although such sensing technologies have been employed for breath testing, their usage for measuring the gases of fecal samples has remained limited [62-66].

One of the main technological requirements for correctly sensing gases from the fermentation of distal colonic fecal samples is the establishment of a nearly oxygen-depleted atmosphere. The colonic environment is known to be almost anaerobic with the oxygen level measured to be below 2% vol [8,71,72]. Direct human colonic gas measurements suggest that significant amounts of CO_2 and H_2 exist in the colon [8], and that these gases play important roles in influencing the ecosystem of the microbiota of the colon and as such colonic gas production. There are also reliable suggestions that measurable concentrations of NO_x and H_2S can be found in the colon [73-77]. N_2 also naturally exists in the colon [8]. As a summary, Table 1.1 presents the range of concentrations of the colonic gases.

To simulate the colonic headspace environment, *in-vitro* fecal fermentation approaches conventionally consist of flushing the chamber headspace with inert gases for inducing neutrality of the microbial activities [8,20,78]. In reality, the introduction of CO_2 and H_2, which naturally take part in the metabolic pathways of the microbiota, into the head space of the *in-vitro* incubator should be fully explored to assure that their effects are revealed. Such explorations have been carried out for *in-vitro* simulation of animal gastrointestinal tract [22,79] but mostly ignored in the studies of the human feces sample incubation.

The anaerobic conditions of the colon also hinder the incorporation of many low-cost commercial gas sensors, including semiconducting transducers, as their correct functions

need reactions between gas species and surface chemisorbed oxygen at elevated temperatures [80,81]. This limits anaerobic gas sensor technologies to optical, thermal conductivity-based calorimetric, physisorptive charge transfer and selected electrochemical-based gas sensors [80]. These sensors do not need oxygen in their operation and, hence, may be suitable candidates for realizing low-cost *in-vitro* gas measurement systems for real-time measurement of fermentation gases.

Table 1.1. Average gas concentrations in healthy colonic gas environment from various sources

	Number of participants	N_2 (%vol)	O_2 (%vol)	H_2 (%vol)	CO_2 (%vol)	CH_4 * (%vol)	H_2S (ppm)	NO*x* (ppb)
Suarez, Furne [72], 1997	16	22.2 ±12.2	3.3 ±1.9	34.3 ±17.5	34.7 ±14.7	5.6 ±10.4	29 ±40	
Steggerda [71], 1968	5	61.2	3.6	19.8	8.1	7.3		
Levitt [8], 1971	11	64 ±21	0.69 ±0.5	19 ±16	14 ±7	8.8 ±9		
Herulf [76], 1998	6							460 ±60
Lundberg [75], 1994	12							45 ±7

* It is important to consider that CH_4 only appears in some of the samples and the average only belongs to them. Nearly >80% of the human subjects did not produce any CH_4 in their colons.

1.1.2 Gas profiling

In addition to gas sensing technologies, gas profiling also deals with extracting meaningful characteristics from different sensing data (pressure, temperature and headspace gas mixing ratio) which are available in quasi-closed pressure regulated anaerobic fermentation systems. Gas profiling results in the generation of the GPP, an insightful set of parameters, which includes the gas production quantity, composition and kinetics throughout the whole fermentation duration. Informative, straightforward and concise, the GPP is utilized for diagnostics, analysis and control of fermentation and their correlated biological processes.

In order to completely extract GPPs in such fermentation systems, there are two important issues which must be taken into account. These are for accurately assessing the total gas production, gas composition and the kinetics of gas production. The first concerns determining the total gas production by measuring the cumulative pressure using reliable pressure sensors [82-84] and translating the data into correct gas production according to the *ideal gas law*. The second is about measuring the concentration of gases in the system using sensors with high selectivity and accuracy as mentioned earlier.

Ideally, after acquiring the correct pressure and gas sensing data, the GPPs can be fully estimated. Although it is desirable to understand the behaviour of fermentation systems, and this necessitates obtaining equations for accurately calculating GPPs in closed and pressure regulated systems, there is nevertheless, a limited scientific literature detailing the comprehensive sets of equations necessary for such calculations, and it is possible that some reported systems may produce inaccurate estimates of GPPs [85].

In many earlier reports on quasi-closed systems that may also allow venting, the total gas production is measured using pressure sensors but such works, despite their important

contributions, generally exclude incorporation of gas sensors or automated regulators [82,83,86]. In others systems, gas production measurements are determined by assessing the vented gas, which is advantageous as it interferes less with the reactor, whilst ignoring the effect of gas presence in the headspace [5,25,87,88]. In a few advanced methods, both vented and headspace gases are taken into account in the total GPP calculations, though even in these methods, the equations used are based on simple assumptions [3,26,84,89]. In several reports, gas productions were measured continuously using respirometers and by introducing mass flow equations; however, neither changes in headspace pressure and temperature nor gas solubility in liquid were taken into account [3,26]. In two other reports, gas solubility was included in the calculations though, again, changes in headspace pressure were ignored [84,89]. Recently, Hannah et al reported on the development of a mathematical formulation for GPP calculations, for fermentations where only a single post-incubation analysis of headspace gas was available [89]. While this method is attractively simple and sufficient for many applications, it is based on the assumption that the composition (i.e. the percentage of CO_2 and the percentage of CH_4) of the fermentation gas does not change during the course of the fermentation.

The current commercial systems for GPP calculation ignore important factors such as internal pressure changes or the presence of gas contained in the headspace. Furthermore, none of existing methods include embedded gas sensors in the fermentation model [90-93] as required in fermentation systems such as *in-vitro* fecal incubation or AD.

1.1.3 Gas components in anaerobic digestion

AD is the process of decomposing organic wastes by different microorganisms in an oxygen-free environment. AD is utilized in many applications such as biogas production and

wastewater treatment [94]. AD presents many advantages including relatively energy efficient treatment, reduced pollutant by-products and fertilizers as secondary-products [94-96]. AD is very suitable for treating high strength wastewater with concentrations above 4 kg/L of chemical oxygen demand (COD), while the limit for aerobic digestion is less than 1 kg/L [2,94,97].

1.1.3.1 Monitoring of anaerobic digestion

Monitoring and controlling AD processes are essential for increasing the efficiency of organic wastes degradation and conversion to biogas, maximizing process yield and assuring process stability [29,96,98]. Monitoring AD is a multi-variable and complex procedure based on parameters such as volatile acids (VA), pH, buffering capacity, organic removal (usually measured in terms of total solids (TS) and volatile solids (VS) [27,99,100]), dissolved gas and biogas production profiles [29,96,98]. Identifying high distinction parameters that provide early warnings for process complications is vital to enable operators to intervene process failure realization [27,29,98].

VA are frequently mentioned as efficient early warning indicators [29,98,101,102] considering that VA accumulation implies process imbalance [103] and are important intermediates in methanogenesis [104,105]. Analyzing different components of VA helps in process diagnostics [101,103]. However, *in-situ* measuring of VA accurately, continuously and automatically requires high maintenance, skills and costs [29,100,105-107].

Measuring pH directly from the liquid is relatively simple for indicating a process imbalance. Different microorganisms can function in specific ranges of pH [29,108,109] and pH normally drops together with VA accumulation [98]. However, in a well-buffered system, pH changes are usually slow and non-distinguishable [106,110]. Buffering capacity (alkalinity) is

good digester imbalance indicator, as VA accumulation reduces buffering capacity earlier and in higher magnitude than pH [29]. However, it has been reported as insensitive in several scenarios [28]. In some industrial treatment plants, the main objective is the removal of organic wastes as opposed to biogas production, hence organic removal is an important indicator of process efficiency [27,111,112]. However, organic removal is generally analyzed in laboratories with bulky and expensive equipment and the procedure can be too long [29].

Alternatively, accurate, continuous and *in-situ* measurements of biogas components, both in the liquid and headspace simultaneously, have the potential for providing sufficient real-time process characterization as an effective early indicator. These biogas components including CO_2, CH_4 and H_2 appear in the metabolic pathways of microorganisms and are highly informative (in comparison to pH and buffering capacity). Additionally, compared to measuring alternative parameters such as VA, TS and VS, assessing gas components is generally simpler and involves lower costs.

1.1.3.2 Gas components in anaerobic digestion

AD gas products fulfill different roles in the digestion process including intermediate, final product and inhibitor, while having a high correlation to different VA. The main gas products of AD include CO_2, CH_4 and H_2 [104,113].

It has been reported that different fermentation pathways are greatly influenced by high levels of dissolved H_2 whereas at low levels, H_2 and acetate producing pathways are favoured [114]. During acetogenesis, the main products are acetates, H_2 and CO_2 [104,115,116] and while low dissolved H_2 concentration is vital for acetogen bioactivity [114,117], H_2 is found as an important electron donor in transitioning to methanogenesis [117,118]. In methanogenesis,

different types of methanogenic bacteria reduce acetate, H_2 and CO_2 to form CH_4, satisfying their energy needs [104,113,114,117].

The H_2 level in biogas is linked to the imbalance between different microorganisms [27,119] and excess amount directs electrons flow from methane to VA production [31,114], which then inhibit acetogens from degrading butyric and propionic acids [120]. Furthermore, H_2 production is strongly correlated to VA [30] and H_2 increases together during a system overload [28]. Consequently, H_2, both in liquid and gas phases, is an important and sensitive process indicator as a control parameter. Although H_2 responds quickly to an overload of fast degrading organics, it only mildly responds to loading with slow degrading organic matter [121] and, by itself, can be insufficient for early prediction of moderate and slow overloading [30,31,122,123]. As such, additional monitoring of other gases is also required.

Monitoring CH_4 production rate helps in mitigating process imbalance in continuous flow stirred tank reactors and provides an effective basis for process control [124]. Tracking CH_4 was recommended by Liu *et al* [125] as an important online indicator and demonstrated a good correlation with VA accumulation [101]. Moreover, low production of CH_4 together with high levels of H_2 and CO_2 appear as what preclude methanogens to prevent the accumulation of VA and H_2 [101,114,118].

CO_2 is directly linked to the alkalinity level and eliminates the need for probing, which can be subjected to fouling [126]. Moreover, fluctuations in pH are strongly observed in CO_2 production [112,127] therefore abnormal levels of CO_2 is a good indication of process imbalance.

1.1.3.3 Sensing methods and limitations of gas components

Existing literature for gas-phase measurements present gas chromatography (GC) [29] and infra-red (IR) sensing for CO_2 and CH_4 [128] and electrochemical (EC) sensing for H_2 [128]. Additionally, many commercial systems are capable of measuring the total gas production which is important but not quite informative and can provide delayed response relating to process instability [128].

In reality, poorly dissolved gases like H_2 and CH_4 show low mass transfer coefficients from the liquid to gas-phase, resulting in higher accumulation in the liquid, sometimes up to 80 times, relative to the theoretical calculation based on the equilibrium between the gas-phase and liquid-phase according to *Henry's law*. Therefore, measuring CH_4 and H_2 in both phases is required in order to monitor an AD effectively [32,129,130].

In liquid-phase, in order to measure CO_2, CH_4 and H_2, researches traditionally use high pressure liquid chromatography (HPLC) and near infra-red spectroscopy (NIRS) which involve preliminary liquid processing [105,107], trained operators [29] and high maintenance costs since expensive sensing components operate in highly toxic and corrosive environment [105]. In limited studies, measurements of dissolved H_2 were conducted by Koruda *et al* [32] and Strong *et al* [31] by covering an EC sensor with a protective membrane. Although these techniques are *in-situ*, accurate and continuous, the sensors are sensitive to H_2S [32], featuring complicated calibration procedures or long preparation time [30,31]. Other approaches use membranes and gas diffusion to sense dissolved H_2 with mass spectrometry (MS) [33,34], flame spectrophotometry [131], or measuring partial pressure with trace gas analyzer [30]. These methods can be bulky, expensive and not suitable for long term operations due to membranes' bio-fouling.

1.2 Motivations

Most of the direct methods for sensing colonic gases are invasive in their nature and involve notable discomfort for subjects, limiting their continuous and large scale applications. Other methods such as breath tests and whole-body calorimetry are non-invasive but incur significant inaccuracies and may be influenced by other sources of interferences in the living body. Measuring gases *in-vitro* contains many advantages and has the potential to overcome these approaches limitations. However, current methods for sensing colonic gases *in-vitro* are either bulky, expensive, offline or require high skilled operators and as a result their on-going application on large number of individuals is generally difficult. Moreover, current methods consist of sensing a limited range of gas species which can hinder important biological processes. These processes are potentially observed in the relationship between different gas types and their dynamics (Table 1.1).

In this PhD research, in order to address the limitations of *in-vitro* intestinal gas sensing and to reveal the valuable GI insight, the author develops a new, real-time, low-cost and portable gas sensing technology. The new technology is specially designed to sense colonic gases including CO_2, CH_4, H_2, H_2S and NO*x*, produced by incubated human fecal sample *in-vitro* in an anaerobic environment. The portability of the system allows it to be easily utilized outside the lab and its cost-affectivity is a key for mass scale applications.

Conventional approaches for simulating gut environment during fecal incubation *in-vitro* generally use 100% inert gas which is preliminary flushed into the headspace. However, these approaches often ignore the importance of supplying the reactor with gases, such as CO2 and H2, which are involved in the metabolic pathways and are essential to the microbiome during fermentation (Figure 1.1).

Considering the limited literature detailing the contribution of these supplemented gases on the simulated human gut environment, as part of the work of this PhD research, the author will use his new *in-vitro* intestinal gas sensing technology and apply it to several anaerobic environments. Consequently, the author will investigate these environments' impacts on the resulted GPPs and their implications to the microbial activities.

Gas profiling in the aforementioned fermentation systems is of high importance for exploiting the rich information contained in the production of gas components and serves different applications and a variety of purposes. Methods for calculating GPP are explained in some of the existing literature. However, these methods do not represent a comprehensive approach and often lack several components which contribute to the overall GPP. These components include: embedded gas analysis, gases contained in the headspace, gases released from the system, dissolved gases and the headspace's internal pressure and temperature variations. These partial and non-standardized calculations result in the estimation of GPP which may hinder biological processes or lead to wrong conclusions.

In the subsequent stage of this PhD work, in order to complete the missing knowledge detailing the calculation of GPP in such fermentation systems, the author proposes a new gas fermentation model and provides a rigorous and comprehensive method to generate GPP from the available sensing data. The new method will avoid inaccuracies which may be involved in partial calculations used in other works and, overall, in order to increase the value from the GPP.

Eventually, in the final stage of this PhD research, the candidate focuses on the implementation of gas profiling in both gas and liquid phases to obtain comprehensive gas profiling for assessing the health of AD. Gas components in AD processes, both in headspace and in liquid, contain invaluable information with respect the health of digesters' microbial activities. These gas components can potentially replace parameters such as VA, pH,

alkalinity and organic removal, which are relatively difficult to measure or provide partial information. While continuous gas analysis in the gas-phase is well established, the relationship with gas components in the liquid-phase has not been shown. The information gained from co-measurement of gas and liquid media components can enhance the monitoring of and control over anaerobic digesters to effectively provide early warning for imbalances and failures. In addition, current methods for sensing gases in liquid-phase are either bulky, expensive, sensitive to bio-fouling and susceptible to liquid medium toxics or require high operating expertise.

In this PhD research, in order to enhance the monitoring capability of AD processes *in-situ* by measuring gas components in both phases, simultaneously, and, in order to address the limitations of measuring gas components in liquid-phase, the author harnesses the new technology designed for sensing intestinal gases and develops a novel, relatively simple, technique which allows *in-situ* measurements of CO_2, CH_4 and H_2 in liquid-phase as well. Furthermore, in order to identify indications for AD processes' health and to explore the potential of gas components as early warning parameters, the author investigates patterns and inter-correlations between the gases in both phases in both balanced and imbalanced AD processes.

1.3 Objectives

This thesis is primarily focused on gas profiling for quasi-closed pressure regulated anaerobic fermentation systems. The work is presented in three main stages in the form of human fecal incubation *in-vitro*, expansion of the gas profiling model and wastewater treatment by AD *in-situ*.

Current approaches for gas profiling in quasi-closed pressure regulated anaerobic fermentation systems lack real-time, accurate, simple, portable and low-cost gas sensing technologies that can operate in the anaerobic headspace environment and in the incubated slurry. The outcomes of this work have not been reported by any other researcher at the time that the PhD research started.

The research work in this PhD dissertation can be briefly classified under the following objectives:

a) Introducing a new, simple, low-cost and portable gas sensing technology for measuring intestinal gas in anaerobic environments.
b) Exploring the impacts that different anaerobic environments have on the GPP produced during human fecal samples incubation *in-vitro.*
c) Accurately producing the GPP from the variety of sensors utilized in fermentation system in real-time, by developing a new model that incorporates many gas fermentation parameters.
d) Measuring gas components of AD processes in both liquid and gas phases using a novel gas profiling technology.
e) Enhancing AD monitoring by investigating AD process imbalances and failures utilizing gas components patterns.

1.4 Thesis organisation

This thesis is mainly dedicated for addressing limitations and inadequacies of gas profiling in quasi-closed pressure regulated anaerobic fermentation systems.

In Chapter 2 the author details the development of a low-cost, portable, simple technology for real-time *in-vitro* sensing of colonic gases in the anaerobic headspace of incubated human

fecal samples. The author lays out the considerations incorporated in the synthesis of such a technology together with validation tests. Then, the author uses the system to explore the impacts of different anaerobic environments on the GPP of incubated fecal samples. Finally, he investigates the effect of highly fermented fibres by comparing the GPPs with and without added substrates.

In Chapter 3 the author develops a rigorous fermentation model and introduces a novel mass-flow equation for accurately extracting GPPs from the sensing data of such systems in real-time. The author validates the accuracy of the new mass-flow equation utilizing the intestinal gas sensing technology from Chapter 2. In addition, the author demonstrates the performance of the novel fermentation model and shows the impact the newly introduced components in the developed mass-flow equations have on the total GPPs.

In Chapter 4 in order to enhance and improve monitoring in AD processes, the author utilizes the new gas profiling technologies and equations from Chapter 2 and Chapter 3 for developing the gas sensing techniques for AD processes in both liquid and gas phases, simultaneously. The author validates the new technique using a series of AD batch experiments and utilizes the developed approach to investigate AD process imbalances and failures together with the impact that elevated pressure has on the process performance.

Finally, in Chapter 5, the author presents the concluding remarks and the future outlook of the research presented in this thesis.

Chapter 2. GAS PROFILING SYSTEM

2.1 Introduction

In this chapter, the author shows the development of a portable and continuous sensing technology for measuring gases from *in-vitro* fecal sample fermentation. This system enables continuous profiling of gases produced from the incubation of samples that are good representatives of the microbiota of the distal colon. The operative principles of each of the system's components (the gas sensors) are critically discussed and the gas-profiling performance is demonstrated using human fecal samples mixed with a model fiber as a function of simulated colonic gas environment. The effect of different headspace gas mixtures are investigated for understanding their influence on the gas profiles. Additionally, the measurement reproducibility and the system repeatability are also investigated.

The content of this chapter was published as a fully reviewed paper in Sensors and Actuators B journal [132].

2.2 System design guidelines

2.2.1 Considerations for choosing gas sensing technologies in anaerobic environment

A comprehensive discussion regarding the choice of gas sensors based on the conditions of operation is presented in the following sections. These conditions include the operation in an anaerobic environment suitable for culturing the microbiota of the distal colonic samples and the range of gas concentrations. Additionally, considerations about costs are also included as the gas sensors for the incubator-sensor systems are presented for addressing viability for point-of-care units.

Briefly, non-dispersive infrared (NDIR) gas sensors are chosen for measuring CO_2 and CH_4 due to their ability to selectivity measure these gases at the concentration range of $0 - 100\%$ in the anaerobic environment (Figure 2.1a). A low-cost liquid-electrolyte based electrochemical sensor is selected for sensing H_2S in the range of $0 - 2000$ ppm due to its high selectivity, excellent sensitivity and low oxygen requirement to operate in the anaerobic condition (Figure 2.1b). Thermal conductivity calorimetric gas sensor is another low-cost device which is selected for sensing H_2 in the *in-vitro* system (Figure 2.1c). It is currently the most durable and relatively selective gas sensor available in the market which can measure H_2 in the range of $0 - 20\%$ on par with the concentration range of this gas in the colonic environment as indicated in Table 1.1. Physisorption charge-transfer gas sensor is chosen to sense NO*x* in the sub-ppm range given by its low-cost, portability and unique affinity to NO*x* gas (Figure 2.1d) [133].

2.2.1.1 Optical gas sensing platforms

Optical gas sensors rely on the unique fingerprints of target gas molecules such as their optical absorption and emission wavelengths, which can lead to acceptable selectivities and sensitivities, depending on the light sources and detector bandwidths, and also reliability of operation in anaerobic conditions. In practice, highly selective optical sensors require bulky, costly and sophisticated instruments to enable operation whether the sensor technology is fiber optics [134-137], chemilumiscence [138,139] or tunable cavity laser-based sensors [140]. In comparison, NDIR optical sensors have much lower costs, smaller size and complexity [140], which come with a drawback of selectivity loss. Despite this fact, they can still be good candidates for anaerobic measurements of selected gases. In the NDIR configuration, only an IR (generally broadband) light source and two pyroelectric or field effect-based active detectors (one as the sensor and the other as a reference for compensation

of ambient environmental interferences) are incorporated into cells with reflective surfaces (Figure 2.1a). Length has a strong influence on the quality of NDIR sensors, as based on the *Beer-Lambert law* for light absorption, the sensitivity of such gas sensors strongly depends on the light path length within the absorption cell.

The current commercially-available NDIR gas sensors are mainly implemented for sensing of CO_2 and CH_4, two of the main fermentation gases, as these gases have distinct IR absorption bands [140,141]. The achievable sensitivities for CO_2 and CH_4 are normally in the ppm (part per million) to ppt (part per thousand) ranges with light-interactive path length for up to a few centimeters [140]. These specifications satisfy the requirements for sensing CO_2 and CH_4 intestinal gases in concentration ranges suggested by Levitt *et al.* [8] (Table 1.1). Unfortunately, NDIR technologies are not easily adoptable for measuring other target intestinal gases. There is no IR absorption band for H_2. NO*x* and H_2S have absorption bands in the IR light regime but their usual concentrations in the colon are in sub-ppm ranges (Table 1.1). For achieving considerable sensitivity in such ranges, the required path lengths are too long for creating compact NDIR systems [140] and the sensing is limited to chemilumiscence, tunable cavity or other complex or expensive technologies.

2.2.1.2 Electrochemical gas sensing platforms

Electrochemical sensors can be categorized into liquid and solid electrolyte-based. Normally, the former is amperometric and the latter is potentiometric [142,143]. Although the solid electrolyte-based potentiometric sensors have demonstrated several advantages in comparison to those of liquid electrolyte-based amperometric [142], many types of conventional affordable electrochemical gas sensors are still liquid-based.

In liquid electrolyte-type electrochemical sensors (Figure 2.1b), gas molecules diffuse into the porous polymeric membrane, dissolve in the electrolyte (acid or organic-based) and then are catalytically reduced or oxidized on the surface of a sensing electrode (normally made of noble metal catalysts) at room temperature. In the catalytic process, the choice of sensing electrode metal, together with the applied bias voltage, determine the efficiency and the selectivity to a target gas [143]. The catalytic reaction results in the generation of free electrons, producing a current proportional to the gas concentration. A small amount of oxygen is required in the counter electrode for the reaction with the target gas. The oxygen can be found dissolved in the liquid electrolyte. Depending on the volume of the electrolyte, access to this oxygen allows the operation of the sensor in the anaerobic environment for several hours, before being fully depleted. Electrochemical sensors are available for different gases of importance to the gut including H_2S, H_2 and NO*x*, and cannot be sensed optically at low-costs or with the required sensitivities for the colon environment (Table 1.1). The usual detection limit of H_2 in electrochemical sensors is within thousands of ppm range, which is much less than the concentrations found in the colon environment (%vol range as presented in Table 1.1) [8]. The sensitivities for H_2S and NO*x* are normally in the range of ppm or sub-ppm, which is well below to their concentration in the colon environment [73-77]. However, especially for H_2 and NO*x*, the cross-sensitivity of these electrochemical sensors to other active gas species of the gut is extremely large. This means H_2 and NO*x* results using only electrochemical configuration are rendered of no value for selective gas measurements in the colonic environment. Out of all electrochemical sensors, H_2S sensors provide the selectivity and sensitivity required for gas measurements of the gut. H_2 sensors should be used together with other gas sensors to compensate for the cross-talk.

2.2.1.3 Calorimetric gas sensing platforms

Calorimetric gas-sensing platforms are generally divided into catalytic-bead and thermal-conductivity (TC) configurations [144,145]. In the former method, a bead is heated followed by the catalytic oxidation of gas species, which results in heat release. However, this method requires oxygen to support the catalytic reaction and is not suitable for working in anaerobic conditions. On the other hand, TC sensors are non-combustible and can operate without the presence of oxygen, and are thus suitable for gas-sensing in the anaerobic colon environment. Their sensing mechanisms are based on different thermal conductivity of the active heating element usually made of noble metals (*e.g.*, platinum) in the presence of a target gas compared to the reference heating element (Figure 2.1c). The sensitivity of a TC sensor is within the ppt (part per thousand) range, which is much lower than those of NDIR and electrochemical gas sensors. However, as suggested in the literature [8,71,72], the concentrations of major colonic gases such as H_2, CO_2 and CH_4 are in the range of %vol illustrating the challenges TC sensors face in measuring such colonic gases in a multiple-gas environment while maintaining reasonable sensitivity. There are reliable TC-based gas sensors for measuring H_2 from the microbiota of the gut, and, as their response to H_2 is more than an order of magnitude higher than CO_2 and CH_4, they can be used for the application presented in this paper.

2.2.1.4 Physisorption-based charge-transfer gas-sensing platforms

For NO*x*, electrochemical gas-sensing platforms have significant cross-talk with many other gases, and chemiluminescent sensors are too expensive and bulky. As such, they are not suitable for reliable and low-cost point-of-care colonic gas systems. NO*x* has strong paramagnetic properties [146]. Upon the physisorption of NO*x* gas molecules onto the

surface of a certain group of materials, a charge transfer occurs without the need for oxygen. The efficient charge transfer between NO*x* and the sensitive material depends on the relative positions of their electronic band structure [133]. The physical attractive forces in physisorptive sensors are fundamentally different from those in conventional semiconducting gas sensors that generally rely on chemisorption of gas species [147,148]. In the physisorption process, a simultaneous interaction of magnetic dipoles and surface-induced dipoles can take place, which results in a relatively strong NO*x* affinity to the sensitive material compared to other non-paramagnetic colonic gases of CO_2, CH_4, H_2S and H_2. This implies that the physisorption-based charge-transfer gas-sensing platforms (PCT) can be suitable candidates for selective NO*x* sensing in this PhD work due to their capability of operating in anaerobic environments.

Carbon nanotubes [149], conducting polymers [150] and graphene [151] have been investigated as the possible candidates for physisorption of gas molecules. These materials demonstrate poor gas selectivity, although exhibit excellent sensitivities (in the sub-ppb range). The recent emergence of earth-abundance two-dimensional (Figure 2.1d) metal chalcogenides has been shown as a significant breakthrough for NO*x*, H_2S and NH_3 sensing [152-156]. In particular, the developed NO*x* gas-sensor based on 2D tin sulfide (SnS_2) has demonstrated high sensitivity (sub-ppm range) and superior selectivity to NO*x*, and excellent reversibility at low operating temperatures without the presence of oxygen [133]. Therefore, this sensor was chosen to be incorporated into the author's *in-vitro* anaerobic gas sensing system for NO*x* sensing.

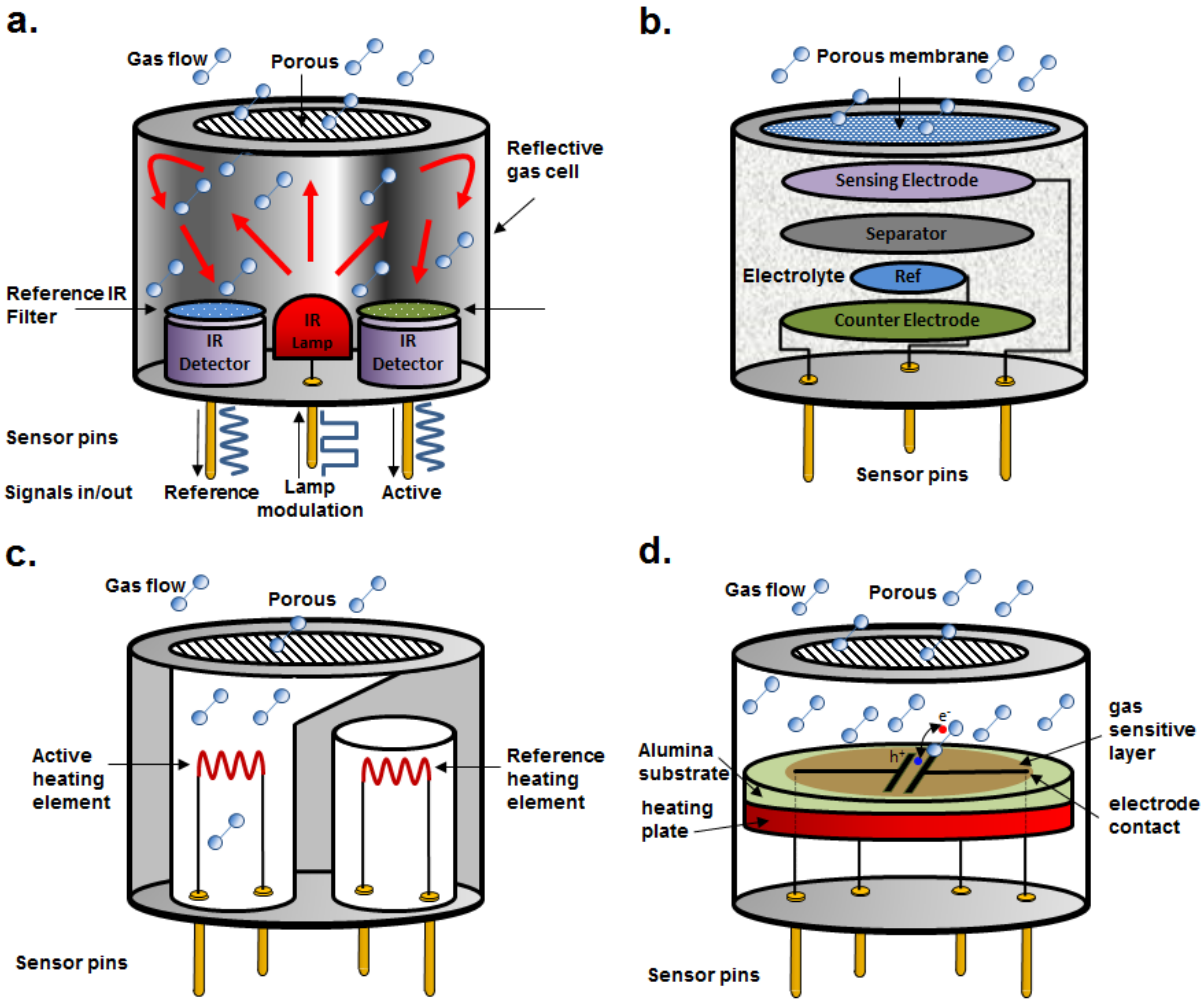

Figure 2.1. Low-cost and small size gas sensors configurations chosen for the anaerobic conditions presented in this chapter: **a.** optical NDIR; **b.** electrochemical; **c.** thermal conductivity; **d.** physisorption based charge transfer sensors.

2.2.2 Considerations for gas production measurement of colonic samples

The *in-vitro* gas system for fecal samples should be able to measure the total gas production and concentration of each gas individually. From these measurements, the production of each gas can be obtained. The measurement of total gas production is based on the real-time measurement of pressure changes in the headspace (Figure 2.2) obtained by a pressure sensor, followed by converting the real-time pressure change value into the transient total gas

production volume according to both *Avogadro's* and *ideal gas laws* [157]. The gas production of individual gas species was calculated according to *Dalton's law* [157], in which the total pressure exerted is equal to the sum of the partial pressures of the individual gases and the partial pressures are linked to the total pressure by the relationship in a mixture of non-reacting gases. Additionally, according to these principles the sub-gas production was calculated *via* the product of the total gas production and the gas species concentrations in the headspace. The gas production rates were calculated using the time derivative of the cumulative gas production.

The formulation of the gas production calculation is as follows:

$$V^+ = n^+ \cdot 22.41 \cdot 1000 \text{ [mL]} \quad 2.1$$

where $n^+ = P^+ \cdot \frac{V_h}{RT_h}$; n^+ is the gas produced in mol; P^+ is the transient headspace pressure increment due to gas production in kPa; V_h [mL] is the headspace volume in the container; T_h[K] is the headspace's temperature measured in Kelvin and *R* is the gas constant = 8.314472 $J \cdot K^{-1} \cdot mol^{-1}$.

The transient production of the individual gas species can be calculated according to *Dalton's law* [157], in which the total pressure exerted is equal to the sum of the partial pressures of the individual gases and the partial pressures (P^k) are linked to the headspace pressure (P_h) by the relationship in a mixture of non-reacting gases:

$$P^k = C^k \cdot P_h \quad 2.2$$

where C^k is the real-time headspace concentration of the gas species *k* in the fixed volume V_h.

Fermentation events are assessed by analyzing the kinetics of the fecal fermentation, derived from the accumulated gas production volume of each target gas species as:

$$GP^k(t_j) = \frac{V_h}{RT_h}\sum_{n=1}^{j} C^k(t_n)P^+(t_n) \text{ [mL]} \quad 2.3$$

where $GP^k(t_j)$ [mL] is the sub-gas production of gas species *k* at time t_j.

Gas production rates are calculated using the time derivative of the gas production volume integrated over a 10-min length normalized triangular window (T_{10}):

$$\text{gas production rate (t)} = \frac{1}{10}\int_{t-5}^{t+5} \dot{y}(\tau)\cdot T_{10}(\tau - t)\, d\tau$$

where y(t) stands for cumulative gas production as a function of time (t) and $\dot{y}(\tau) = \frac{dy}{d\tau}$ is its derivative at time.

Reproducibility of gas production measurements and repeatability of the *in-vitro* gas sensing system are assessed by repeating the studies in feces from three volunteers. The samples are incubated with and without the FOS substrate in the type 1 headspace gas environment (100% inert gas). The gas production results are presented as mean values ± standard errors.

2.3 Experimental setup

2.3.1 System integration

As presented in Figure 2.2, the developed *in-vitro* gas sensing system consists of three main modules. The first is a glass septa bottle filled with fecal slurry. The second is a gas-sensor array composed of an acrylonitrile-butadiene-styrene (ABS) adapter that accommodates four gas sensors: one NDIR sensor for CO_2 and CH_4 (purchased from © SGX Sensortech, United Kingdom); one electrochemical sensor for H_2S (purchased from © SGX Sensortech, United Kingdom); one TC sensor for H_2 (purchased from © SGX Sensortech, United Kingdom); and one PCT gas sensor for NO*x* (developed at RMIT based on SnS_2 technology [133]) in a gas-

seal manner. The third module is adopted from an automated gas pressure regulator (ANKOM Technology, USA), which consists of a gas pressure transducer, a temperature sensor, a controlled venting valve, an electronic control unit and a radio-frequency transceiver. This module is designed to record temperature, small pressure changes in the headspace and maintain a near constant pressure environment. All three modules are gas-sealed using lubricated rubber gaskets.

2.3.2 Measurement protocol and signal processing

Electronic boards connected to the sensors to collect the analogue signals digitize them and transmit the processed and coded signals to a computer where the data are recorded in real-time. The digital data are interpreted as gas concentration by applying them into a pre-computed fitted curve. The fitted curves are designed according to the characteristics of the sensors and their associated electronics and contain parameters from the calibration tests. The sensors continuously operate to provide live data, which are recorded by the computer software at the intervals of 5 s. Similar to the gas-sensors electronic boards, the pressure regulator module senses pressure changes in the headspace and transmit the data to the computer through a RF transceiver where they are converted into real-time total gas production.

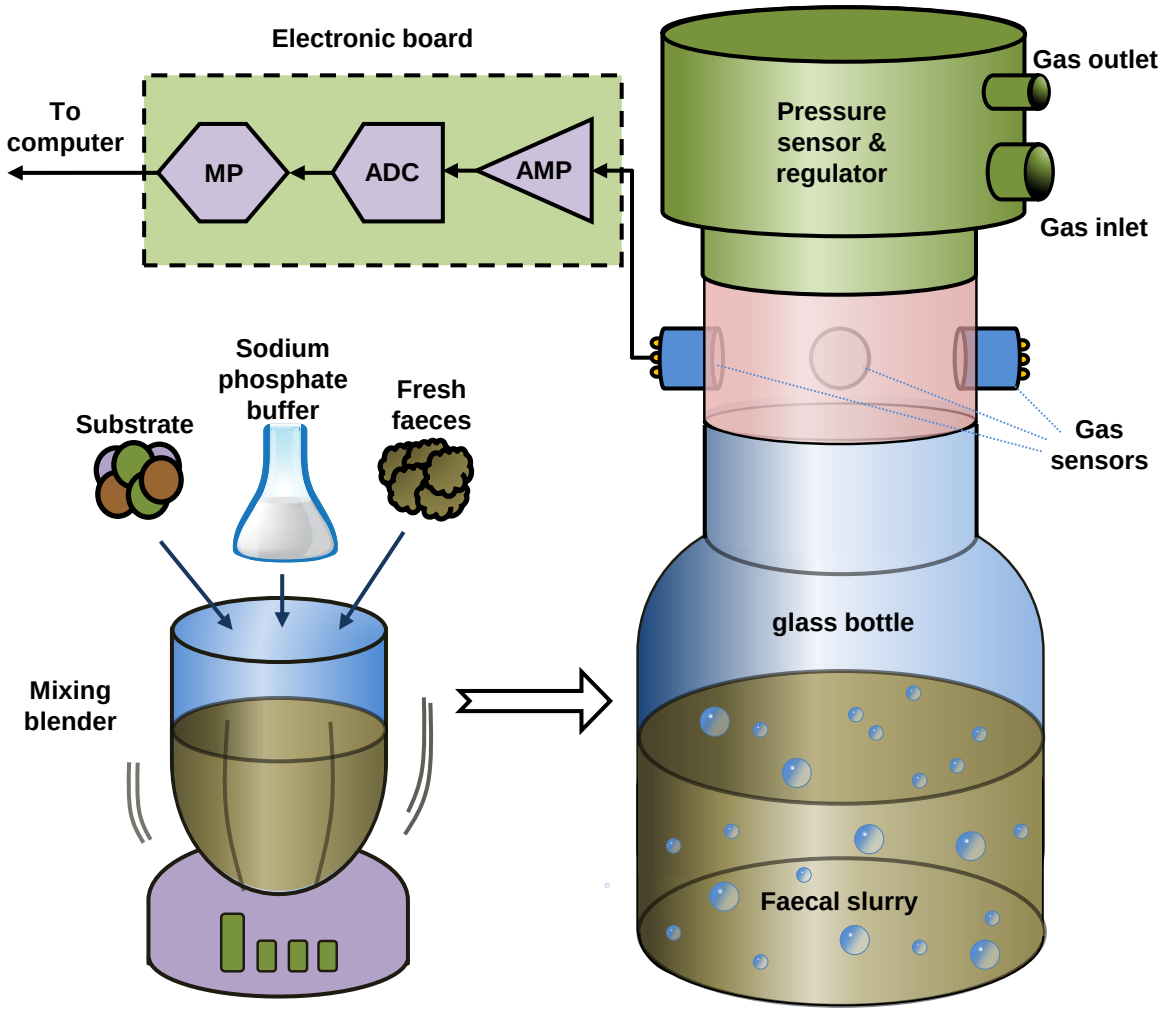

Figure 2.2. Illustration presenting the steps for the preparation of the fecal samples and the schematic of the *in-vitro* fecal fermentation gas measurement system with the incorporated sensors and data acquisition unit.

2.3.3 System calibration

The system was calibrated with target gases of industrial standards, which are 1%vol CH_4, 5%vol CO_2,1% vol H_2, 56 ppm H_2S and 10 ppm NO_x in balanced inert gas (e.g. N_2 or Ar). The introduction of the inert gas is to simulate the formation of an oxygen-free environment for the *in-vitro* fermentation and promotion of methanogens that only thrive in such a condition.

Pre-calibrations to assess the cross-sensitivities of the sensors, when exposed to all target gases at typical concentrations, are conducted at the laboratory. Table 2.1 presents the outcome of these measurements and proves that a sufficiently low level of cross-sensitivity exists, which is a crucial parameter for the successful implementation of the system for measuring the gases of the simulated colonic environment.

Table 2.1. Performance and cross-sensitivities of gas sensors

	NDIR – CH_4	NDIR – CO_2	Electrochemical	TC	PCT
1%vol CH_4	1%	<0.1%	<0.06 ppm	<0.14%vol	<0.8 ppm
5%vol CO_2	<0.1%	5%	<0.1 ppm	<0.05%vol	<0.8 ppm
56 ppm H_2S	0%	0%	56 ppm	0%vol	<0.4 ppm
1%vol H_2	0%	0%	<5 ppm	1%vol	<0.3 ppm
10 ppm NO*x*	0%	0%	0 ppm	0%	10 ppm

2.3.4 Preparation of fecal samples and mimicking the colon environment

Healthy volunteers, without known past GI disorders, were recruited for the study and were guided not to alter their diets during the experiments period. The experiments were conducted under ethical approval obtained from Monash University Human Research and Ethics committee (CF15/2454). Feces were defecated naturally into a sealed container then kept in an anaerobic environment at 37 °C and were used within 1.5 h of passage. In order to mimic the colon environment, the system is placed in a 37°C water bath equipped with a shaker of

50 shakes per min that simulates the colon temperature and motility [20]. An inoculum is prepared by mixing freshly collected human feces from a healthy volunteer with the sodium phosphate buffer (pH 7) to make up the 160 g/L slurry and achieve similar pH level to that of colon lumen. For some experiments, 1 g of substrate (fructooligosaccharides, FOS, BENEO-Orafti, Belgium) was added into the inoculum when 50 mL fecal slurry is injected into the incubation chamber to ensure minimum fermentation event occurs before the start of experiment. FOS is an indigestible carbohydrate [158] that is rapidly fermented by the colonic microbiota to produce short-chain fatty acids (including butyrate, acetate and propionate) and fermentation gases (H_2, CH_4 and CO_2). FOS was chosen as a model substrate for the fecal microbiota to better understand gas profiles produced as a result of different headspace mixture gases and against a blank reference not only for its fermentation characteristics, but also because it is clinically relevant. FOS is present in many foods (such as wheat and onions) and is fermented *in-vivo* as shown by hydrogen breath testing, one of the key components of the diet that is reduced in order to relieve symptoms of irritable bowel syndrome [48,159-161].

Although the importance of pressure distribution along the human GI track is still scientifically unclear [40], *in-vivo* measurements of pigs' GI track indicated that the pressure conditions in the colon are slightly above atmospheric pressure [162]. Since human's digestive system is very similar the pressure regulator in the system was set to maintain the internal pressure as low as reasonably practicable, at 1 psi above the atmospheric pressure. This ensured the simulation of the colon environment in the headspace in terms of pressure while enabling a stable functionality of the *in-vitro* fermentation system and steady reading of the sensors that are intrinsically sensitive to pressure variations.

While forming an anaerobic environment for mimicking the colon headspace, the incubator is purged with different mixtures of gases for 1 min to sufficiently fill up the whole headspace.

These headspace gases are made using only inert gases of Ar and N_2, or mixtures of these gases with different concentrations of H_2 and CO_2.

The correlations between the simulated gas environment and the colonic gas profiles were investigated from 1 h incubation of fecal slurry from one subject with 1g of FOS to understand the behavior of the colon microbiota. Although all experiments were continued for 4 h, the pH fell after the first hour and the incubation environment was no longer similar to the human colon after this duration. The repeatability of the measurements was assessed by repeating the studies using feces from three different volunteers.

2.4 Results and Discussions

2.4.1 Effect of headspace gas mixtures:

Two sets of experiments were conducted. In the first set, the effect of the head space gas mixtures on the *in-vitro* gas production was explored. Three gas mixtures explored were as follows: (type 1) 100% inert gas; (type 2) 6.5% CO_2 balanced with inert gas and (type 3) 5.5% CO_2, 5% H_2 balanced with inert gas. These mixtures were chosen based on the actual typical measurements of the headspace gases in the human gut according to Table 1.1. The gas profiles for these *in-vitro* fermentation experiments are shown in Figure 2.3. The changes of the rates (kinetics) of gas production are presented in Figure 2.4. As expected, the addition of 1 g FOS to the fecal samples excites the microbiota to induce H_2, CO_2, CH_4 and H_2S gas production.

The free energy of the chemical equations for producing CH_4 and H_2S pathways are used in some of the discussions and extracted from the past literature [42,43]. For CH_4, the major production pathway is to convert 4 mol H_2 and 1 mol CO_2 to 1 mol CH_4 with a free energy of -130 kJ/mol *via*:

$$4H_2 + CO_2 \rightarrow CH_4 + 2H_2O \quad (2.4)$$

The production pathway of H_2S is more thermodynamically favourable. As reported, 4 mol of H_2 is consumed to produce 1 mol of H_2S with a free energy of -152.2 kJ/mol in the presence of sulfur sources as:

$$4H_2 + SO_4^{2-} + H^+ \rightarrow HS^- + 4H_2O \quad (2.5)$$

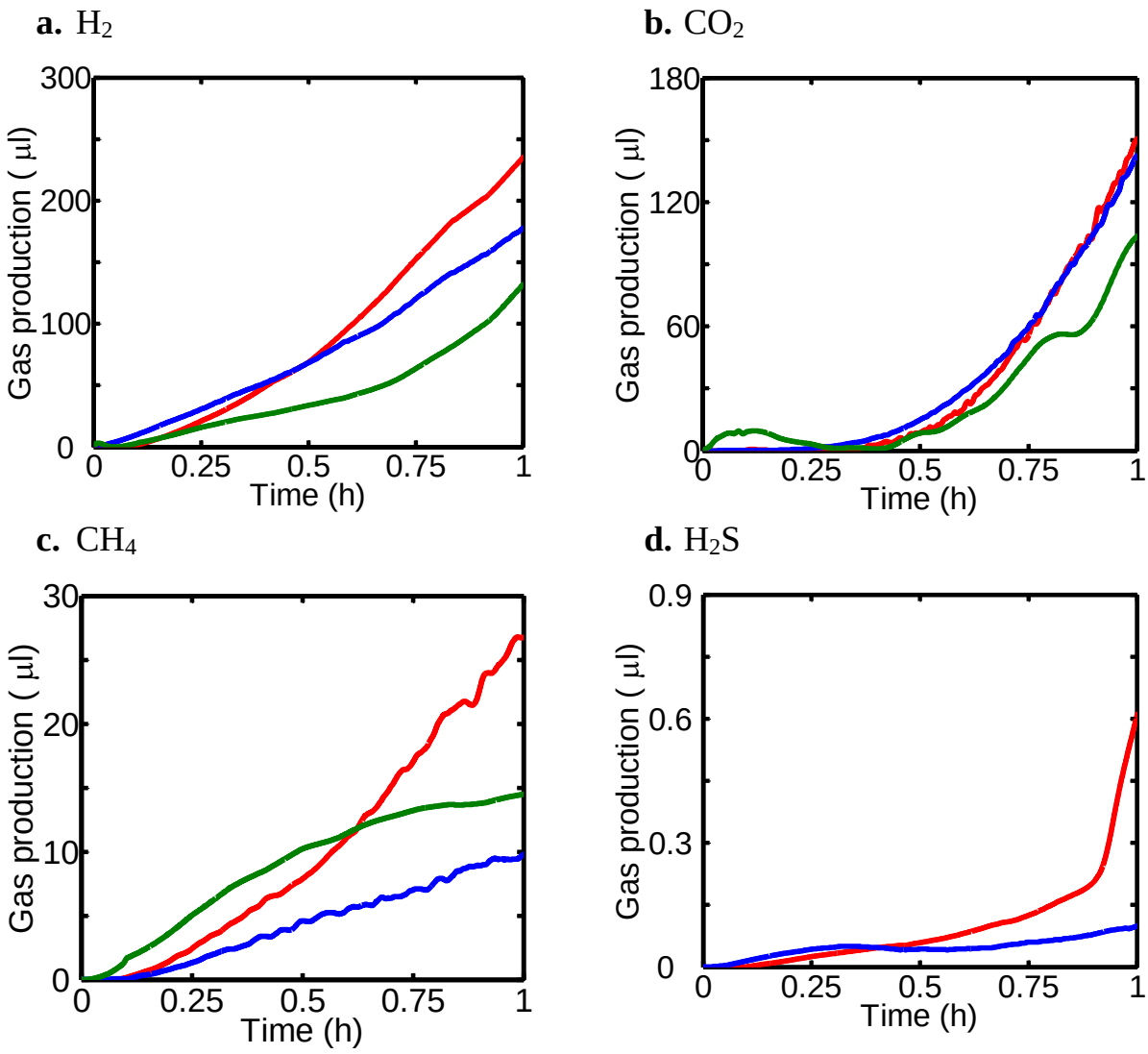

Figure 2.3. *In-vitro* colonic gas production of fecal fermentation with FOS substrate in different anaerobic environments (blue line: type 1 condition with 100% inert gas; red line: type 2 condition with 6.5% CO_2 balanced with inert gas; green line: type 3 condition with 5.5% CO_2 and 5% H_2 balanced with inert gas): (a) H_2, (b) CO_2, (c) CH_4, (d) H_2S.

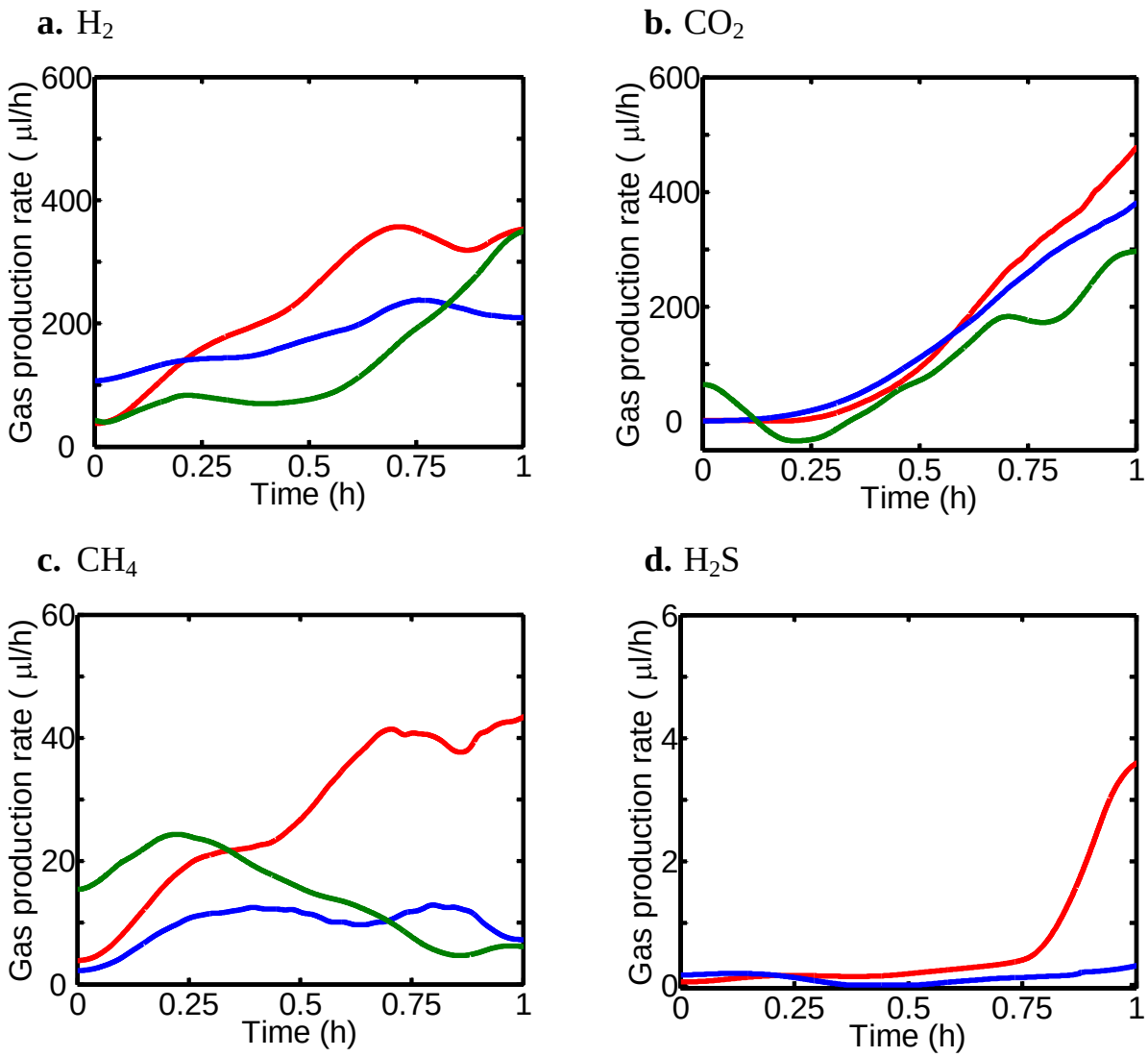

Figure 2.4. *In-vitro* colonic gas production kinetics of fecal fermentation with FOS substrate in different anaerobic environments (blue line: type 1 condition with 100% inert gas; red line: type 2 condition with 6.5% CO_2 balanced with inert gas; green line: type 3 condition with 5.5% CO_2 and 5% H_2 balanced with inert gas): (a) H_2, (b) CO_2, (c) CH_4, (d) H_2S.

H_2 gas profiles: As shown in Figure 2.3a, the alteration of the headspace environment greatly influenced the pattern of H_2 gas production. While the production occurs almost instantly at the beginning of fermentation in the type 1 condition (only N_2 headspace), there are ~ 0.1 h delays in the production events for both types 2 and 3 conditions (when either only CO_2 or

when CO_2 and H_2 together exist in the headspace), indicating that, in a CO_2 rich environment, the produced H_2 gas is quickly consumed by other metabolic pathways instead of being released into the headspace [163]. Furthermore, the production level with the type 1 mixture is slightly greater than other incubation gas environments during the first 0.5 h of fermentation, possibly indicating that the metabolically produced H_2 is not being consumed significantly for that period [163]. However, while the gas production rate in type 1 conditions remains relatively constant, the type 2 condition (only CO_2 added) leads to rapid increases of the kinetics for between 0.2 and 0.7 h of the fermentation processes, which results in greater production than that of type 1 condition after the 0.5 h mark (Figure 2.4a). The production level for type 3 (both H_2 and CO_2 in the headspace) was the smallest compared with the other headspace gas types at the beginning and the rate remained almost constant in the first 0.5 h. However interestingly, there was a marked increase in the rate of H_2 gas production in the second half of the fermentation process in type 3 conditions, indicating that the consumption of metabolic H_2 had not been reduced (Figure 2.3a and Figure 2.4a).

CO_2 gas profiles: In comparison to H_2 patterns, completely different profiles were observed for the CO_2 gas production (Figure 2.3b). At the beginning of the fermentation (for up to 0.4 h), low production levels are seen for all headspace types, reflecting that the produced CO_2 is rapidly consumed by a variety of metabolic pathways (such as producing short-chain fatty acids) [164,165], regardless of the simulated colon gas environment. After 0.4 h, the rates of production of CO_2 gas levels increased in all conditions. At this point, both the production rates of types 1 and 2 headspaces were larger than that of type 3 in which H_2 was present (Figure 2.4b). The changes were linked to the CH_4 productions presented below.

CH_4 gas profiles: As shown in Figure 2.3c, a delay in the CH_4 production was the shortest for type 3 condition (presence of H_2), while it is the longest in the complete inert gas

environment (type 1). Such production characteristics can be linked to the delay in the production of H_2 (Figure 2.3a), in which an opposite trend is observed (shortest for type 1 and longest for type 3). This implies that a significant amount of the initially produced H_2 gas is fed in the metabolic activity of methanogens that are also regulated by the type of gas in the environment. The rate of CH_4 production for the type 3 conditions started to decrease after 0.3 h and reached a plateau at 0.85 h (Figure 2.4c), possibly indicating apoptosis of certain methanogens after reaching the saturation of their growth. On the other hand, the CH_4 production rate of the type 1 condition is relatively constant but at a smaller magnitude for the duration of the fermentation, suggesting that the complete inert gas environment does not promote the growth of methanogens (Figure 2.4c). Although it starts with a relatively small level, the type 2 gas environment (that includes CO_2 but not H_2) leads to a rapid increase in the CH_4 production level from 0.2 h as shown in Figure 2.4c, which eventually results in the highest level of production at the end of the fermentation procedure compared to other 2 incubation conditions.

H_2S gas profiles: The type 3 condition was not able to be applied for H_2S as the response of H_2S electrochemical sensor is saturated in the presence of a high concentration of H_2. The patterns for H_2S gas production in types 1 and 2 conditions are presented in Figure 2.3d. A small H_2S production was observed in the first 0.5 h of fermentation period for both headspace type gases, while there were sudden increases in the production kinetics for type 1 and 2 conditions at 0.6 and 0.5 h, respectively, suggesting the elevation of the metabolic activities of SRB after these durations (Figure 2.4d). The initial introduction of FOS does not instantly boost H_2S production. Additionally, the level of H_2S production is always more than one order of magnitude smaller than that of CH_4. These observations suggest that the produced H_2 gas is more favorably fed into the CH_4 production rather than H_2S. This can be

possibly due to the relatively smaller number of SRB than methanogens presented in the colonic samples and their different activation time-frames during the fermentation process.

NOx gas profiles: As expected from the past literature [75,77], colonic fecal samples of healthy human subjects did not produce detectable NO*x* (Figure 2.5) and NO*x* is only seen when nitrogen containing substrates are added or samples belong to subjects with disorders [7, 8].

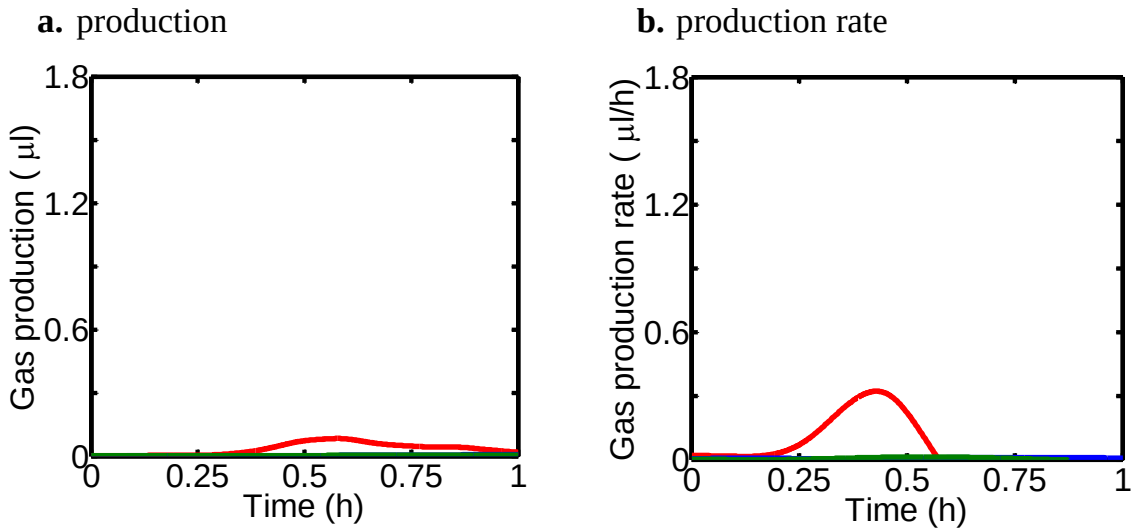

Figure 2.5. (a) NO*x* gas production profile and (b) its production rate of fecal fermentation with FOS substrate in different anaerobic environments (blue line: type 1 condition with 100% inert gas; red line: type 2 condition with 6.5% CO_2 balanced with inert gas; green line: type 3 condition with 5.5% CO_2 and 5% H_2 balanced with inert gas).

2.4.2 Comparison of blank samples vs samples with added fibre:

The author subsequently conducted a series of pilot tests on the measurement capabilities of the *in-vitro* gas system. The aim was to verify that the *in-vitro* gas system was able to detect differences in gas production from a highly fermentable substrate and assess whether a large

amount of gas could exceed the detection limits of the system. The use of type 2 mixture of 6.5% CO_2 balanced with inert gas was used as the headspace gas as per previous experiments produced the largest gas concentrations for all gases. As shown in Figure 2.6 and Figure 2.7, significant amounts of H_2, CO_2 and CH_4 gas production were detectable in comparison to those with the blank inoculum. The absence of FOS, total bacterial fermentative activity slowed down and the overall gas production decreased (Figure 2.7a-c), while, in presence of FOS, the total production remained relatively high.

Production of H_2 and CH_4: H_2 production when FOS was added was higher than in the blank after 0.25 h (Figure 2.6a). According to the gas production pathways presented in

Figure **1.1**, it is likely that, immediately after the FOS is added, most of H_2 is consumed to produce CH_4. As described in the introduction, such an observation may be of relevance to the altering the dietary intake of FOS in the management of constipation or diarrhea since CH_4 slows colonic motility and is linked to constipation [13].

CO_2 production: As shown in Figure 2.6b, CO_2 was initially produced at a similar rate for the blank sample, but then production rate of blank remained low as almost all of the produced CO_2 was rapidly consumed after 0.25 h, presumably eventually being transformed to acetate and amino acids [164].

H_2S production: The H_2S profiles are shown in Figure 2.6d and Figure 2.7d in comparison to the blank sample which showed a steady increase in H_2S, the system appeared to detect lower levels of H_2S produced from fermentation of FOS. There was a rapid increase in the production of the H_2S in the presence of FOS after 0.9 h. It seems that at this point a rapid colonization of the SRB occurs. This ability of reducing H_2S production by incorporating FOS in the diet suggests that FOS may influence the pathogenesis and/or clinical course of

IBD and colon cancer due to the close clinical association between these gastrointestinal diseases and the colonic H_2S level [166].

NOx production: similar to the previous section and as expected from the past literature [75,77], colonic fecal samples of healthy human subjects did not produce detectable NO*x*.

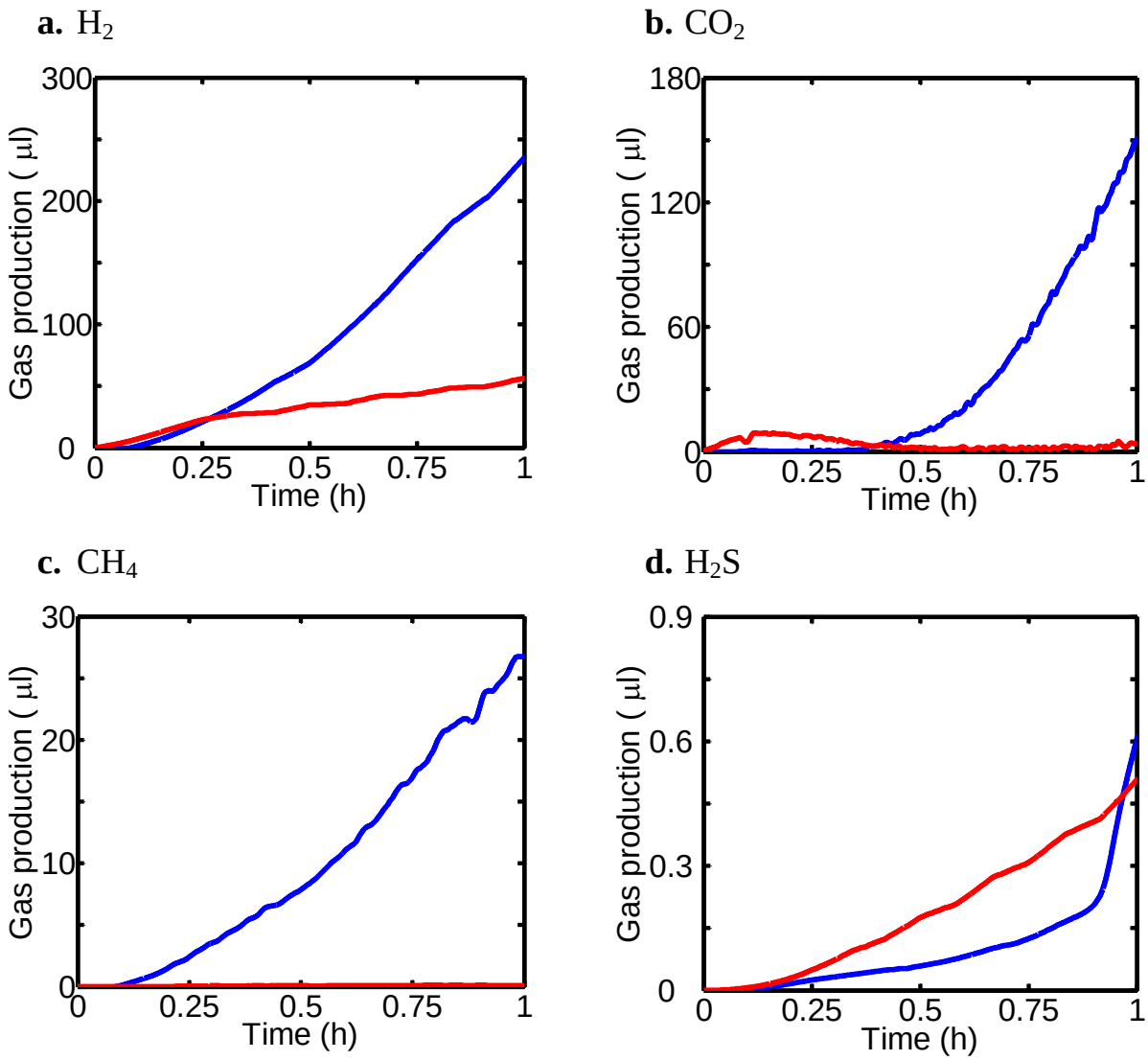

Figure 2.6. *In-vitro* colonic gas production of fecal fermentation using type 1 anaerobic environment (100% inert gas) with and without the FOS substrate. Value are mean (n = 3) ± SE. (blue line: FOS, red line: BLANK): (a) H_2, (b) CO_2, (c) CH_4, (d) H_2S.

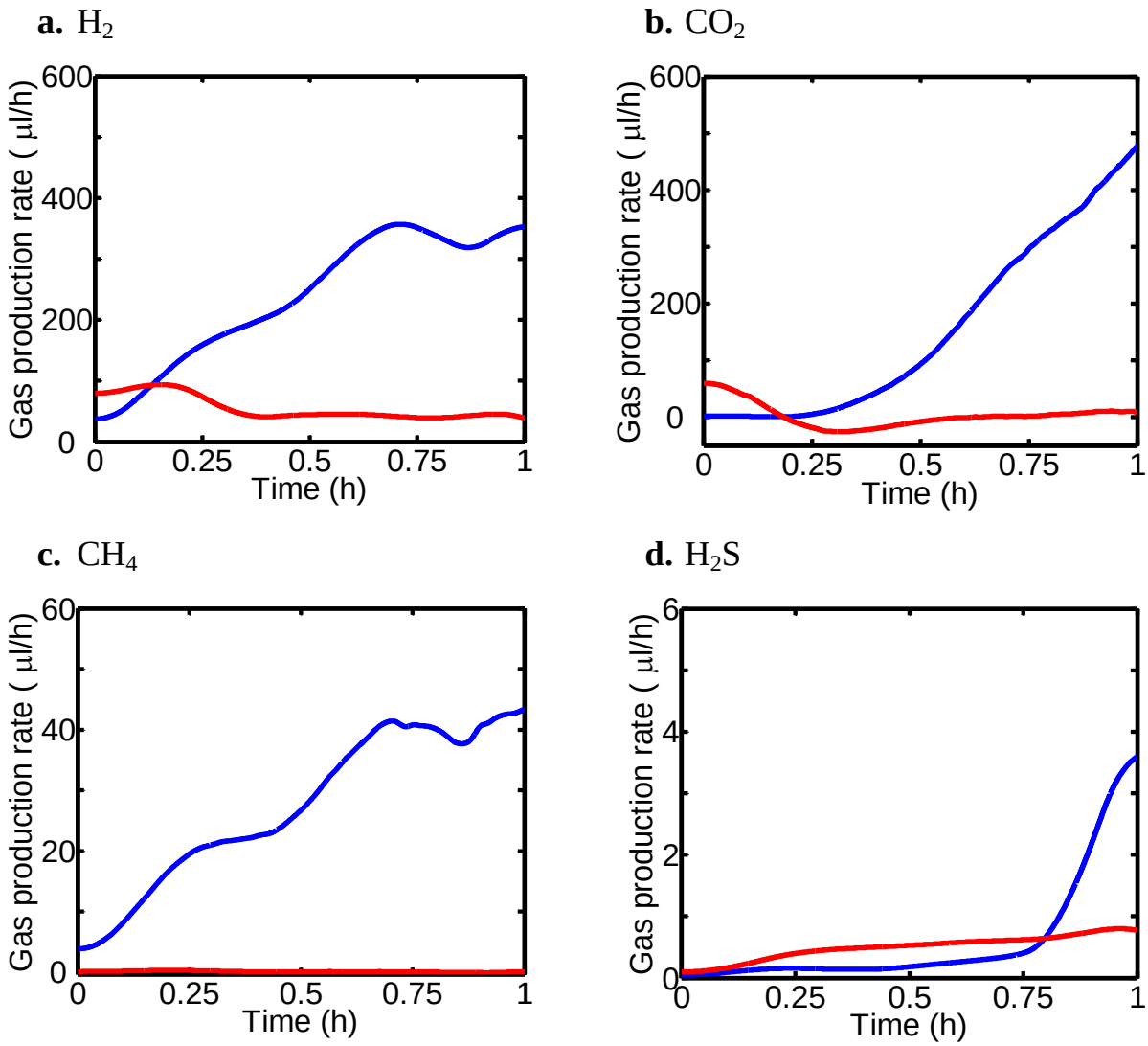

Figure 2.7. *In-vitro* colonic gas production kinetics of fecal fermentation using type 2 anaerobic environment (6.5% CO_2 balanced with inert gas) with and without the FOS substrate (blue line: BLANK, red line: FOS): (a) H_2, (b) CO_2, (c) CH_4, (d) H_2S.

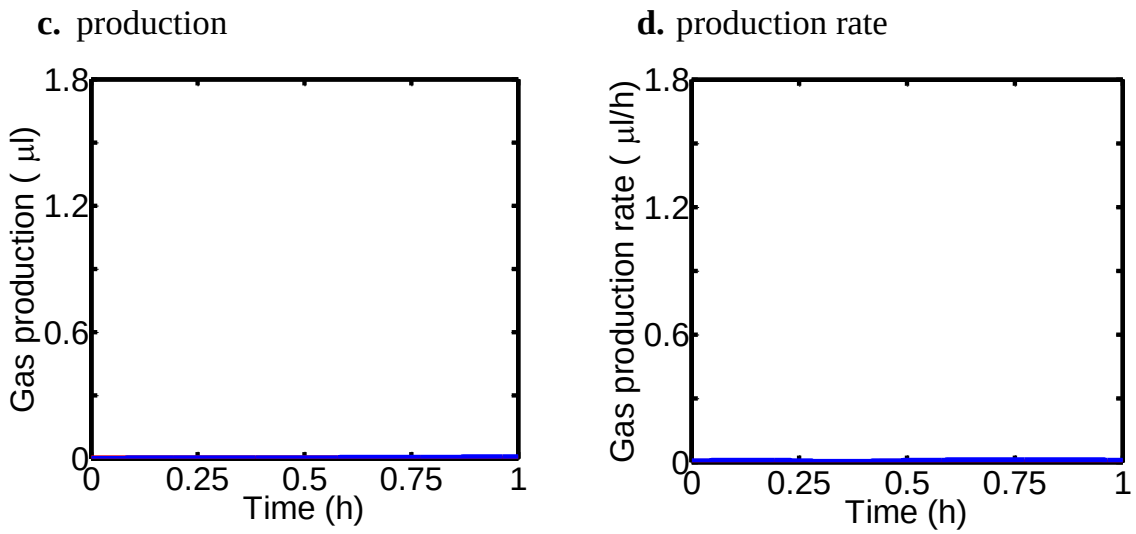

Figure 2.8. (a) NO*x* gas production profile and (d) its production rate of fecal fermentation in type 2 anaerobic environment (6.5% CO_2 balanced with inert gas) with and without the FOS substrate (blue line: blank, red line: FOS).

2.4.3 Reproducibility and repeatability investigations:

The author also conducted investigations on the reproducibility of results and repeatability of the *in-vitro* gas system using fecal samples from three different volunteers. The samples were incubated with and without the FOS substrate in the conditions similar to those presented in Section 2.4.1 and 2.4.2. 100% inert gas environment was selected as the headspace incubation gas. According to Table 2.2 and Table 2.3, all three replicate runs exhibited different gas production behavior with the FOS substrate compared to those without any substrate, in which the addition of FOS resulted in significant increases of H_2, CO_2 and CH_4, but does not favor H_2S production. These outcomes are in good agreement with those presented in Section 2.4.2. In addition, although some noticeable variations on the fecal gas production volumes are observed amongst the three samples especially after 0.5 h incubation (Table 2.2), the trends of their gas production patterns and kinetics (Table 2.3) are comparable. This indicates acceptable reproducibility of the results and repeatability of the *in-vitro* gas system.

Table 2.2. *In-vitro* colonic gas production of fecal samples fermentation in type 1 anaerobic environment (100% inert gas) from three different human fecal samples with the FOS substrate and without (blank). The presented values are the mean (n = 3) ± standard error

Time (h)	**H_2 (µl)**		**CO_2 (µl)**		**CH_4 (µl)**		**H_2S (µl)**	
	Blank	FOS	Blank	FOS	Blank	FOS	Blank	FOS
0.25	29.5±2.0	36.6±1.8	0.1±0.2	0.8±0.8	1.2±1.6	5.6±1.5	0.1±0.03	0.1±0.002
0.5	45.5±3.6	67.3±3.7	3.7±4.0	6.7±3.9	0.8±0.6	12.3±1.0	0.4±0.1	0.2±0.03
0.75	45.8±6.7	103.3±4.0	7.3±7.5	33.4±9.2	0.6±0.7	22.3±5.0	0.7±0.1	0.3±0.03
1	60.0±3.7	163.5±22.7	12.1±10.1	95.7±7.3	0.7±0.7	35.1±10.6	1.1±0.2	0.4±0.1

Table 2.3. *In-vitro* colonic gas production kinetics fecal samples fermentation in type 1 anaerobic environment (100% inert gas) from three different human fecal samples with the FOS substrate and without (blank). The presented values are the mean (n = 3) ± standard error.

Time (h)	**H_2 (µl/h)**		**CO_2 (µl/h)**		**CH_4 (µl/h)**		**H_2S (µl/h)**	
	Blank	FOS	Blank	FOS	Blank	FOS	Blank	FOS
0.25	78.1±3.5	124.5±7.9	9.4±10.2	14.1±9.0	11.3±2.0	26.8±2.6	0.9±0.3	0.5±0.1
0.5	20.4±21.5	128.7±13.8	15.0±15.6	74.4±20.4	6.3±5.7	34.3±15.5	1.0±0.3	0.5±0.01
0.75	38.7±4.6	219.8±68.0	17.2±12.6	196.9±25.7	9.4±1.6	49.0±25.4	1.5±0.1	0.2±0.2
1	27.3±10.9	218.5±63.3	38.9±43.5	416.0±140.1	9.4±0.4	56.5±35.9	1.3±0.3	0.6±1.0

2.5 Conclusions

The author successfully developed an *in-vitro* fecal-fermentation gas-measurement system for continuous profiling of the colonic gases of H_2, CH_4, CO_2 and H_2S in real-time. The pressure in the incubation chamber was regulated to eliminate possible interference from its fluctuations. The performance of the system was evaluated using the healthy human fecal samples incubated with and without a type of highly-fermentable fiber as a representative added substrate. The effect of different gas mixtures for the headspace was investigated and the ideal mixture defined. Good repeatability of the *in-vitro* gas sensing system and acceptable reproducibility of the gas production profiles were also demonstrated using human fecal samples collected from different volunteers.

The author demonstrated that the type and concentration of the colonic gases could be accurately measured using low-cost, portable gas-sensor technologies and colonic gas

production patterns and kinetics could be defined, providing unique and valuable insight in the intestinal gas production pathways and bacterial metabolic activities of the human colonic microbiota. These advantageous features of the system make it a unique tool in comparison to conventional off-line, expensive and bulky *in-vitro* fermentation systems currently available for research and commercial assessments. Given that intestinal gas may be used as unique biomarkers for many gut disorders, this accurate, real-time, cost-effective and portable system deserves further study to determine its place as a medical tool that might have roles in diagnostics, and in assessing the effects of diet and therapeutic agents on the gut microbiota.

Chapter 3. GAS PROFILING CALCULATION

3.1 Introduction

In the previous chapter the author introduced the technology of gas sensing in quasi-closed, pressure regulated and anaerobic fermentation systems while focusing on incubated human fecal samples. In order to process the signals produced by the developed system, the author used basic calculations that contain inaccuracies and potentially can cause errors in the estimated GPP (section 2.2.2). To mitigate the inadequacies presented in Chapter 1, the objectives of this chapter are to introduce a novel gas production mathematical model together with comprehensive mass flow equations. This model allows for the calculation of GPPs based on measuring the output signals from common closed incubation systems or systems with automated pressure regulation. The model is parametric, versatile and includes the incubation chamber physical configurations and measured data. Moreover, it consequently revealed the fermentation profile of the incubated sample in high detail. Last, the validity and significance of the approach was assessed using an *in-vitro* lab experiment.

The content of this chapter was published as a fully reviewed paper in Sensors and Actuators B journal [167].

3.2 Materials and Methods

3.2.1 Representation of the fermentation system with embedded sensors

A sealed incubation vessel equipped with pressure and temperature sensors, outlet automatic regulation valve and an array of gas sensors is described in schematic representation in Figure 3.1.

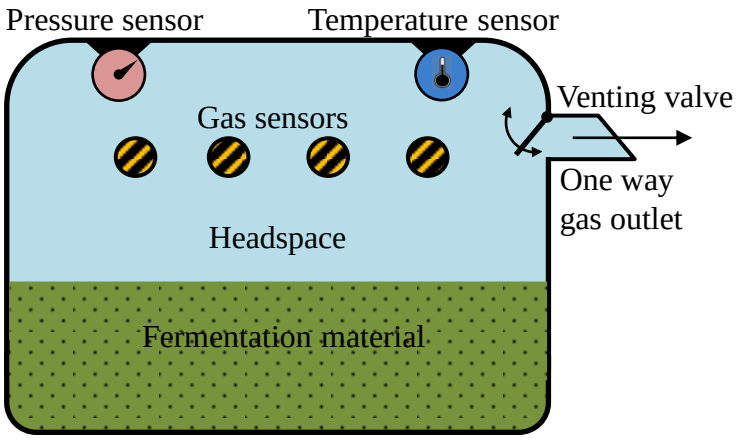

Figure 3.1. The schematic representation of a closed and pressure regulated fermentation system

Headspace gas environment is preliminary consist of the gas mixture flushed into the headspace. However, this flushed into headspace gas is gradually replaced with the gas produced by the fermentation material. During the process, the headspace internal pressure (P_i [psi]) and temperature (T_i [K]) are recorded at equally spaced (Δ_t [h]) time points ($t_i = i\Delta_t$ [h]) for $i = 0,1,2,\dots,n$. Throughout the incubation, fermentation gas is being accumulated in the headspace which increases the headspace pressure P_i. The headspace is vented when P_i reaches a certain pressure threshold (P_{th} [psi]) in which the outlet valve is opened for a very short time of τ_v. During this venting event P_i drops and the excess gas is released as demonstrated in the example in Figure 3.2. This short venting window is much smaller than the sampling interval ($\tau_v \ll \Delta_t$) as seen in a venting event close-up presented in Figure 3.2b. For the system to operate with minimal error, the pressure control mechanism should apply a high monitoring rate in order to screen the headspace pressure and to measure the pressure difference right before and right after the venting event (Figure 3.2b). This pressure difference is added to P_i to create another parameter, which is called cumulative pressure (CP_i [psi]) as seen in Figure 3.2a. Evidently, the sampling rate for CP_i is the same as P_i. CP_i represents the sum of all incremental pressure changes in the headspace that can be

employed for calculating the amount of gas released during the venting events as will be explained in section 3.2.3. The internal pressure monitoring rate ($1/\tau_v$), in most cases, should be much higher than the gas dynamics in the headspace ($1/\Delta_t$). It should be considered that this monitoring rate is practically not useful for GPP calculations. In general, for the majority of fermentation systems, gas concentrations are not changed rapidly. Sampling gases at the relatively high monitoring rates of internal pressure only create an excess number of samples which, for common incubation durations ranging between few hours and few weeks, overloads the signal processing units.

At the beginning of the fermentation, both internal pressure and cumulative pressure increase identically until the first venting event takes place (Figure 3.2a). When a venting event takes place, P_i decreases, while obviously the CP_i keeps increasing. As such, CP_i by definition accounts for the pressure drops that occur as the result of the venting events that may take place within the *i*th interval (t_{i-1}, t_i) as seen in Figure 3.2b.

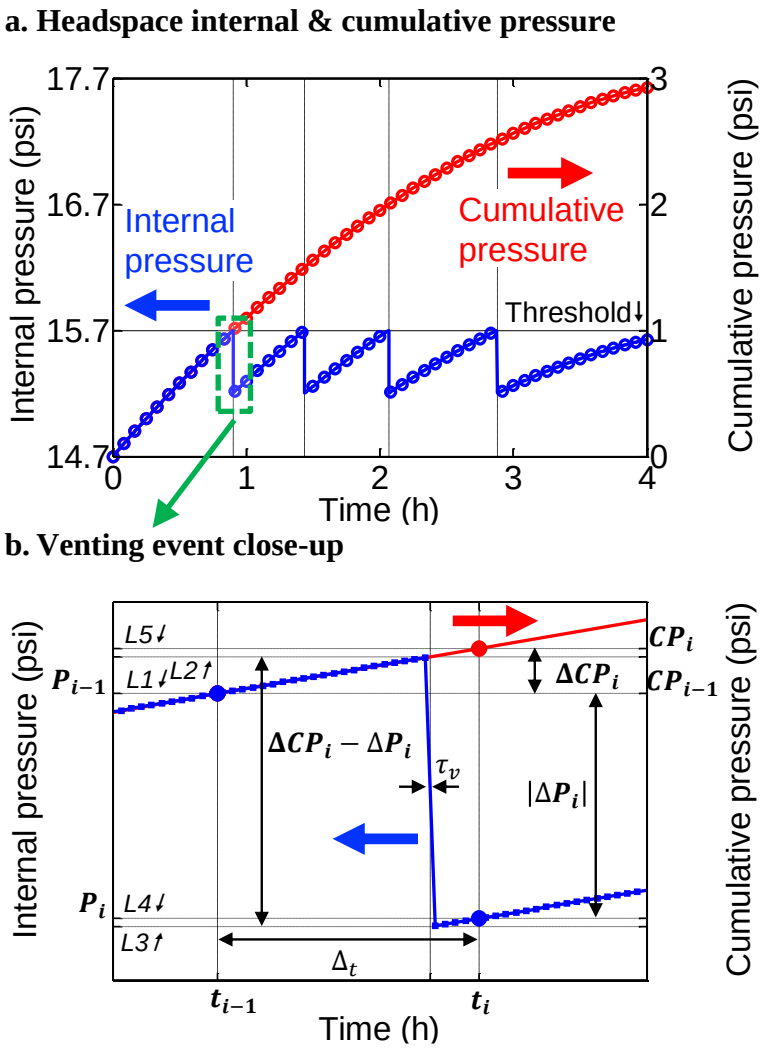

Figure 3.2. Example of the headspace internal pressure (P_i) and cumulative pressure (CP_i) vs time during incubation in a closed vessel with ─ internal pressure ● internal pressure samples ● cumulative pressure samples (**a**) internal pressure and cumulative pressure for a 4 h duration example. The internal pressure value in this example starts at the atmospheric pressure of 14.7 [psi] (**b**) ith interval venting event close-up (shown by the dotted box in (a)). The monitoring intervals of the venting system is shown by ▪ (observed every τ_v) which is conducted at a much shorter interval than the actual sampling interval (Δ_t). L1: P_i and CP_i at t_{i-1}, L2: P_i right before the venting event, L3: P_i right after the venting event, L4: P_i at t_i, L5: CP_i at t_i.

Before introducing the GPP incubation model some definitions, formulations and adjustments of the different signals are presented in the following sections.

3.2.2 Gas production calculation

Fermentation gas production Δn_i [mmol] during the *i*th interval is calculated using the headspace pressure increment value during the *i*th interval which is obtained as $\Delta CP_i = CP_i - CP_{i-1}$. Not affected from venting events, ΔCP_i is proportional to Δn_i according to the *ideal gas law* and *Avogadro's law* [157]

$$\Delta n_i = \frac{V_h}{RT_i} \Delta CP_i \text{ [mmol]} \tag{3.1}$$

where T_i is the headspace average temperature during the *i*th interval in Kelvin as mentioned before; V_h is the head-space volume in mL and R is the gas constant that is equal to 1.205912 [L·psi·K^{-1}·mol^{-1}]. According to *Avogadro's law*, under a defined standard temperature and pressure conditions (STP) of atmospheric pressure P_{atm} = 14.7 [psi] and T_0=273.15 [K], one mole of gas occupies $\frac{RT_0}{P_{atm}} = 22.41$ [L] which allows the direct conversion of a pressure increment to a volume of produced gas as expressed in the form of the following conversion factor γ_i:

$$\gamma_i = \underbrace{\frac{RT_0}{P_{atm}}}_{22.41\ L} \cdot \frac{V_h}{RT_i} \left[\frac{\text{mL}}{\text{psi}}\right] \tag{3.2}$$

According to this, the incremental volume of gas ΔV_i [mL] (at STP) produced during the *i*th interval can be calculated as:

$$\Delta V_i = \gamma_i \cdot \Delta CP_i \text{ [mL]} \tag{3.3}$$

Observation of the different fermentation events and their originating biological processes are carried out examining the cumulative volume of fermentation gas produced. The total cumulative gas production ($TCGP_{\mathrm{i}}$ [mL]), defined as the total amount of gas produced at the end of the *i*th interval, is given by the following equation:

$$TCGP_{\mathrm{i}} = \sum_{j=1}^{i} \Delta V_j \quad [\mathrm{mL}] \tag{3.4}$$

3.2.3 Venting events

Venting events take place independent of the gas sampling events. Recording both P_i and CP_i enable the calculation of the amount of gas released in every venting event according to:

$$V_F^i = \gamma_i(\Delta CP_i - \Delta P_i) \quad [\mathrm{mL}] \tag{3.5}$$

Here $\Delta P_i = P_i - P_{i-1}$ is the headspace internal pressure variation for the *i*th interval (Figure 3.2b) and V_F^i represents the volume of gas vented out in the venting event or events that take place during the *i*th interval. Without pressure regulation, no venting event takes place ($V_F^i = 0$), the internal pressure would increase at the same rate as the cumulative pressure. When a venting event or events take place within the *i*th interval (Figure 3.2b), the difference between ΔCP_i and ΔP_i is proportional to the amount of gas released from the headspace (V_F^i [mL]) according to equation (3.5).

3.2.4 Effective headspace volume

During the incubation, the headspace can be kept at a desired temperature. The internal pressure increases as gas is produced and in order to calculate the headspace gas constituents, the following equivalent headspace volume is defined:

$$V_e^i = \frac{T_0}{T_i} V_h + \gamma_i \cdot (P_i - P_{atm}) = \frac{T_0}{T_i} \frac{P_i}{P_{atm}} V_h \text{ [mL]} \quad (3.6)$$

Here V_e^i is a mathematically defined headspace volume appearing as an equivalent volume at the STP condition, which is extracted from the actual headspace volume (V_h). This parameter is introduced in order to simplify future calculations of gas mixing ratios.

3.2.5 Gas analysis

Gas analysis is implemented using a low-cost and portable array of gas sensors specially chosen to record the gas components in the headspace as presented in Chapter 2 [132]. The sensors are pre-calibrated with known concentrations of target gases and in specific temperature (T_{cal} [K]) and pressure conditions (P_{cal} [psi]).

Headspace gases mixing ratio is represented by $C_i = (C_i^1, C_i^2, \dots, C_i^K)$, comprised of *K* different gas species, is continuously sensed during the incubation and recorded at t_i by an array of gas sensors, for which the values of the sensor outputs at t_i are presented by $S_i = (S_i^1, S_i^2, \dots, S_i^K)$. As headspace conditions can vary during the incubation process, two correction factors are introduced in order to accurately interpret gas sensor signals:

Pressure: According to the *ideal gas law*, and assuming that pressure differences are within ±10% of calibration pressure point, a first order approximation that impacts pressure sensor reading variation is given by the following pressure compensation factor (PCF_i):

$$PCF_i = \frac{P_i}{P_{cal}} \quad (3.7)$$

***Temperature*:** According to *Charles's law*, gas molecules tend to expand proportionally to the gas temperature, *i.e.* a fixed volume contains less gas molecules as temperature increases and as a result the reading of the gas sensors is reduced relative to the reading with the same

conditions at a lower temperature. This effect of temperature is accounted for by the following correction factor (TCF_i):

$$TCF_i = \frac{T_{cal}}{T_i} \tag{3.8}$$

Applying these factors establishes a relationship between the *k*th gas sensor reading ($S_i^k, k = 1,2, \dots, K$) and the headspace's *k*th gas concentration (C_i^k) :

$$S_i^k = C_i^k \times PCF_i \times TCF_i \tag{3.9}$$

$$C_i^k = S_i^k \times \frac{T_i}{T_{cal}} \times \frac{P_{cal}}{P_i} \tag{3.10}$$

3.2.6 Solubility adjustment

Part of the fermentation gas may dissolve in the liquid slurry of volume V_s where it is held during the incubation and not detected by the pressure sensor. Accordingly, the GPP is corrected by adding the dissolved amount of gas to the volume of the *k*th gas type ($k = 1,2, \dots, K$) according to *Henry's law* as follows:

$$DG_i^k = (P_i C_i^k - P_{atm} C_0^k) V_s H_{cp}^k \text{ [mL]} \tag{3.11}$$

where (H_{cp}^k [psi^{-1}]) is the solubility constant of the *k*th gas specie ($k = 1,2, \dots, K$).

3.2.7 Formulations and definitions

- $\tilde{C}_{\mathrm{i}} = \left(\tilde{C}_i^1, \tilde{C}_i^2, \ldots, \tilde{C}_i^K\right)$ represents the gas composition array of ΔV_i at the *i*th interval comprised of *K* different gas species sensed during the incubation.
- $C_F^i = \left(C_F^{i,1}, C_F^{i,2}, \ldots, C_F^{i,K}\right)$ is the vented volume composition array and headspace mixing ratio array at venting event at time t_F comprised of *K* different gas species sensed during the incubation.
- $CGP_i = (CGP_i^1, CGP_i^2, \ldots, CGP_i^K)$ is the cumulative gas production array after the end of the *i*th interval comprised of *K* different gas species for their cumulative gas productions.
- $DG_i = (DG_i^1, DG_i^2, \ldots, DG_i^K)$ is the dissolved gas array at the *i*th interval comprised of *K* different gas species which are sensed during the incubation.

3.2.8 GPP incubation model

An amount of fermentation gas (ΔV_i) at a composition of $\tilde{C}_{\mathrm{i}}$ is released from the liquid during the *i*th interval into the headspace. It is assumed that the headspace gas environment is well circulated in the current model and that the fermentation gas mixes rapidly and completely with the existing gas environment. Since the rates of fermentation and subsequent release to the headspace are much lower than the sampling rate, one can assume that $\tilde{C}_{\mathrm{i}}$ remains relatively constant during the *i*th interval.

During this interval, at time t_F^i ($t_{i-1} \leq t_F^i \leq t_i$), and after an amount of gas of volume Δ_i' (mL) had already been produced ($0 \leq \Delta_i' \leq \Delta V_i$), an amount of gas of volume V_F^i and of composition C_F^i is released from the headspace outlet during a short venting event. The parameters are shown in Figure 3.3.

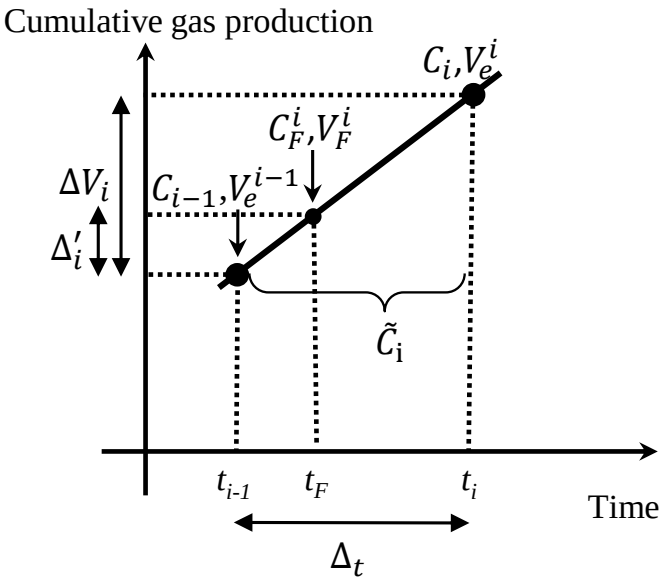

Figure 3.3. A demonstration of cumulative gas production vs time - single interval description of gas produced in a closed vessel including a venting event at time t_F.

As a result, the headspace gas environment at time t_i differs from the one at time t_{i-1} after adding the fermentation/released gas and discarding the vented gas, as demonstrated by the schematic in Figure 3.4.

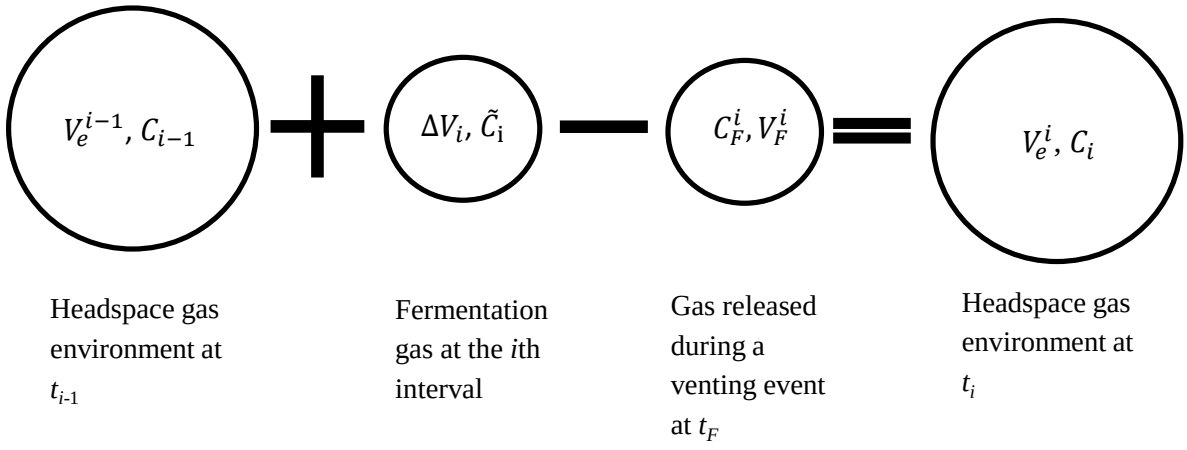

Figure 3.4. Fermentation and released gas impact on headspace gas environment at the end of the *i*th interval.

In order to calculate C_F^i, the *i*th interval is dissected into two parts: just before the venting event (Figure 3.5) and straight after the venting event (Figure 3.6).

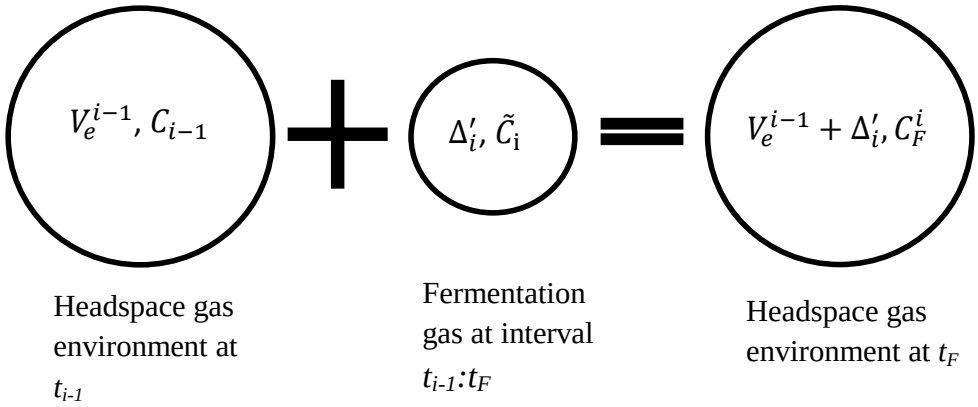

Figure 3.5. Fermentation and released gas impact on headspace gas environment just before the venting event.

$$C_F^i = \frac{V_e^{i-1} \times C_{i-1} + \Delta_i' \times \tilde{C}_\mathrm{i}}{V_e^{i-1} + \Delta_i'} \tag{3.12}$$

Immediately after the venting event, headspace gas environment mixing ratio does not change but contains less gas molecules, hence the calculation of C_i according to the schematic presented in Figure 3.6.

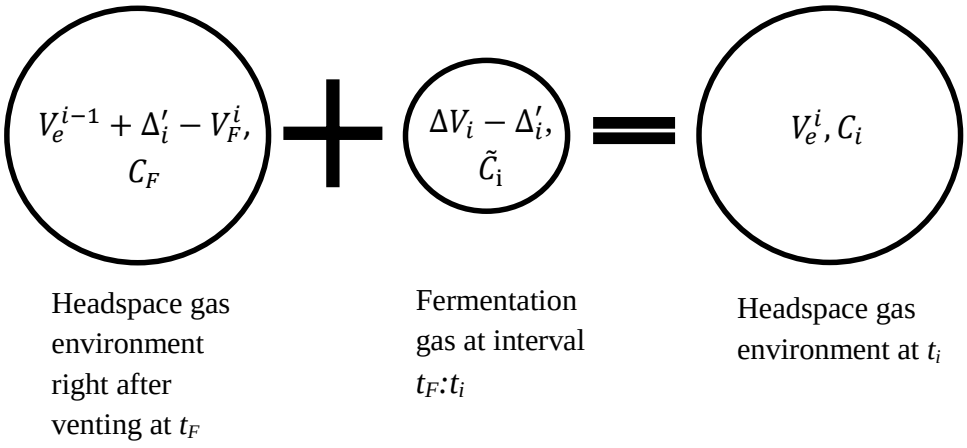

Figure 3.6. Fermentation and released gas impact on headspace gas environment just after the venting event.

$$C_i = \frac{\left(V_e^{i-1} + \Delta_i' - V_F^i\right) \times C_F^i + (\Delta V_i - \Delta_i') \times \tilde{C}_\mathrm{i}}{V_e^i} \tag{3.13}$$

Finally, the fermentation gas produced and released at the *i*th interval and cumulative released gas are given by the following equations:

$$\Delta V_i \tilde{C}_\mathrm{i} = V_e^i C_i - V_e^{i-1} C_{i-1} + V_F^i C_F^i \quad [\mathrm{mL}] \tag{3.14}$$

$$CGP_i = V_e^i C_i + \sum_{j=1}^{i} V_F^j C_F^j \quad [\mathrm{mL}] \tag{3.15}$$

In reality C_F^i, Δ_i' and t_F aren't measured as the venting event takes place between the sampling points. When the venting event takes place immediately after the *i*th interval begins ($\Delta_i' \to 0$) we have $C_F^i \to C_{i-1}$ and when it takes place just before the end of the *i*th interval ($\Delta_i' \to \Delta V_i$) we have $C_F^i \to C_i$. While the gas produced during the *i*th interval is much smaller with respect to the headspace volume ($\Delta V_i \ll V_e^i$), headspace gas environment change is very small ($C_{i-1} \approx C_i$) and together with solubility correction, the following mass flow equation for gas production, in a closed and pressure regulated system, is introduced as:

$$CGP_i \cong V_e^i C_i + \sum_{j=1}^{i} V_F^j C_j + DG_i \quad \text{[mL]} \tag{3.16}$$

3.3 Results and Discussions

3.3.1 Demonstration of the new incubation model

The suggested comprehensive calculation of GPP is tested using an *in-vitro* system designed for incubating fecal matter to imitate the environment of the human colon (see below). As seen in Figure 3.7, the *in-vitro* system was comprised of three modules: (I) A glass bottle filled with fecal slurry. (II) An array of gas-sensors embedded into an acrylonitrile-butadiene-styrene (ABS) adaptor. The sensor array includes one electrochemical sensor for H_2S (SGX Sensortech); one non-dispersive infrared sensor for CO_2 and CH_4 (SGX Sensortech); and one thermal conductivity sensor for H_2 (SGX Sensortech). (III) An automated gas pressure regulator with pressure and temperature sensors, electronic control components, a venting valve and RF transceiver (ANKOM Technology) designed to record T_i, P_i and CP_i, while regulating the headspace pressure around P_{th}.

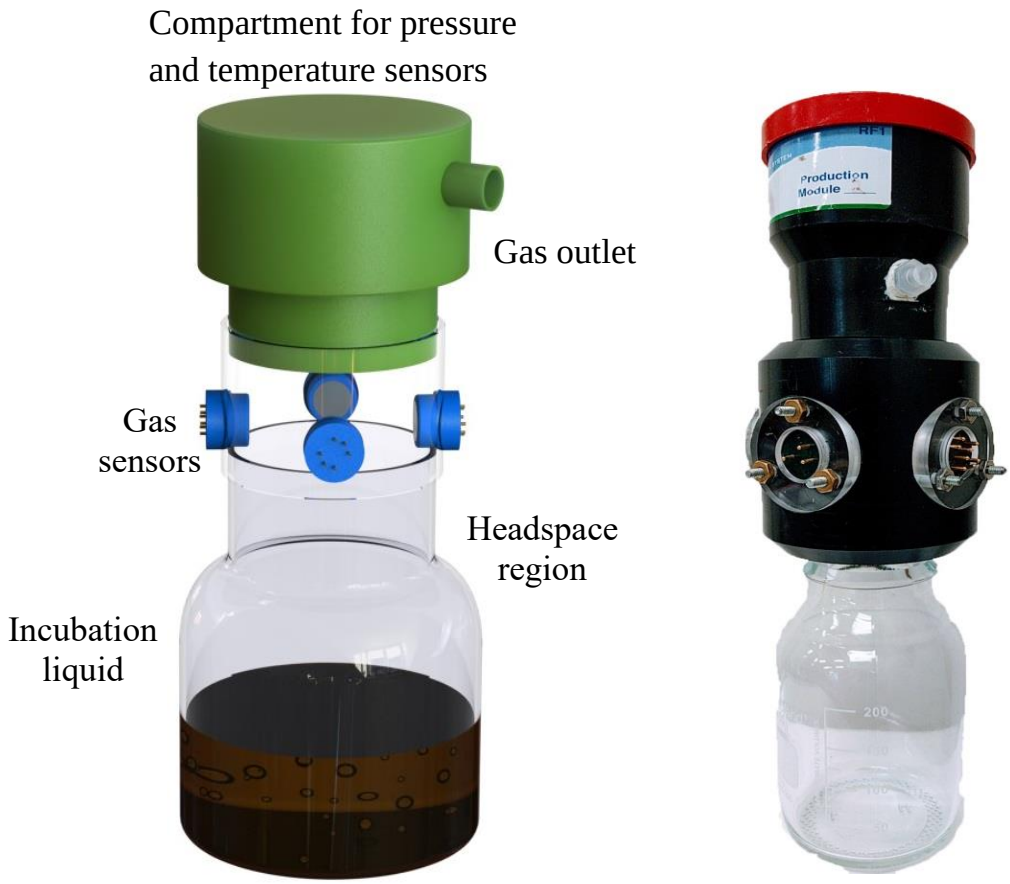

Figure 3.7. A 3D representation of the of the fecal matter fermentation in an *in-vitro* incubation system and a photo of the actual system.

A slurry containing human feces was used as the fermentation material, to produce the dissolved gases that were then released into the headspace. To mimic the colon environment, the system was placed in a 37°C water bath equipped with a shaker that applied 50 shakes per min [20]. Feces from a healthy human volunteer were used to provide the inoculum for fermentation. The incubation medium contained approximately 160 g feces/L and sodium phosphate buffer (pH 7) was used to simulate the pH in the colon. As substrate for the fermentation, 1 g of substrate (fructooligosaccharides, FOS, BENEO-Orafti) together with 50 mL fecal slurry and additional 10 mL of buffer are inserted to the vessel simultaneously,

ensuring minimum fermentation occurs before the start of incubation. FOS is a carbohydrate [158] that is rapidly fermented by the colonic microbiota to produce short-chain fatty acids and fermentation gases (including H_2, CH_4, H_2S and CO_2) as well as water vapor. Internal pressure, cumulative pressure and gas sensors signals were continuously recorded at t_i ($i = 0,1,2 \ldots 48$) with Δ_t=5 min for a total period of 4 h while P_{th} is set to 1 psi above P_{atm} and with venting event of τ_v =100 msec length. The 320 mL headspace volume was flushed with flushing gas (N_2) for 1 min before starting the incubation in order to form a colon like anaerobic environment.

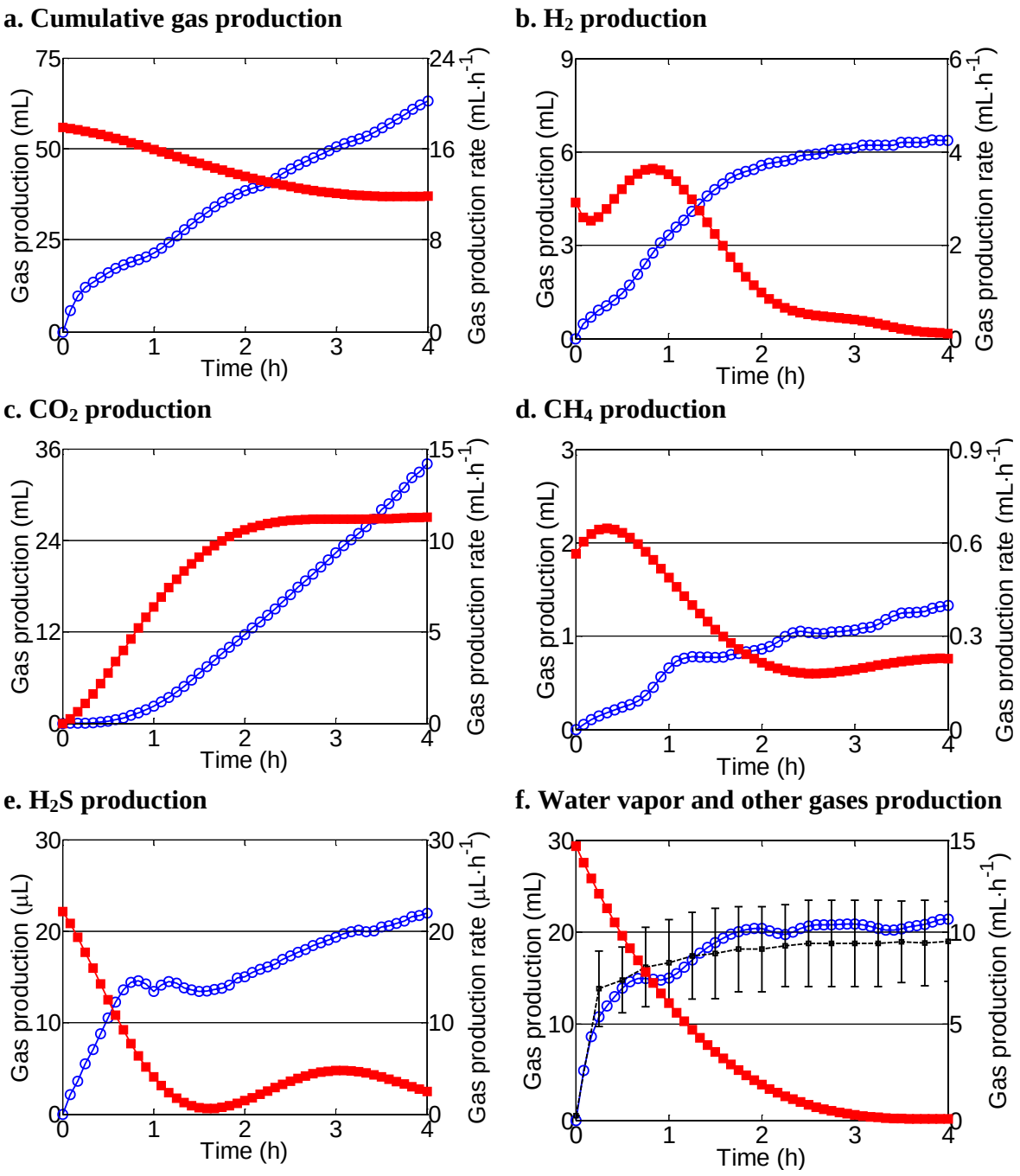

Figure 3.8. *In-vitro* colonic gas production by fecal fermentation of FOS substrate demonstrating GPP for different gas species (⊖ cumulative production (mL) - left y-axis, ■ production rate (mL/h) – right y-axis, --- water vapor measurement independent experiment): **(a)** Total production **(b)** H_2 production **(c)** CO_2 production **(d)** CH_4 production **(e)** H_2S production **(f)** water vapor and other gases production**.**

Total gas production: By the end of the four hour incubation, approximately 63 mL of total gas had been produced. At the beginning of the fermentation, the rate of total gas production was approximately 17.9 mL/h, but this decreased to approximately 11.9 mL/h after 4h. Interestingly, the production rate of total gas was approximately constant throughout the 4 h of the incubation whereas the rates of production of individual gas species varied greatly during the time course of the incubation. The diverse patterns in the rates of production of the different gas species during the incubation revealed in this study demonstrate the potential for this type of analysis to provide new insights into the fermentative process.

***H_2 gas profiles*:** By the end of the four hour incubation, approximately 6.4 mL of H_2 had been produced. At the beginning of the fermentation, the rate of total H_2 production was approximately 3.2 mL/h, but by 4h, H_2 production had ceased.

***CO_2 gas profiles*:** By the end of the four hour incubation, approximately 35 mL of CO_2 had been produced. At the beginning of the fermentation, the rate of total CO_2 production was negligible, but by 4h, the rate of CO_2 production had increased to approximately 11.3 mL/h.

***CH_4 gas profiles*:** By the end of the four hour incubation, only approximately 1.3 mL of CH_4 had been produced. At the beginning of the fermentation, the rate of CH_4 production was approximately 0.6 mL/h, but this decreased to approximately 0.23 mL/h by the end of the incubation. Production of CH_4 was negligible in comparison to the main two gases of H_2 and CO_2, indicating the subject is more likely not to be a CH_4 producer [168].

***H_2S gas profiles*:** production of H_2S increased rapidly in the first hour of incubation with maximum rate of 22.2 µL/h. After 1 h H_2S production rate was suppressed to as low as 0.6 µL/h. It has been suggested that this type of suppression effect on the rate of H_2S

production may be due to FOS which inhibits sulfide reducing bacteria responsible to the formation of H_2S gas [132].

Water vapor and other gases: the production of water vapor and other gases were estimated by calculating the difference between the total gas production and the sum of CO_2, H_2, CH_4 and H_2S. As one can see cumulative productions of water vapor and other gases saturate toward the end of the incubation period with production rate decreasing towards zero. Furthermore, water vapor GPP was measured independently by using the same system and applying similar conditions but instead of fecal slurry, an equivalent amount of sodium phosphate buffer (+99% water) was used. As described in the black dashed line in Figure 3.8f the total production of water vapor was approximately 19±4 mL after 4 h of incubation, mostly due to humidity elevation from 0%, as featured in the flushing gas, to 100% during the incubation. The author consider that the finding, in which two independent measurements of water vapor production resulted in similar values, validates the accuracy of the suggested calculation.

3.3.2 Investigation of incubation model components

In order to understand the impact of each component in the incubation model presented as the mass flow equation (3.16), a series of scenarios was conducted. In each scenario, one or more components of this equation was excluded or substituted with a fixed value in order to assess its contribution to the GPP.

The impact of an individual or a group of components is demonstrated on CO_2 GPP calculation presented previously in Figure 3.8c. The components selected are the vented gas, headspace gas, effective headspace volume (V_e^i) and gas sensor compensation. The outcomes are shown in Figure 3.9. Solubility impact is considered negligible and not included. The following scenarios are considered:

***Vented gases*:** excluding the gas vented out of the vessel from equation (3.16) (described as $V_F^i = 0$) results in the following mass flow equation:

$$CGP_i = V_e^i C_i + DG_i \quad [\text{mL}] \tag{3.17}$$

The impact of not including vented gas is a decrease of 2.16 mL (6.3%) volume of gas produced after 4 h and 1 mL/h (8.6%) in the production rate. Vented gas volume increases with the incubation time. Hence, for longer incubation durations, excluding it from the calculation will result with higher difference as incubation time extends.

Headspace gas: headspace volume is the major part the vessel volume (84%) in the discussed example where most of the gas produced is contained and not vented out. Excluding headspace gas from equation (3.16) (described as $V_e^i = 0$) results in the following mass flow equation:

$$CGP_i \cong \sum_{j=1}^{i} V_F^j C_j + DG_i \quad [\text{mL}] \tag{3.18}$$

The impact is a significant reduction of 31.9 mL (94%) of the total volume produced and 10.3 mL/h (91%) reduction in the production rate after 4 h. Systems with small headspace volume running for longer periods of incubation times will be impacted less as most of the gas produced will be in the form of vented gas.

Effective headspace volume: if the mathematically defined headspace volume (V_e^i) defined in equation (3.6) is approximated as the headspace volume (appeared as $V_e^i = V_h$) equation (3.16) transforms into the following mass flow equation:

$$CGP_i \cong V_h C_i + \sum_{j=1}^{i} V_F^j C_j + DG_i \quad [\text{mL}] \tag{3.19}$$

This results in an increase of 1.5 mL (4.3%) volume of gas produced and 0.5 mL/h (4.5%) in the production rate after 4 h. In the above example, $P_{th} = P_{atm} + 1$psi and water bath temperature of 37° C were applied. With higher P_{th} and lower temperature, the impact of such an approximation will increase.

Gas sensor compensation: Without using sensor compensation factors, designed to compensate for the vessel's temperature and pressure differences to the sensor's calibration point, equation (3.16) simplify into the following mass flow equation:

$$CGP_i \cong V_e^i S_i + \sum_{j=1}^{i} V_F^j S_j + DG_i(S_i) \quad [\text{mL}] \tag{3.20}$$

Here, $DG_i(S_i)$ means the incorporation of S_i^k in equation (3.11) instead of C_i^k. As a result, the GPP would experience a reduction of 1.7 mL (5%) in the calculated volume of gas produced after 4 h and 0.6 mL/h (5.2%) reduction in the calculated production rate. Thus, if the sensor calibration factor is not taken into account, the resulting error can be significant.

Cluster of components: Excluding a combination of three *vented gases*, *sensor compensation and headspace effective volume* (scenarios 1, 3 and 4 altogether) from equation (3.16) results in the following mass flow equation:

$$CGP_i \cong V_h S_i + DG_i(S_i) \quad [\text{mL}] \tag{3.21}$$

It generates an impact by reducing 2.3 mL (7%) of the calculated production volume and reducing 1 mL/h (9.1%) in the calculated production rate after 4 h of incubation.

a. Cumulative gas production

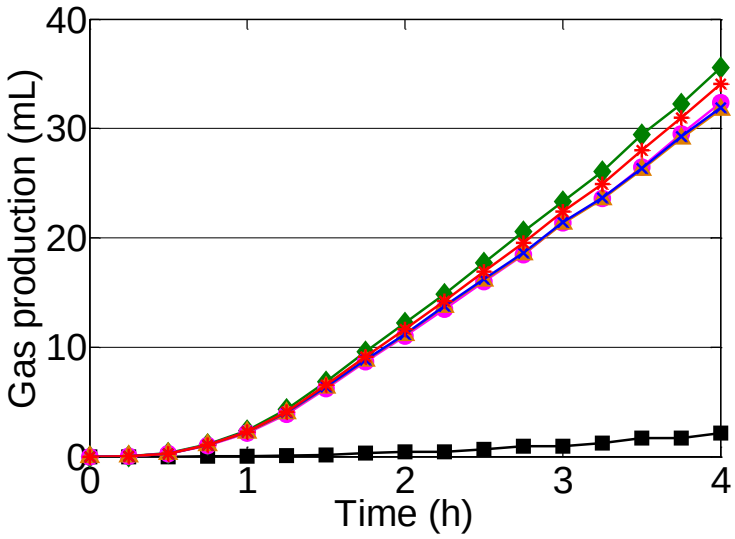

b. Gas production rate

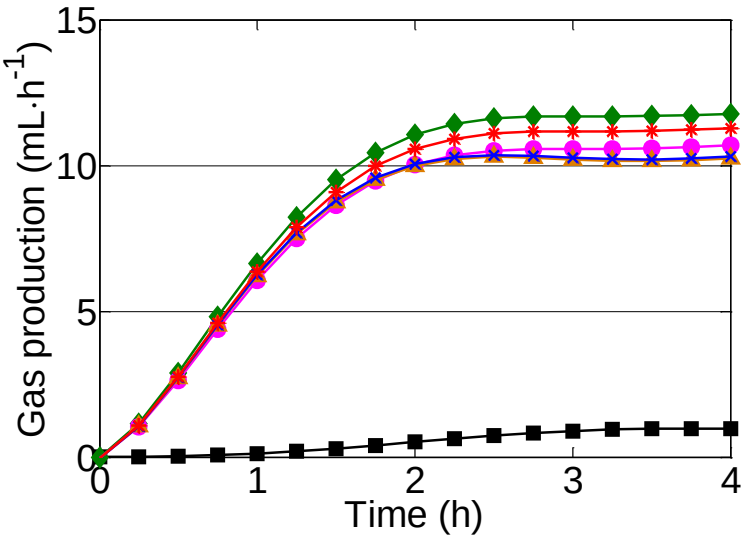

Figure 3.9. Deviations from the real measurements of cumulative gas production (mL) and gas production rate (mL/h) as a result of parameter modification in equation (3.16). Here, *in-vitro* colonic CO_2 gas production from fecal fermentation with FOS substrate is used as an example. The deviations from the actual measurement (shown by ✱ in the complete model) is seen after modification of different parameters and assessing their impact on the GPP. The different scenarios are as follows: ■ is produced by excluding headspace gas, ✕ produced by excluding vented gas ◆ when $V_e^i = V_h$, ● is produced by excluding sensor compensation factors, ▲ is produced by excluding a combination of a cluster using three parameters of vented gas, degeneration of V_e^i and sensor compensation factors.

3.4 Conclusions

In this chapter, the author showed the development of a versatile and parametric fermentation model which enables calculation of GPP in closed or pressure regulated fermentation systems which are gas inlet free. Fermentation systems are common in many industries including those associated with the production of food, chemicals and pharmaceutics. The components of GPPs are accurately described by the novel mass-flow equation (3.16) which takes into account gas sensors inputs such as headspace gas mixing ratio, internal pressure, cumulative pressure, and temperature.

The performance of the model was demonstrated using an *in-vitro* system, designed for incubating fecal matters in conditions similar to those in the human colon. The data modeled was that routinely available from gas sensors including headspace gas mixing ratio, internal pressure, and temperature and the model enabled prediction of total cumulative gas production, GPP and estimation of the production of water vapor. The kinetics of the different gas species were fully taken into consideration. The developed calculation procedure was validated by matching two independent measurements of water vapor – one with incubating water based buffer in an *in-vitro* system and the other through the new mass flow equation (3.16).

The contribution of individual components of the novel mass flow equation and a combination of these components were parametrically investigated and then tested on an *in-vitro* colonic gas production from fecal fermentations with FOS substrate as an example. The impact of the different test scenarios on cumulative gas production and gas production rate ranged between 4.3% to 94% and 4.5% to 91%, respectively. A novel component, which is introduced in this paper for the first time, is the effective headspace volume that is responsible for 4.3% of the total production and 4.5% of the production rate, respectively. Whereas, apart from the gas contained in the headspace, the combined contribution of vented

gas, effective headspace volume and sensor compensation accounts for up to 7% of the cumulative production and 9.1% of the production rate.

In conclusion, with respect to existing methods, which lack one or more components or continuous gas analysis, the suggested calculation method is comprehensive and may potentially impact the outcomes significantly. The method can be scaled and applied to applications in biogas or wastewater plants, food production or even for biological reactors including those describing rumen and human colonic reactions, allowing accurate assessment of GPP, exerted gas and other figures of interest.

Chapter 4. GAS PROFILING OF ANAEROBIC DIGESTERS

4.1 Introduction

In the previous two chapters the author developed the gas profiling technology for quasi-closed and pressure regulated anaerobic fermentation systems. In this chapter, the author adds a new dimension to the profiling technology and develops a novel technique for measuring gas components in the liquid medium as well as in the headspace. In the work presented in this chapter, the author's main objective is to introduce sensing arrays for simple, low-cost, continuous, *in-situ*, and automated gas measurement in both liquid and gas phases, specifically adapted to the anaerobic digester's headspace and the corrosive slurry environments. Here, the author choose to focus on CO_2, CH_4, and H_2 as they are the predominant biogas products in AD processes. Although other gases, such as H_2S and ammonia [29,96,169], are valuable indicators, focusing on CO_2, CH_4 and H_2 is satisfactory in order to fulfil the main objective in this chapter. This platform can be expanded for measuring other gases and is recommended in chapter 5 for future work. The suggested approach utilizes commercial sensors protected by silver embedded polydimethylsiloxane (PDMS) membranes [170,171] that prevent bio-fouling by inhibiting bacterial overgrowth, reducing the impact of caustic vapors and allowing real-time measurement of the dissolved gases partial pressures. This new technique overcomes many current challenges in measuring gas components, helps operators in obtaining real-time process characterizations, process optimization and stabilizing digesters operation.

In the following sections, the author details the application of the developed sensor array on an AD in a series of batch experiments for evaluating the accuracy, reproducibility, and longevity of the measurements. Additionally, the impact of inoculum aging and elevated

pressure conditions on the digestion characteristics is investigated to further evaluate early warning capability of the developed system.

The content of this chapter has been submitted as a full paper to Water Research journal and currently under review.

4.2 Materials and Methods

4.2.1 Fermentation system

The developed system consists of four main units as shown in Figure 4.1: (a) standard laboratory glass bottle of 250 mL, (b) two sets of gas sensor-arrays that are placed into cylinders made of machined high-density polyethylene (HDPE), stacked up using a middle piece adapter and designed to hold up to 3 gas sensors each. The bottom array is used for measuring liquid-phase gas concentrations, while accommodating one NDIR dual sensor for sensing CO_2 and CH_4 and one TC sensor for assessing H_2 gas (all purchased from © SGX Sensortech). The top array is used for measuring the headspace gas concentration, with similar sensors and an outlet valve for headspace flushing, (c) The third unit consists of a gas pressure regulator unit (ANKOM Technology, USA) to keep the headspace pressure constant using a pressure actuator and continuously recording the internal pressure value with a sensor. It also contains a temperature sensor and electronic modules and (d) the fourth unit includes electronic circuits and a PC for simultaneous data acquisition of gas and pressure sensors.

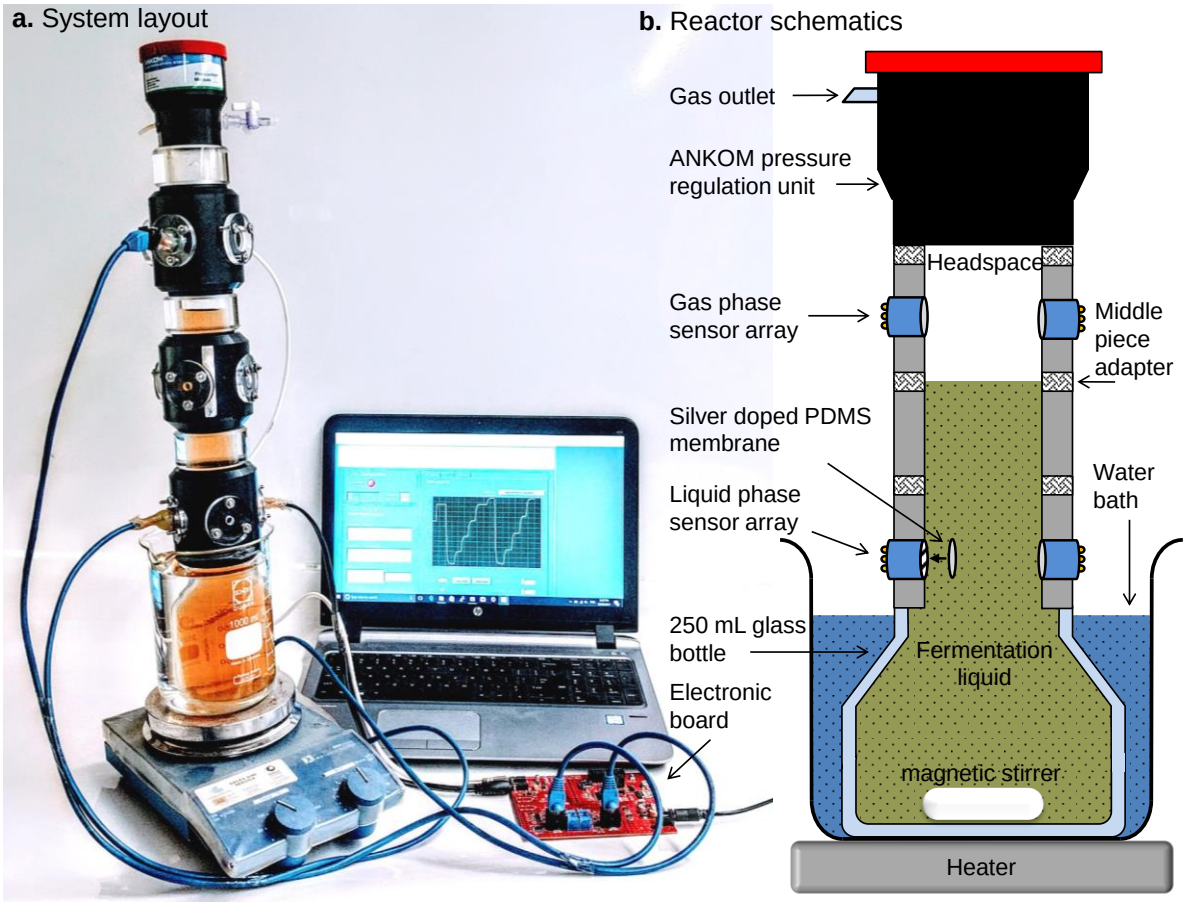

Figure 4.1. AD simulation system (a) system layout (b) reactor schematics

4.2.2 Evaluation and calibration of the system

In order to accurately measure gas concentration in liquid, protect gas sensors from caustic substances found in the slurry (fermentation broth) and to prevent bio-fouling, 70 µm thick silver embedded PDMS membranes, especially designed and produced at RMIT [170,171] were placed on the packaging to protect the submerged sensors in the liquid medium. The membrane and sensors' packaging created a miniature headspace (Diameter: 20 mm, Length: 10 mm) around the sensing elements. The small volume of the miniature headspace (3 mL), and proximity to the liquid medium, ensure rapid equilibrium between the inside the sensor container and the liquid environment near the membrane. The system allows the real-time

measurement of the dissolved gas partial pressures which can be converted into the gas concentration in liquid using *Henry's law* and the equilibrium solubility constants in water at 37ºC for CO_2, CH_4 and H_2 which are obtained as 229.6, 10.1 and 6.9 $\frac{\mu Mol}{L \cdot KPa}$, respectively [172].

Membranes were also applied to the headspace sensors in order to reduce the exposure of the sensors to ongoing high humidity and caustic vapors.

Before and after AD experiments were conducted, the sensors were calibrated against target gases of industrial standards including three separate gas bottles of 50%vol CH_4, 50%vol CO_2, and 1%vol H_2, respectively, balanced with N_2 for simulating anaerobic gas environment demonstrating similar accuracy as presented in Chapter 2. The liquid sensors were calibrated by adding water to the system instead of slurry and saturating it with the different gas mixtures.

4.2.3 Experiment procedure

4.2.3.1 Characteristics of substrate and inoculum

Food waste used in this study was the organic fraction of municipal solid waste (OFMSW) according to the specifications found in [173]. Due to highly biodegradable nature of the OFMSW, a batch of synthetic food waste was prepared using compositional data from the Victorian garbage bin recipe collected by Sustainable Victoria, Australia [173]. The synthetic food waste was stored in small containers at −20ºC and the characteristics of the samples were obtained at regular intervals to examine any variations.

The inoculum used in these experiments was collected from the anaerobic digester of Melton Recycled Water Treatment Plant, Melbourne, Australia, operated at mesophilic conditions (37ºC). The characteristics of the food waste, TS, VS and VA of inoculum, are presented in Table 4.1.

Table 4.1. Inoculum and food-waste composition

Sample	TS%	VS%	VA (g acetic acid/L)	pH	Density (g/mL)
Food waste	26.73±1.07	24.93±0.27	5.37±0.08	5.02	1.018
Inoculum	2.72±0.01	2.01±0.01	0.73±0.05	7.55	1.02

4.2.3.2 Experimental methodology

AD batch experiments were conducted to evaluate the biogas signatures. Tests were carried out using slurry at a food waste to inoculum ratio of 1:2 g/g VS. Preliminary to the experiment, the slurry was added to the reactor, while covering the liquid-phase sensor array as shown in Figure 4.1b. The reactor headspace was flushed with 100%vol N_2 (0% humidity) for two minutes in order to mimic a digester's anaerobic environment and the pressure regulation level was set to 1 psi above atmospheric pressure (14.7 psi). The glass bottle was nearly fully submerged in a 37ºC water bath, while mixed with a magnetic stirrer at 50 rpm for ensuring sludge's homogeneity (Figure 4.1b). Immediately after flushing, all valves were closed and the experiment commenced with data recording at 1 min intervals. In addition to gas and pressure measurements, digestate parameters including TS, VS and VA were analyzed before and after every batch experiment.

4.2.4 Analytical methods

TS and VS were measured according to APHA methods 2540B and 2540E [174]. VA were determined by calorimetric techniques using HACH (Model: DR/4000 U) spectrophotometer according to the method 8196. Sample were centrifuged (Eppendorf 5702, Germany) at 4.4 rpm for 15 mins and then filtered through 0.45 μm filter paper (mixed cellulose-ester

membrane filter, Advantec, Japan), to measure the VA content. The composition of biogas was verified using a gas chromatography (Varian 450-GC, Varian Australia Pty Ltd., Netherlands) equipped with a packed column (GS Carbonplot 113-3132, 1.5 μm, 30 m* 0.320 mm, stainless steel, Agilent Technologies Inc., Australia) according to the method described by Zahan *et al.* [99].

Cumulative gas production was calculated according to the calculations presented in Chapter 3 and normalised to the amount of experiment food waste. The gas production rate was calculated using the derivative of the cumulative gas production as described in Chapter 3.

4.3 Results

During the experiments, the same batch of inoculum was used at different periods after collection: aged for 13 days, 41 days, 46 days and 55 days where the corresponding experiments are named as AD13d, AD41d, AD46d and AD55d, respectively. Meanwhile, the inoculum was stored in a sealed container at 37ºC without feeding.

Gas measurements were evaluated in two sets of AD batch experiments. The first set, AD13d, was used for validating the system accuracy and longevity as well as demonstrating its sensing capability in both liquid and gas phases. Inoculum aged within two weeks of collection is considered fresh according to biochemical methane potential (BMP) batch AD experiment standards [175-177]. The response of AD batch experiment using fresh inoculum was used for benchmarking the system with reference to previous reports [31-34,99,177-181].

The second set of AD batch experiments, using aged inoculum AD41d, AD46d and AD55d, was conducted to identify gas signatures from possible process imbalance and failures as a result of ageing.

Utilizing the suggested system, gas profile signatures were explored, for revealing the advantages of monitoring gas components by providing early warnings of process instability. In addition, the system reproducibility was demonstrated using aged inoculum in two sequential experiments.

4.3.1 Demonstration of the gas measurements and system validation

The system's capability in providing online and continuous monitoring of gas profiles for AD processes was tested. The process included the measurement of gas profiles in both liquid and gas phases in addition to demonstrating the system's accuracy and longevity as shown in Figure 4.2 and Table 4.2.

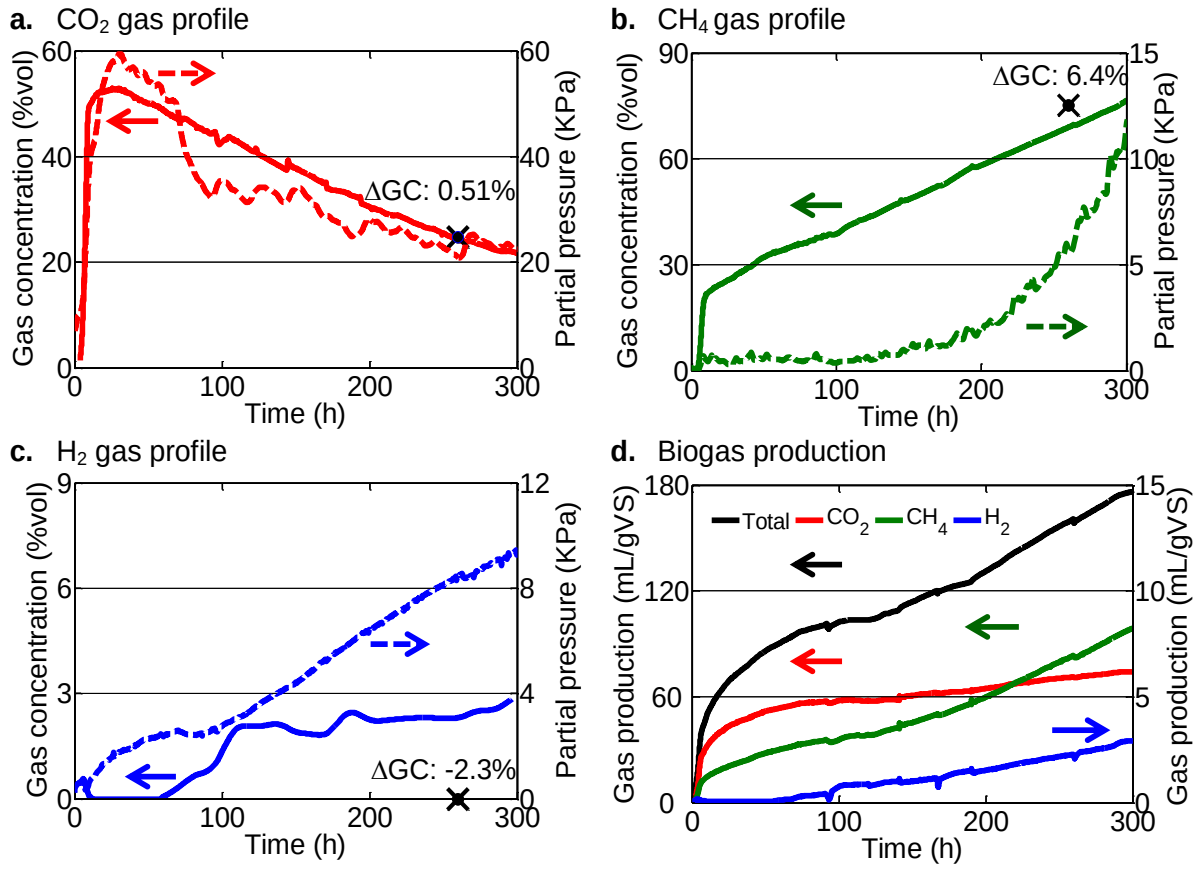

Figure 4.2. Anaerobic digestion of food waste using wastewater inoculum (AD13d), demonstrating system's complete functionality over 300 h together with sensor's accuracy using gas-phase GC (✕) analysis at 260 h: **(a)** CO_2 profile **(b)** CH_4 profile **(c)** H_2 profile **(d)** cumulative biogas production.

The accuracy of the system was validated using GC analysis of the gas-phase (Figure 4.2a-c). Here ΔGC (%vol), which represents the difference between GC measurement and the gas sensors readings, is less than 6.4%vol for all gas types. Additionally, the 300 h operation of the system, consists of pressure regulation, pressure recording and gas sensing in both gas and liquid phases, is presented to demonstrate longevity.

CO_2 measurements (Figure 4.2a) show production in two intervals. In the first interval (0-15 h), CO_2 levels in both phases increased rapidly and reached peak levels of 53%vol and 60 kPa in gas-phase and liquid-phase, respectively. In the second interval (15-300 h), CO_2 level linearly decreased to 22%vol in the headspace and to 23 kPa in the liquid.

Synchronized with the CO_2 profile, CH_4 gas-phase profile occurred during similar production intervals (Figure 4.2b). At the end of the first interval (15 h), CH_4 concentration in the headspace reached 22%vol and monotonically increased during the second interval to 75%vol at 300 h. However, unlike the gas-phase, the CH_4 partial pressure in the liquid-phase was significantly lower relative to the headspace before 100 h, after which the production accelerated and exceeded 12 kPa by 300 h (Figure 4.2b). Moreover, the difference in the production intervals is not observed in liquid-phase.

The two production intervals can be identified in the H_2 gas profile as well (Figure 4.2c) while H_2 levels in the second interval were significantly higher. During the second interval, H_2 levels in the liquid increased linearly to 9 kPa at 300 h whereas the gas-phase concentration increased at a lower rate reaching 3%vol due to constant gas evacuation from the headspace.

Cumulative biogas production (Figure 4.2d), obtained from the gas-phase concentration and total release of gas components [167], consisted of 176 mL/gVS after 300 h where the

dominant gas produced was CH_4 with 99 mL/gVS (56.3% of the total gas) followed by CO_2 with 74 mL/gVS (42%) and H_2 with 3 mL/gVS (1.7%).

In terms of digestion analysis, within the 300 h of digestion, the removal of TS and VS consisted of 28.8% and 34.6%, respectively (Table 4.2a). VA concentration increased to 2.2 g/L from 0.84 g/L.

Table 4.2. Digestion analysis of food waste AD by wastewater inoculum

Parameter	**a. Digestate AD13d**	**b. Digestate AD46d**
TS %	2.8±0.02	3.2±0.01
VS %	2.04±0.01	2.2±0.06
VA(g acetic acid/L)	2.2±0.14	3.1±0.07
TS removal %	28.8±0.01	18.3±0.3
VS removal %	34.6±0.01	29.5±0.5

4.3.2 Gas profiles for aged inoculum

First, a typical experiment with an aged inoculum (AD46d) is demonstrated and gas profile signatures for its AD are presented in Figure 4.3. Subsequently, differences between a failed AD, where aged inoculum was used, and the balanced and working AD demonstrated in the previous section, are highlighted.

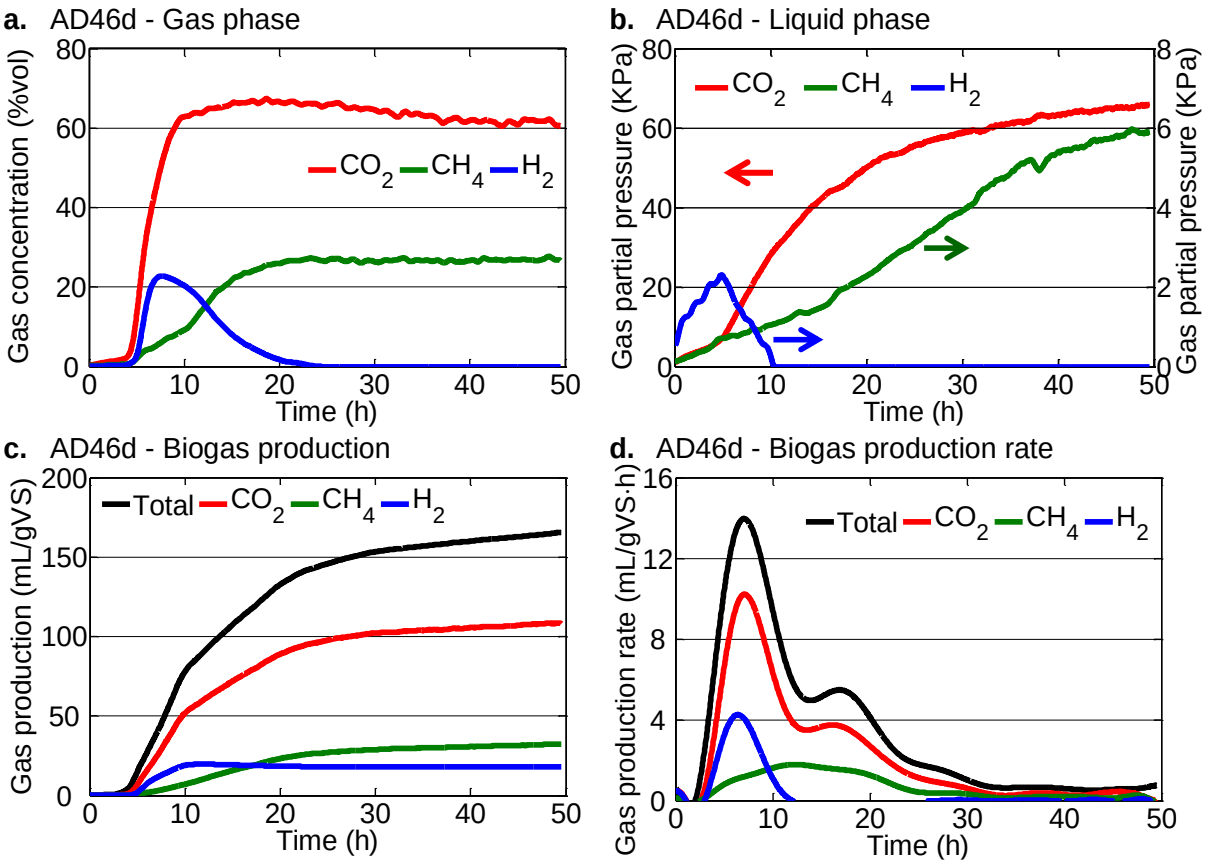

Figure 4.3. AD of food waste using aged wastewater inoculum (AD46d), demonstrating liquid and gas phase analysis: **(a)** gas-phase profile **(b)** liquid-phase profile **(c)** cumulative biogas production **(d)** biogas production rate.

The gas-phase analysis (Figure 4.3a) shows the rapid increase of CO_2 concentration after 4 h that peaked at 66%vol after 15 h, followed by H_2 production reaching 23%vol after only 8 h and by 21 h almost no H_2 presence was observed. CH_4 production initiated slowly after 5 h, afterwards, the concentration in the headspace was increased to 26%vol at 20 h and remained constant.

CO_2 was the dominant gas measured in the liquid as shown in Figure 4.3b. Synchronized with the gas-phase, liquid CO_2 partial pressure started increasing after 4 h and reached 66 kPa by 50 h. However, unlike the gas-phase, CH_4 and H_2 partial pressures were significantly

lower where CH_4 concentration increased monotonically to 6 kPa at 50 h, where H_2 level stayed below 2.2 kPa. H_2 appeared first in the liquid-phase at 0 h, peaked at 5 h and gradually reduced until it became undetectable (10 h).

Cumulative biogas production (Figure 4.3c) consisted of 165 mL/gVS after 50 h for which the dominant gas was CO_2 with 108 mL/gVS (66.7% of the total gas) followed by CH_4 with 32 mL/gVS (19.5%) and H_2 with 18 mL/gVS (10.9%). The remaining gas production ascribed to water vapor and other gases [167].

In regards to digestion analysis (Table 4.2b), within 7 days of digestion, 18.25% and 29.5% of TS and VS, respectively, were removed while VA concentration increased from 0.84 to 3.05 g/L.

Another indicator considered was pH. In all experiments, the pH value was set to 7.4 at the start, fell to ~6.5 when CH_4 started to increase and then exceeded 7.8 at the 50 h duration.

Considering that no gas production was seen after 30 h the remainder of the digestion experiments were limited to 50 h duration.

4.3.3 Comparison of aged and fresh inoculum

The effect of inoculum ageing on the digestion process was explored by comparing AD13d, AD46d and AD55d samples of different ages. All batches operated under the same process conditions. Inoculum ageing seemed to be separating the measurements into two groups of fresh (age < 14 d) and aged (age > 45 d). The first 50 h digestion profiles are presented in Figure 4.4-Figure 4.6.

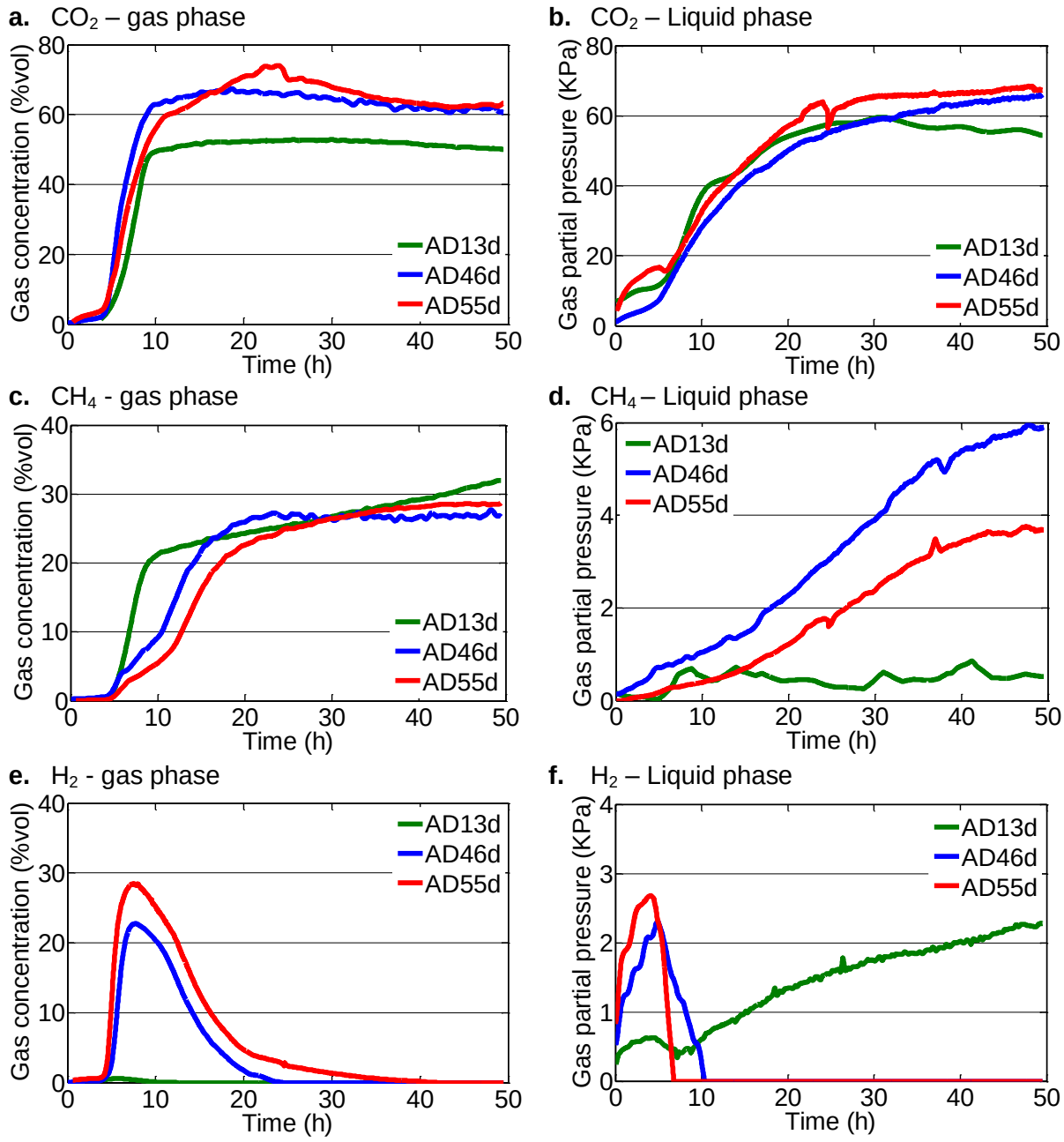

Figure 4.4. AD of food waste using wastewater inoculum, demonstrating gas analysis in gas-phase and in liquid-phase *vs* time for different inoculum ages: **(a)** CO_2 in gas-phase **(b)** CO_2 in liquid-phase **(c)** CH_4 in gas-phase **(d)** CH_4 in liquid-phase **(e)** H_2 in gas-phase **(f)** H_2 in liquid-phase.

Gas-phase (Figure 4.4) - CO_2 profiles in the gas-phase of aged inoculums (AD46d and AD55d) were ~20% higher than that of fresh inoculum (AD13d) as presented in Figure 4.4a.

Although CH_4 concentrations at 50 h were relatively close for all samples, it increased faster and linearly for fresh inoculum while plateaued for the aged inoculums (Figure 4.4c). While H_2 concentration in the gas-phase was negligible for fresh inoculum, it was significant for aged inoculum (Figure 4.4e). H_2 concentration increased with the inoculum age, reaching 28.5%vol in AD55d (Figure 4.6a).

Liquid-phase (Figure 4.4) – similar to the gas-phases, CO_2 levels in liquid-phases after 30 h were higher for the aged inoculum and emerged with almost similar kinetics as in the gas-phase. While CH_4 values were minimal for the fresh sample, they exceeded up to 6 kPa at 50 h for aged inoculum (Figure 4.4d). In liquid, H_2 was detected for the fresh inoculum throughout most of the first 50 h at 0-2.2 kPa levels, while for the aged inoculums H_2 levels increased rapidly in the first 5 h to 2.7 kPa and weren't detected after 10 h (Figure 4.4f).

Gas production (Figure 4.5) – After 50 h of digestion, the total production was 70%-80% higher for aged inoculum (Figure 4.5a) where the main difference originated from CO_2 production as shown in Figure 4.5b. Similarly to gas-phase (Figure 4.4), CH_4 total production wasn't impacted significantly by the inoculum age as seen in Figure 4.5c and Figure 4.6d but initiated, together with the other gases, 3 h earlier for fresh inoculum as seen in Figure 4.6c. One of the major differences, which also seen in the gas-phase analysis, was the significantly higher H_2 biogas production for aged inoculum (Figure 4.5d).

VA accumulation rate (Figure 4.6b) - the accumulation rate of VA, defined as 1 mg of acetic acids per L and per day of digestion, increased with inoculum age and was roughly 3 times higher for the aged inoculum than fresh sample (Figure 4.6b).

Production lag (Figure 4.6c) – the production lag was measured by how long it took for the total cumulative biogas production to reach mL/gVS. As per Figure 4.6c, fresh inoculum

production started within 1 h, while for aged inoculum it took roughly 4 times longer to initiate a substantial gas production.

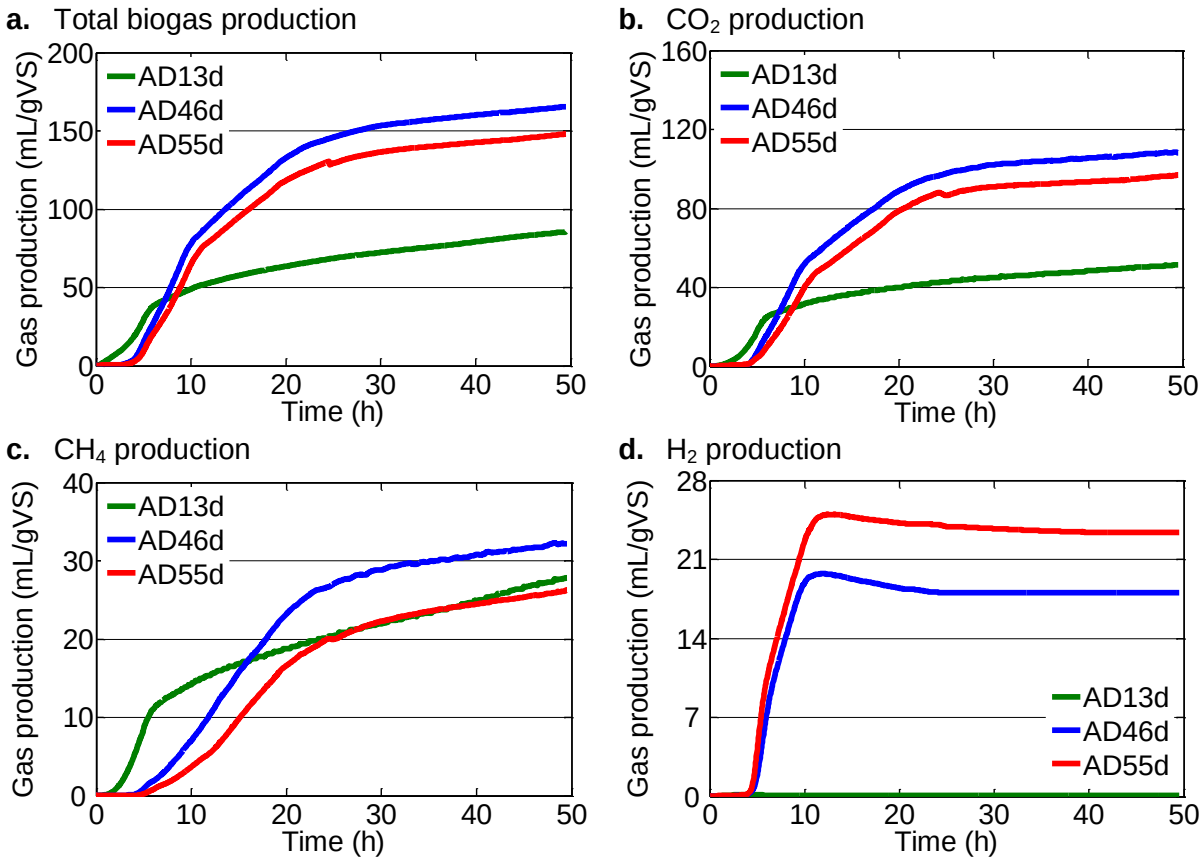

Figure 4.5. AD of food waste using wastewater inoculum, demonstrating biogas production for different inoculum ages *vs* time: **(a)** total cumulative biogas production **(b)** CO_2 cumulative production **(c)** CH_4 cumulative production and **(d)** H_2 cumulative production**.**

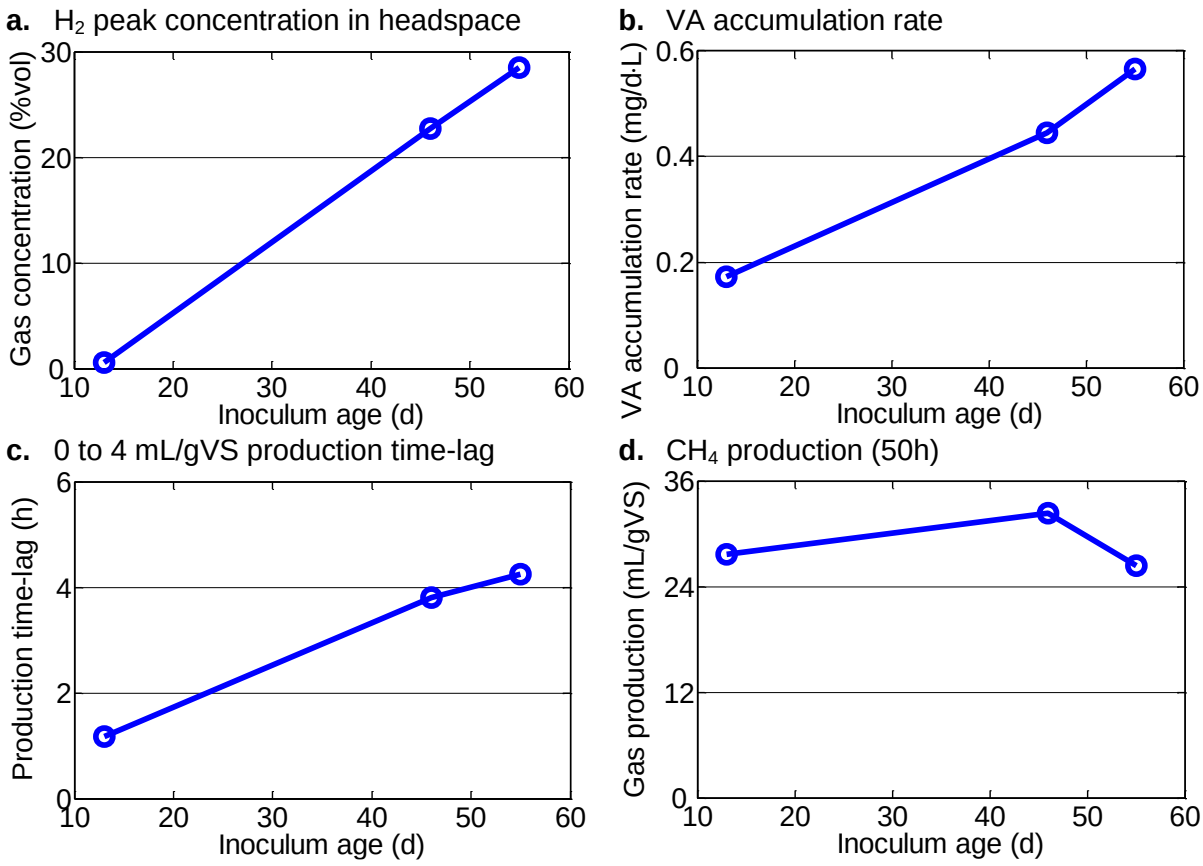

Figure 4.6. AD of food waste using wastewater inoculum, demonstrating process figures of merit *vs* inoculum age: **(a)** H_2 peak concentration **(b)** VA accumulation rate **(c)** total biogas production time lag to first 4 mL/gVS **(d)** CH_4 production after 50 h.

From Figure 4.6a-c one can observe a nearly linear correlation between the inoculum age and the peak H_2 concentration in gas-phase, the VA accumulation rate and the production time-lag. The finding shows that as the inoculum is aged it is more likely to enter an imbalanced state and fail when the same process conditions are applied.

Solids removal (Table 4.2) – relative to fresh inoculum, VS and TS removals for aged inoculum were, on average, 25% and 43% lower, respectively.

The inoculum and food waste were analysed after 76 days in storage where less than 10% differences were found in comparison to its analysis after collection (Table 4.3).

Table 4.3. Inoculum and food-waste composition before and after 76 days in storage

Parameter	Food waste		Inoculum	
	0 days	**76 days**	**0 days**	**76 days**
TS %	26.73±1.07	26.84±0.69	2.72±0.01	2.70±0.02
VS %	24.93±0.27	24.87±0.73	2.01±0.01	1.99±0.04
VA(g acetic acid/L)	5.37±0.08	5.39±0.02	0.73±0.05	0.66±0.03

4.3.4 AD at elevated pressure conditions

The effect of elevated pressure in the headspace was investigated with two consequent batch experiments using inoculums with similar ages, namely, AD41d and AD46d. According to the author's experiments, the 5 day difference between the two batches should not result in more than 10% variation in the biogas production. As such, the differences seen beyond this range should be due to the pressure effect.

While the pressure in AD46d was continuously regulated throughout the whole experiment, AD41d's pressure regulator was turned off at 19 h. The pressure in the headspace of AD41d gradually accumulated together with the continuous production of biogas, reaching 7 psi above the pressure level of AD46d. This created an elevated pressure headspace condition. The difference in the process performance is presented in Table 4.4, Figure 4.7 and Figure 4.8.

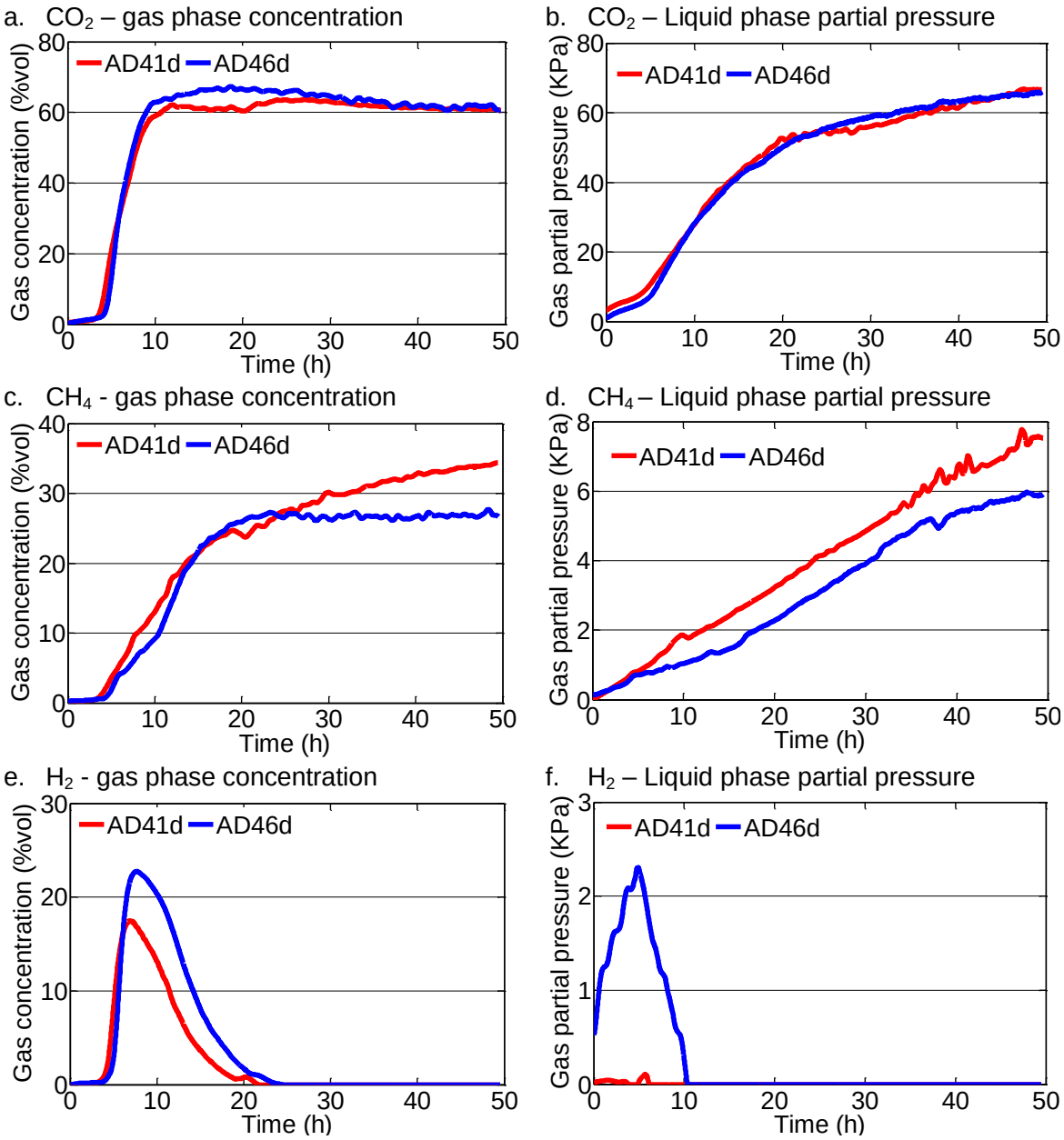

Figure 4.7. Anaerobic digestion of food waste by wastewater inoculum demonstrating gas analysis in both gas-phase and liquid-phase *vs* time at different headspace pressure conditions (red: AD41d – elevated pressure conditions, blue: AD46d – constant pressure conditions): (a) CO_2 concentration in gas-phase (b) CO_2 partial pressure in liquid-phase (c) CH_4 concentration in gas-phase (d) CH_4 partial pressure in liquid-phase (e) H_2 concentration in gas-phase (f) H_2 partial pressure in liquid-phase.

Gas profile (Figure 4.7) – The gas profile of AD41d and AD46d, both in liquid-phase and gas-phase, are similar in quantity and kinetics while the main difference was elevated levels of CH_4 in gas-phase after 19 h and H_2 in both phases. The difference in CH_4 likely originates from non-linear response of the NDIR sensor to elevated pressure which the pressure compensation algorithm, based on the *ideal gas law*, didn't correct completely. The difference in H_2 profiles was not related to the difference in pressure conditions as it occurred before 19 h and discussed in the next section.

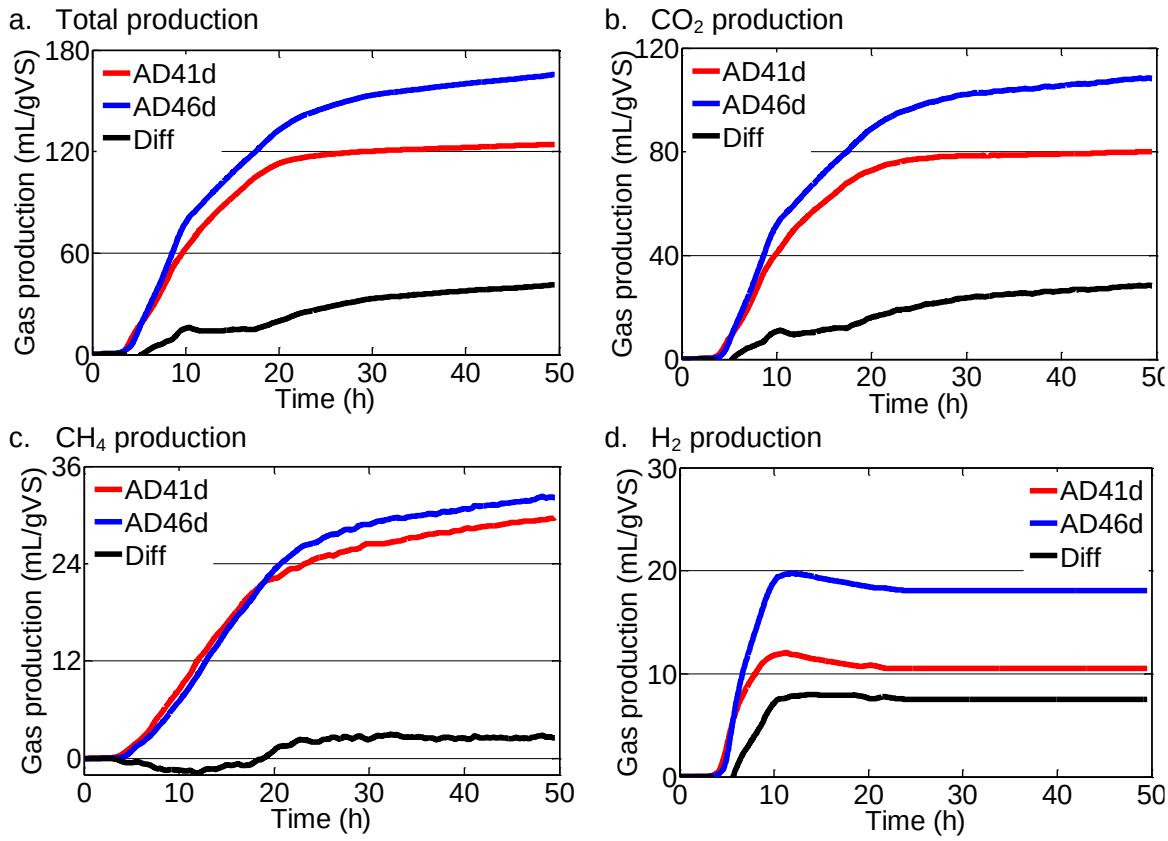

Figure 4.8. AD of food waste by wastewater inoculum demonstrating gas production *vs* time at different headspace pressure conditions (red: AD41d - elevated pressure conditions, blue: AD46d – constant pressure conditions, black - difference): (a) total cumulative biogas production (b) CO_2 cumulative production (c) CH_4 cumulative production (d) H_2 cumulative production.

Gas production (Figure 4.8) – during the first 19 h of digestion, gas production profiles of both AD41d and AD46d showed similar patterns. However, after AD41d headspace started pressurising (19 h), a deceleration in biogas production rate was observed in AD41d. At 50 h, relative to AD46d, the biogas produced was 24%, 26%, 13% lower in AD41d for total biogas production, CO_2 and CH_4, respectively. The impact on H_2 production was minimal as most of H_2 produced before 19 h for both AD41d and AD46d.

Digestion analysis (Table 4.4) – in AD41d VA level was 29% higher than in AD46d which is linked to gas production inhibition [103]. In addition, the organic removal was lower in AD41d.

In [182], batch anaerobic digestion trials were conducted with high pressure conditions (3-90 bar) demonstrating less degradation rate and less biogas production in comparison with digestion in lower pressure conditions. This report is in agreement with the author's finding which approves the ability of the developed system to provide useful and accurate AD characterization.

Table 4.4. Digestion analysis of food waste AD by wastewater inoculum AD41d &AD46d

Parameter	**AD41d**	**AD46d**
TS %	3.7±0.1	3.2±0.01
VS %	3.2±0.03	2.2±0.06
VA(gAceticAcid/L)	4±0.05	3.1±0.07
TS destruction rate %	5.4±0.7	18.3±0.3
VS destruction rate %	7.4±0.5	29.5±0.5

4.3.5 System reproducibility

System reproducibility was assessed using the first 19 h of AD41d and AD46d, two batch experiments with comparable inoculum age and identical process conditions in the first 19 h. After 19 h the pressure conditions altered of AD41d as mentioned in the previous section. Gas profiles in liquid-phase and gas-phase were compared and the variations were quantified using coefficient of variation (CV). The CVs were calculated for 6-19 h when gas levels were above the detection error. Besides H_2 and CH_4 in liquid-phase, Minor differences were observed between the two sets of data and the recorded CVs levels were below 20% at 6-12 h and below 10% at 12-19 h (Figure 4.9). Since levels of CH_4 in liquid were close to the sensor's sensitivity, its CV levels reached 29% at 9-10 h but were mostly below 25% at 6-19 h. H_2 in gas-phase (Figure 4.9e and Figure 4.9f) was sensitive to inoculum age as mentioned in section 4.4.4. In liquid-phase, H_2 was only observed in AD46d, it is possible that less H_2 gas was produced for AD41d and completely consumed for methanogenesis or propagated rapidly to the headspace as discussed earlier in this chapter.

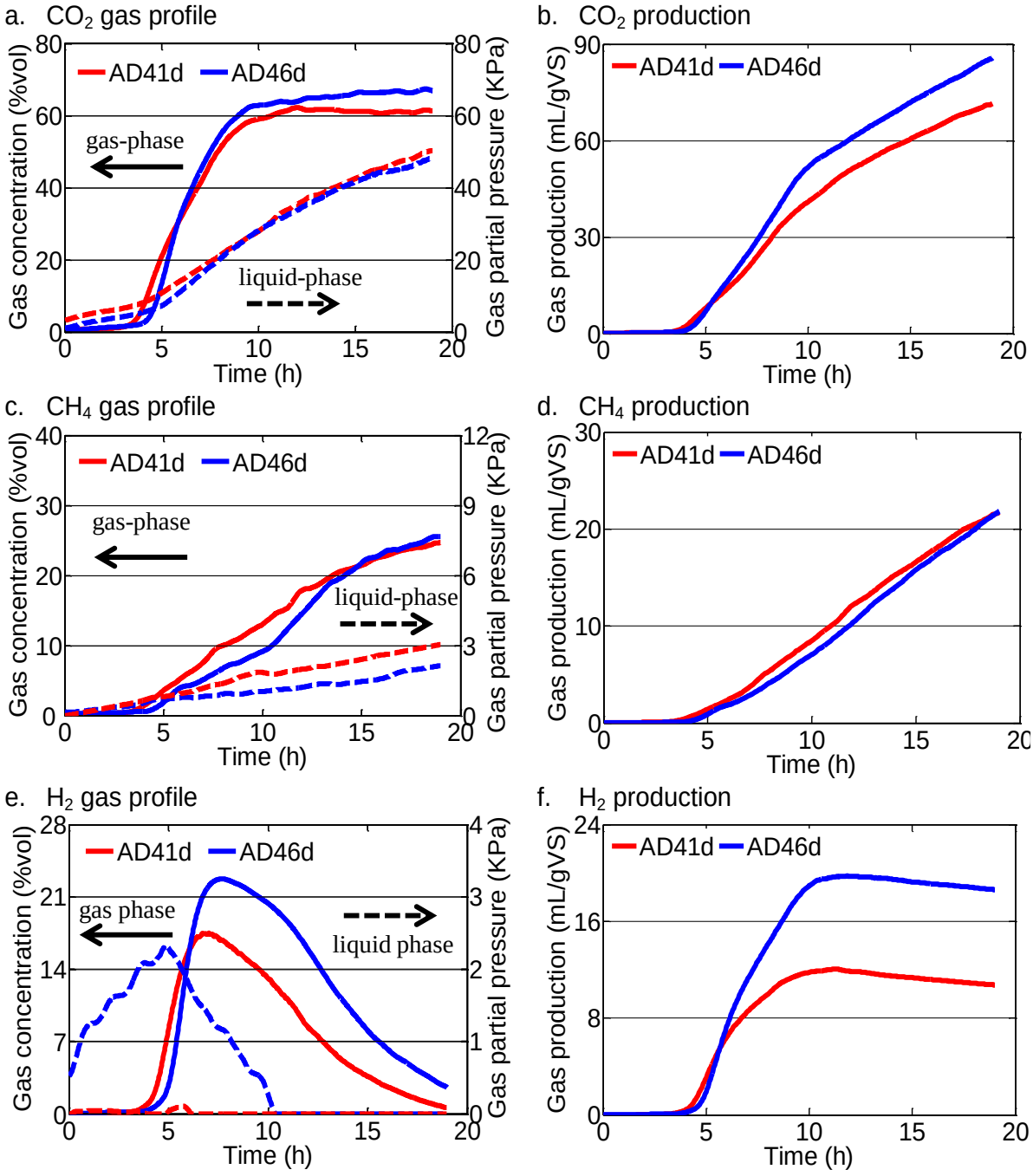

Figure 4.9. AD of food waste using wastewater's inoculum demonstrating system's 19 h reproducibility of gas production and gas analysis (gas-phase and liquid-phase) with two batch experiments (red – AD41d, blue – AD46d): (a) CO_2 gas profile: ─ gas-phase ▪▪ liquid-phase (b) CO_2 cumulative production (c) CH_4 gas profile: ─ gas-phase ▪▪ liquid-phase (d) CH_4 cumulative production (e) H_2 gas profile: ─ gas-phase ▪▪ liquid-phase (f) H_2 cumulative production.

4.4 Discussion

4.4.1 System validation

The accuracy of the system was also confirmed by biogas production and the digestion analysis in comparison to published literature. The biogas production matched previous reports of equivalent AD [177-180]. Additionally, the removal percentage of TS and VS match other BMP reports considering the relatively shorter experiment length [99,177,179]. Finally, VA concentration increased to 2.2 g/L from 0.84 g/L which represents balanced process as it out of the inhibition range [181].

In Figure 4.2, the author showed a strong correlation between CO_2 in liquid and gas phases which confirms the accurate sensing of dissolved CO_2 and can be attributed to its high solubility/release-ability in comparison to other gases. However, the quantity and kinetics of CH_4 in liquid-phase were poorly correlated with the gas-phase. The results indicate that the produced CH_4 preferentially propagated into the headspace instead of being dissolved in the liquid. This phenomenon can be attributed to methane's poor solubility and low mass transfer in AD [130].

The dissolved gas concentrations in liquid were calculated using the gas partial pressures (Figure 4.2a-c) and the solubility constants found in Section 2.2. According to this conversion, the dissolved gas ranges were in the order of 2-14 mMol/L, 0-121 µMol/L and 0-62 µMol/L for CO_2, CH_4 and H_2, respectively. CO_2 levels in liquid matched the CO_2 levels in the gas-phase while CH_4 levels were in agreement with other reports [33,34]. H_2 levels were significantly lower than failure conditions levels of 400 µMol/L and 695 µMol/L reported in [32] and [31], respectively. Other reports mentioned that process imbalance happens when H_2 concentration is within 0.05-80 µMol/L [30,31,33,34]. The author attributes the difference of those reports in comparison to his findings to their relatively short experiments (0-20 h) and

different H_2 measurement methodologies. The advantage of the suggested *in-situ* partial pressure measurement is in its simplicity and low contamination risk which can eliminate inaccuracies faced by other methods. In conclusion, it is derived that the availability of dissolved H_2 supports methanogenesis throughout the 300 h in the balanced process (Figure 4.2c).

The system was found to be reasonably reproducible except for H_2 and CH_4 in liquid. Since levels of CH_4 in liquid were close to the sensor's sensitivity, CV levels reached 29% at 9-10 h but were mostly below 25% during 0-19 h. High CV values for H_2 are likely to stem from H_2 sensitivity to inoculum age as seen in Figure 4.6a. Figures and discussions can be found in Supporting Information.

4.4.2 Gas profiles for fresh inoculum

When fresh inoculum was used (AD13d) a continuous production of biogas, consisting mainly of CH_4, was observed for 300 h. CH_4 methanogenesis regulates VA accumulation [101,104,113,114,117,118]. Therefore, the high levels VS and TS removals, the low levels of VA accumulated after 300 h and the high production of biogas, particularly CH_4, can all be attributed to a consistent and healthy methanogenesis phase throughout the whole experiment. In addition to his results being in agreement with previously published reports, the author concludes that AD13d was a typical, balanced and high yielding AD process.

All gas profiles indicate two production intervals, separated before and after 15 h. For H_2 the first interval is remarkably lower as possibly the available H_2 in the first interval was consumed for the rapid production of CH_4. These production intervals are likely associated with different types of organic substances and their degradability. The first interval occurred

when readily degradable organic materials were digested, followed by the second interval, representing the digestion of slowly degradable organic materials [99].

4.4.3 Gas profiles for aged inoculum

AD46d was considered as a failed AD process and can be explained by decomposing AD46d GPP to a series of different production intervals, which were easily identified through several production rate peaks (Figure 4.3d). The first interval (lag phase) lasted 5 h and identified with low gas production. The second interval (5-10 h) started after H_2 became available in the liquid-phase and featured high biogas production, mainly consisting of H_2 and CO_2, and the corresponding production rates that peaked at 8 h with 10 mL/gVS·h and 4.3 mL/gVS·h, respectively. The third interval (10-25 h) featured 50% reduction in the total production rate and involved only CO_2 and CH_4. H_2 production is minimal during this interval and seen only in the liquid-phase at low values which suggests that H_2 has been consumed for methanogenesis or evacuated from the headspace. In terms of CH_4 production profile, the second and third intervals were merged into a single interval that started slowly at 5 h and peaked at 11 h (1.7 mL/gVS·h). The lag in the CH_4 production was associated with the time took for H_2 and CO_2 to become available for methanogenesis. Similar to the aforementioned AD with the fresh inoculum, the second and third intervals were related to the digestion of readily degradable and slow degradable organic materials, respectively [99]. Although the first three intervals were observed in AD13d, here a process failure was identified starting at the fourth interval (25-32 h). In this interval, a significant deceleration in all gas production rates was observed, which was then followed by the last interval (death phase), where total production rate was lower than 0.8 mL/gVS·h.

A correlation was seen between the lack of H_2 in the headspace after 21 h (Figure 4.3a) and the deceleration of CH_4 production after 26 h (Figure 4.3d). It is known that significant part of methanogenesis occurs by using CO_2 and H_2 and as such lack of H_2 dampens the total CH_4 production [104]. H_2 appeared first in liquid and then in the headspace and after 21 h was no longer detected in both phases. It is reasonable to assume that H_2 in the liquid was consumed to support methanogenesis and the remnant propagated to the headspace. Possibly, H_2 in the gas-phase has been either fully consumed or evacuated from the headspace which then led to a notable reduction in CH_4 production for the rest of the experiment.

Most of the biogas in AD46d was produced during a 10 h period in the second and third intervals (5-10 h) and similar to the previous section, it preferentially propagated into the headspace instead of being dissolved in the liquid. Consequently, H_2 level, and therefore CH_4, in the liquid were significantly lower than if they were calculated based on their corresponding headspace concentrations. This phenomenon, however, has less effect on CO_2 measurement in the liquid, considering its high solubility.

Relative to AD13d, here VS and TS removals were, 17% and 37% lower, respectively (Table 4.2). The high amount of VS removal can explain the rapid biogas production and suggests that the majority of VS were digested in the first 1-2 d. Whereas, the relatively low TS removal implies that the early failure of the AD process (~30 h) left the slow degradable organic materials indigested. Moreover, VA concentration was 40% higher than AD13d and included in the VA's inhibition range [181]. Perhaps the high level of VA was the cause of the reduced biogas production after 30 h [103]. The comparison between fresh and aged inoculums is further discussed in the next section.

Naturally, pH should decrease with increasing VA [98]. However, considering that VA have increased in all experiments and that the digestion was inhibited after 30 h, pH was found to be an unreliable indicator for assessing the health of the digestion since the expected trends

were not reflected clearly in pH measurements. In small batches like the experiments demonstrated in this chapter, the presence of other factors such as ammonia and phosphate can dominate the balance and hence increase alkalinity [110].

4.4.4 Comparison of aged and fresh inoculum

When aged inoculum was used, all gas species exhibited high production in the first 24 h, which overtook the production of the fresh sample (Figure 4.5). However, gas production rates decreased significantly for aged inoculum followed by high accumulated VA in the liquid and temporarily high concentration of H_2 in both phases (Figure 4.4 and Figure 4.6). Furthermore, when fresh inoculum was used, production rates stayed high within 300 h duration (Figure 4.2d), primarily consisted of CH_4. The average accumulation rate of VA was roughly 3 times lower and H_2 was mainly found in liquid at modest levels.

It can be suggested that when aged inoculum was used, the process resulted in food intake overload, featured with high bio-activity, high VS removal, low TS removal and high biogas production in the first 24 h and followed by significant bio-activity deceleration after 30 h (Figure 4.3d). Furthermore, aged inoculum digestion resulted in high levels of VA and short H_2 pulse that are linked to process imbalance [27,28,31,103,112,114,119,126,127]. Conversely, fresh inoculum demonstrated a more balanced process with high organics removal, lower accumulated VA and lower H_2 production that could enable continuous production of biogas exceeding 300 h (Figure 4.2) in a sealed digester and without additional feeding. It is possible that for aged inoculum, methanogenesis was inhibited and was not effective in processing the rapidly increased levels of H_2 and VA to CH_4 which inevitably, lead to the digester failure [28,103]. It is also possible that fresh inoculum's methanogens

were efficient in reducing H_2 and VA to CH_4 while regulating the digester and enabled biogas production for a longer period of time [118].

The inoculum composition didn't change significantly whilst it was stored (Table 4.3) and dissolved H_2, by itself, couldn't reliably provide an indication of process failure despite reports suggesting its high sensitivity to overload in specific processes [28]. Relying on indicators such as VA and dissolved H_2 only, operators can struggle to predict digestion failure in situations such as the food intake overload described in this chapter. Therefore, it is concluded that when these indicators fail to point to a clear indication, monitoring all gas components simultaneously can help to identify a failing batch process very early.

4.5 Conclusions

In the work presented in this chapter, the author introduced a development of low-cost, *in-situ* sensor arrays for continuous gas sensing in both liquid and gas phases, simultaneously. The novel route for gas sensing in liquid demonstrated many unique features and appeared to be very informative; especially with reference to the headspace gas profiles. The system enables real-time and long-term slurry probing for measuring gas partial pressures in liquid and at the same time the gas production in the headspace without any delay or the risk of sample contamination. Accuracy, longevity and reproducibility were validated using a series of batch AD experiments. The proposed approach was applied for real-time analysis of AD with inoculums at different ages. By using the new technology, the author could clearly identify process imbalance and failure when other popular monitoring indicators, such as pH and VA, couldn't give a clear real-time observation. While liquid-phase gas profiling could provide early warnings about the health of the process at the initiation stages, the gas-phase was an indication of health for biogas production. Applying this simple and new technology

in AD processes demonstrates the capability of gas profiles in providing essential monitoring information and their advantages in identifying process signatures that may be hindered by other commonly used indicators.

Chapter 5. SUMMARY AND FUTURE WORK

5.1 Concluding remarks

The author's aim in this PhD research was to address the gas profiling limitations and inadequacies experienced in quasi-closed, pressure regulated and anaerobic fermentation systems. Deriving gas production profile (GPP) is an essential and useful strategy for monitoring, investigating and diagnosing microbial processes which take place in such fermentation systems. In this work, the author targeted intestinal gas sensing, calculating GPP accurately and comprehensively for monitoring gas components found in anaerobic digestion (AD) processes in both liquid and gas phases. Therefore, the objectives of this PhD research included: (a) introducing a new, simple, low-cost and portable gas sensing technique for measuring intestinal gases in anaerobic environments (b) exploring the impacts different anaerobic environments have on the GPP of human fecal samples incubated *in-vitro* (c) accurately generating the GPP from the variety of sensors utilized in a fermentation system (d) measuring gas components of AD processes in both liquid and gas phases using the new gas profiling technology (e) Enhancing AD monitoring capability by investigating AD processes imbalances and failures utilizing gas component patterns.

As such, in order to achieve the research objectives and target the knowledge gaps, the author's work was organized and pursued in three major stages.

In the first stage, the author addressed the first two objectives. The author thoroughly investigated the literature on the available methods and their limitations for sensing intestinal gases *in-vitro*. At the time when this PhD started, sensing technology for colonic gases was partial, bulky, expensive, offline and included only limited. Continuous and simultaneous measurements of intestinal gases including CO_2, H_2, CH_4, H_2S and NO_x were not available and previous studies didn't pay enough attention to inter-correlation between different gases,

their kinetics and, consequently, the associated microbial processes. Therefore, in the first stage, addressing the first objective, the author developed a gas sensing technology for complete, continuous and simultaneous intestinal gas profiling. In addition, to address the second objective, the author used the new sensing unit to explore the impact of different anaerobic gas environment compositions on the GPPs of incubated human fecal samples.

In the second stage of this research, the author investigated the approaches of generating the GPPs from quasi-closed, pressure regulated fermentation systems. Although, many studies in the field included specific calculation methods, they are generally insufficient, inaccurate and not standardized. In order to standardize the GPP calculations, the author developed a rigorous mathematical gas fermentation model for gas production in such systems and addressed the third objective. The model was demonstrated on human fecal fermentation *in-vitro* in response to a high fermentable fibre substrate.

In the third stage, the author investigated the monitoring of gas components in AD processes. Although AD monitoring had been previously investigated, gas sensing technologies used in liquid were generally bulky, expensive or required high maintenance. Additionally, the literature on simultaneous and real-time profiling of multiple gases in both liquid and gas phases were not comprehensive which hindered the insight from the inter-correlation and kinetics of gas components in AD processes. Therefore, based on the development of gas profiling technology in the first two stages, the author developed an *in-situ*, online and low-cost technology for monitoring AD gas components in both liquid and gas phases.

As such, major achievements in each stage of this research are summarized as follows:

5.1.1 Stage 1

- An *in-vitro* low-cost, portable and continuous gas-profiling technology for sensing colonic gases of incubated fecal sample was successfully developed. This new approach accurately sensed CO_2, CH_4, H_2, H_2S and NO*x* simultaneously in an anaerobic environment. Reproducibility and repeatability were validated using healthy human fecal samples from 3 different volunteers, incubated with and without highly fermentable fibre as an added substrate. Gas sensors' accuracy and cross-sensitivities were verified against industrial standard gas tanks and found accurate with sufficiently low cross-sensitivity for a range of colonic gases in the headspace.
- NO*x* was not detected when healthy fecal samples were incubated as expected in previous reports [75,77]. NO*x* was only detected when substrates containing nitrogen were provided (outcomes included in the thesis of collaborator Dr CK Yao [183]). The ability of the new approach in sensing NO*x* for non-healthy subjects has significant insight potential and is recommended for future work.
- The Impact of three types of anaerobic gas environments: (type 1) 100% inert gas; (type 2) 6.5% CO_2 balanced with inert gas and (type 3) 5.5% CO_2, 5% H_2 balanced with inert gas were investigated. It was found that the presence of CO_2 only (type 2) promoted H_2 production which then results in stimulation of CH_4 and H_2S production and matched the familiar colonic gas production pathways (**Figure 1.1**). However, the addition of H_2 externally (type 3) possibly created an excess amount of H_2 which resulted in inhibition of CH_4 and H_2 production relative to supplementing with CO_2 only (type 2).
- Using fructooligosaccharides (FOS), a highly fermentable fibre, as substrate increased the bio-activity of fermentative bacteria and resulted in high production of CO_2, H_2 and CH_4. However, it was clearly observed that introducing FOS reduced the amount

of produced H_2S. Supressing H_2S by supplementing patients' diets with FOS may be a strategy for prevention and treatment of different types of inflammatory bowel disease (IBD) (*i.e.* ulcerative colitis (UC) outcomes included in the thesis of collaborator Dr CK Yao [183])

- This new, low-cost, portable and accurate technology, specially designed for measuring colonic gases in an anaerobic environment can provide invaluable insight on the microbial processes that take place in the human colon. In comparison to commonly used, off-line, bulky and expensive methods, this new approach presented many advantages which make it a unique tool for medical diagnostics in assessing diets and also therapeutics. Unlike other methods, the capabilities this technique can be delivered in a larger-scale and in the form of a clinical and medical tool used outside research laboratories.

5.1.2 Stage 2

- The author developed a rigorous, parametric and versatile gas fermentation model to describe the gas production of quasi-closed, pressure regulated fermentation systems. By introducing novel mass-flow equation, the author demonstrated how the different components of GPPs can be calculated accurately from the available sensing data. The fermentation model was simplified and designed to match with the standards of commercial fermentation systems, making the new technique readily applicable for other researches and engineers in that area.
- The new model was evaluated using the *in-vitro* fecal system developed in Chapter 2 where healthy human fecal sample was incubated with FOS as an added substrate. The GPP generated using the new mass-flow equation and the headspace's sensing data comprised of real-time internal pressure, cumulative pressure, temperature and gas mixing ratio. The produced GPP was verified against two independent

measurements, water vapor and total gas production, which confirmed the method's accuracy.

- The author investigated the influence of the different components, comprising the new mass-flow equation, have on the GPP. Testing a variety of components combinations, the impact of those on the gas production and rates was up to 94%. In comparison to other calculation methods, the effective headspace volume, a newly introduced component, contributed to up to 9.1% in the discussed example. Contributions of different components, comprising the developed model, were potentially greater if longer incubation time, higher internal pressure level, lower temperature or larger headspace were involved.
- The comprehensive design of the suggested model allowed it to be applied in a variety of configurations such as food production processes, biological reactors, biogas plants, wastewater treatment facilities and many more. The ability to include all possible contribution in the calculation of GPP can potentially improve significantly the knowledge derived from the GPP.

5.1.3 Stage 3

- Based on the developments in the first two stages the author of this thesis expanded the gas profiling technique, which was originally designed for measuring intestinal gas *in-vitro*, and developed a real-time, relatively simple, *in-situ* method for measuring gas components in AD processes in both liquid and gas phases, simultaneously. The author verified the novel approach's reproducibility, accuracy and longevity in a series of batch AD experiments.
- Outstanding advantage in measuring dissolved gas were featured in the new approach. Protected by a polydimethylsiloxane (PDMS) membrane, a commercial sensor was used for real-time probing of the digester's liquid medium. Consequently, the

dissolved gases partial pressures were measured *in-situ*, avoiding delays and the risk of contamination, existing in other methods. This *in-situ* technique allowed simultaneous presentation of gas components in both phases and reveals patterns linked to the relationships between different gases and their dynamics. The link to the microbial processes may be hindered by other popular used monitoring parameters which lack this type of presentation. Additionally, while biogas profiling provides an overall indication for the process yield, the liquid-phase profiling provides important information regarding the process health, especially in early stages, which is useful for predicting imbalance conditions.

- The author utilized the new method to explore the impact of inoculum age. In this PhD research, it has been shown that, relative to using fresh inoculum (age < 14 d), when aged inoculum was used (age > 45 days) there was a higher potential for entering an imbalance state and failure. By examining gas components only, the author showed that process imbalances can be clearly observed in real-time, whereas other commonly used parameters, such as volatile acids (VA) and pH, couldn't give evident, in advance, conclusion regarding the health of the digester content.
- The application of this new technology in AD processes showed how profiling gas components could enhance AD monitoring while providing essential, real-time information in both phases. The cost-effectivity and the simplicity of the measurement process presented by the author, together with the combination of gas profiles in both phases simultaneously makes this technique a useful indicator for early warning for process imbalances and failures.

In conclusion, this research project has successfully brought new ideas, knowledge and tools to anaerobic fermentation systems. The outcomes of this PhD research have been published

in peer reviewed scientific journals. A complete list of publications by the author since the beginning of his PhD research project, are presented in the following section.

5.2 Journal publications

The work conducted by the author of this dissertation during his PhD candidature, resulted in 5 journal publications (three as the first author). The list of author's scientific manuscripts is as follows:

- **A. Rotbart**, C. Yao, N. Ha, M.D. Chrisp, J.G. Muir, P.R. Gibson, K. Kalantar-zadeh, J.Z. Ou, Designing an *in-vitro* gas profiling system for human faecal samples, Sensors and Actuators B: Chemical, vol. 238, pp. 754-764, 2017.
- **A. Rotbart**, P.J. Moate, C. Yao, J.Z. Ou, K. Kalantar-zadeh, A novel mathematical model for the dynamic assessment of gas composition and production in closed or vented fermentation systems, Sensors and Actuators B: Chemical, (*Accepted 2017*).
- **A. Rotbart**, Z. Zahan, L. Greve, M. Othman, J.Z. Ou, K. Kalantar-zadeh, Exploring Continuous Gas Sensing in Liquid and Gas Phases for Monitoring Anaerobic Digestion. *Under review.*
- J.Z. Ou, C. Yao, **A. Rotbart**, J.G. Muir, P.R. Gibson, K. Kalantar-zadeh, Human intestinal gas measurement systems: in vitro fermentation and gas capsules, Trends in Biotechnology, vol 33, pp. 208-213, 2015.
- J.Z. Ou, W. Ge, B. Carey, T. Daeneke, **A. Rotbart**, W. Shan, Y. Wang, Z. Fu, A.F. Chrimes, W. Wlodarski, Physisorption-based charge transfer in two-dimensional S_nS_2 for selective and reversible NO_2 gas sensing, ACS Nano, vol. 9, pp. 10313-10323, 2015.

5.3 Conference presentations

In addition to journal publications, the author's work also presented at two conference of annual meeting of the British Society of Gastroenterology (BSG) 2017 Manchester, UK and Australian Gastroenterology Week (AGW) of the Gastroenterological Society of Australia (GESA) 2016 Adelaide, South Australia and the abstracts of the works appeared in *Gut* and *Gastroenterology and Hepatology* journals, respectively:

- **A. Rotbart**, K. Kalantar-zadeh, J. Ou, C. Yao, J. Muir, P. Gibson, PWE-005 New in vitro human faecal fermentation system for diagnosis and treatment of gastrointestinal disorders using continuous intestinal gas profiling, Gut, vol. 66, pp A128, 2017.
- C. Yao, **A. Rotbart**, K. Kalantar-Zadeh, J. Ou, J. Muir, P. Gibson, Modulation of hydrogen sulfide production from fecal microbiota by diet and mesalazine: utility of a novel in vitro gas-profiling technology, Journal of Gastroenterology and Hepatology, vol. 31, pp 7, 2016.

5.4 Recommendations for future work

In order to furthering the knowledge arising from profiling gas components in anaerobic fermentation systems and their associated applications, a number of suggestions for future works are presented as follows:

5.4.1 Exploring H_2S and NOx from fecal sample fermentation of patients

In this PhD research, the author demonstrated a new technology for sensing colonic gases including CO_2, CH_4, H_2, H_2S and NO*x* during incubation of fecal samples from healthy donors *in-vitro*. H_2S and NO*x* are linked to IBD diseases such as UC and Crohn's disease and also more serious disorders such as colon cancer [42,45,54,56,57]. Profiling these gases by applying the gas sensing unit on patients with such disorders can significantly contribute to

their symptom relief and remedy based on correct diagnosis. The configurations of H_2S and NO*x* profiles may explain the mechanisms that drive these disorders, whether they are resulted from bacterial activities or autoimmune reactions [57,184,185]. Additionally, the ability to apply and monitoring the outcomes of co-fermentation of fecal samples from patients with different substrates using the developed gas *in-vitro* sensing unit, will allow researchers in identifying diets and drugs that will prevent, decrease and possibly cure selected gut disorders.

5.4.2 Future models for advanced fermentation systems

In the work presented in this PhD thesis, the author developed a rigorous model for profiling the production of fermentation gases in quasi-close, pressure regulated anaerobic fermentation systems. Although, these types of systems appear in many industrial, farming and medical applications, in some other applications the fermentation systems can also incorporate gas inlets, headspace gas inhomogeneity or slurry feeding. In future works, the model can be expanded to include these components. As a result, the expanded model will provide researchers with a variety of mass-flow equations to allow accurate extraction of GPPs and increase the insight these GPPs can offer for gaining more information.

5.4.3 Monitoring and controlling continuous anaerobic digestions processes

In this PhD research, the author demonstrated a novel technique for real-time and *in-situ* gas profiling in both gas and liquid phases of AD processes, simultaneously. The new technique was demonstrated on a series of batch AD experiments for periods exceeding two weeks. AD for wastewater treatment and biogas production can include continuous feeding [94] in order to utilize the digester's culture for degrading more waste, consequently, increasing the process yield. Using the new technique for gas profiling, in such AD configurations, can help in finding the optimal loading rate that insures maximum yield, while protecting the system

from entering imbalance states. In addition, a control mechanism can be designed that utilizes gas profiles, produced in real-time in such AD processes, to modify the process conditions in order to avoid failures and to enhance yields. Moreover, the author recommends incorporating sensing capacity for H_2S and ammonia in both liquid and gas phases due to their important roles in AD [29,96,169].

REFERENCES

[1] L. Pasteur, Mémoire sur la fermentation applée lactique. Mémoire sur la fermentation alcoolique: Mallet-Bachelier; 1857.

[2] R.E. Speece, Anaerobic biotechnology for industrial wastewater treatment, Environ Sci Technol, 17(1983) 416A-427A.

[3] S.E. Oh, S. Van Ginkel, B.E. Logan, The relative effectiveness of pH control and heat treatment for enhancing biohydrogen gas production, Environ Sci Technol, 37(2003) 5186-5190.

[4] P. Weiland, Biogas production: current state and perspectives, Appl Microbiol Biotechnol, 85(2010) 849-860.

[5] O. Mizuno, R. Dinsdale, F.R. Hawkes, D.L. Hawkes, T. Noike, Enhancement of hydrogen production from glucose by nitrogen gas sparging, Bioresour Technol, 73(2000) 59-65.

[6] M.J. Wolin, The rumen fermentation: a model for microbial interactions in anaerobic ecosystems, Adv Microb Ecol 3(1979) 49-77.

[7] M. Pimentel, R. Mathur, C. Chang, Gas and the microbiome, Curr Gastroenterol Rep, 15(2013) 356.

[8] M.D. Levitt, Volume and composition of human intestinal gas determined by means of an intestinal washout technic, N Engl J Med, 284(1971) 1394-1398.

[9] H.Y. Wang, C.L. Cooney, D.I. Wang, Computer aided baker's yeast fermentations, Biotechnol Bioeng, 19(1977) 69-86.

[10] K.H. Steinkraus, Lactic acid fermentation in the production of foods from vegetables, cereals and legumes, Antonie Van Leeuwenhoek, 49(1983) 337-348.

[11] H. Prevost, C. Divies, Fresh fermented cheese production with continuous pre-fermented milk by a mixed culture of mesophilic lactic streptococci entrapped in Ca-Al ginate, Biotechnol Lett, 9(1987) 789-794.

[12] F. Leroy, L. De Vuyst, Lactic acid bacteria as functional starter cultures for the food fermentation industry, Trends Food Sci Technol, 15(2004) 67-78.

[13] G.H. Fleet, Wine microbiology and biotechnology: CRC Press; 1993.

[14] Y. Kourkoutas, A. Bekatorou, I.M. Banat, R. Marchant, A. Koutinas, Immobilization technologies and support materials suitable in alcohol beverages production: a review, Food Microbiol, 21(2004) 377-397.

[15] C.A. Masschelein, D.S. Ryder, J.-P. Simon, Immobilized cell technology in beer production, Crit Rev Biotechnol, 14(1994) 155-177.

[16] C. Rymer, J. Huntington, B. Williams, D. Givens, In vitro cumulative gas production techniques: history, methodological considerations and challenges, Anim Feed Sci Technol, 123(2005) 9-30.

[17] M. Blu, E. Ørskov, Comparison of in vitro gas production and nylon bag degradability of roughages in predicting feed intake in cattle, Anim Feed Sci Technol, 40(1993) 109-119.

[18] M.V. Moreno-Arribas, M.C. Polo, F. Jorganes, R. Muñoz, Screening of biogenic amine production by lactic acid bacteria isolated from grape must and wine, Int J Food Microbiol, 84(2003) 117-123.

[19] J.Y. Jung, S.H. Lee, C.O. Jeon, Kimchi microflora: history, current status, and perspectives for industrial kimchi production, Appl Microbiol Biotechnol, 98(2014) 2385-2393.

[20] C. Edwards, G. Gibson, M. Champ, B.B. Jensen, J. Mathers, F. Nagengast, C. Rumney, A. Quehl, In vitro method for quantification of the fermentation of starch by human faecal bacteria, J Sci Food Agric, 71(1996) 209-217.

[21] C. Walton, D.P. Fowler, C. Turner, W. Jia, R.N. Whitehead, L. Griffiths, C. Dawson, R.H. Waring, D.B. Ramsden, J.A. Cole, M. Cauchi, C. Bessant, J.O. Hunter, Analysis of volatile organic compounds of bacterial origin in chronic gastrointestinal diseases, Inflamm Bowel Dis, 19(2013) 2069-2078.

[22] D.C. Hernot, T.W. Boileau, L.L. Bauer, I.S. Middelbos, M.R. Murphy, K.S. Swanson, G.C. Fahey Jr, In vitro fermentation profiles, gas production rates, and microbiota modulation as affected by certain fructans, galactooligosaccharides, and polydextrose, J Agric Food Chem, 57(2009) 1354-1361.

[23] S. Karppinen, K. Liukkonen, A.M. Aura, P. Forssell, K. Poutanen, In vitro fermentation of polysaccharides of rye, wheat and oat brans and inulin by human faecal bacteria, J Sci Food Agr, 80(2000) 1469-1476.

[24] J. Nelson, F. Bishay, A. Van Roodselaar, M. Ikonomou, F.C. Law, The use of in vitro bioassays to quantify endocrine disrupting chemicals in municipal wastewater treatment plant effluents, Sci Total Environ, 374(2007) 80-90.

[25] S.K. Han, H.S. Shin, Biohydrogen production by anaerobic fermentation of food waste, Int J Hydrogen Energy, 29(2004) 569-577.

[26] B.E. Logan, S.-E. Oh, I.S. Kim, S. Van Ginkel, Biological hydrogen production measured in batch anaerobic respirometers, Environ Sci Technol, 36(2002) 2530-2535.

[27] J.P. Steyer, J.C. Bouvier, T. Conte, P. Gras, P. Sousbie, Evaluation of a four year experience with a fully instrumented anaerobic digestion process, Water Sci Technol, 45(2002) 495-502.

[28] L. Björnsson, M. Murto, T.G. Jantsch, B. Mattiasson, Evaluation of new methods for the monitoring of alkalinity, dissolved hydrogen and the microbial community in anaerobic digestion, Water Res, 35(2001) 2833-2840.

[29] A.J. Ward, P.J. Hobbs, P.J. Holliman, D.L. Jones, Optimisation of the anaerobic digestion of agricultural resources, Bioresour Technol, 99(2008) 7928-7940.

[30] R. Cord-Ruwisch, T.I. Mercz, C.Y. Hoh, G.E. Strong, Dissolved hydrogen concentration as an on-line control parameter for the automated operation and optimization of anaerobic digesters, Biotechnol Bioeng, 56(1997) 626-634.

[31] G. Strong, R. Cord-Ruwisch, An in situ dissolved-hydrogen probe for monitoring anaerobic digesters under overload conditions, Biotechnol Bioeng, 45(1995) 63-68.

[32] K. Kuroda, R.G. Silveira, N. Nishio, H. Sunahara, S. Nagai, Measurement of dissolved hydrogen in an anaerobic digestion process by a membrane-covered electrode, J Ferment Bioeng, 71(1991) 418-423.

[33] T. Whitmore, D. Lloyd, Mass spectrometric control of the thermophilic anaerobic digestion process based on levels of dissolved hydrogen, Biotechnol Lett, 8(1986) 203-208.

[34] T. Whitmore, D. Lloyd, G. Jones, T. Williams, Hydrogen-dependent control of the continuous anaerobic digestion process, Appl Microbiol Biotechnol, 26(1987) 383-388.

[35] H. Nanto, S. Tsubakino, M. Ikeda, F. Endo, Identification of aromas from wine using quartz-resonator gas sensors in conjuction with neural-network analysis, Sensors and Actuators B: Chemical, 25(1995) 794-796.

[36] M. Peris, L. Escuder-Gilabert, On-line monitoring of food fermentation processes using electronic noses and electronic tongues: a review, Analytica chimica acta, 804(2013) 29-36.

[37] J.Z. Ou, C. Yao, A. Rotbart, J.G. Muir, P.R. Gibson, K. Kalantar-zadeh, Human intestinal gas measurement systems: in vitro fermentation and gas capsules, Trends in biotechnology, 33(2015) 208-213.

[38] K. Kalantar-Zadeh, C.K. Yao, K.J. Berean, N. Ha, J.Z. Ou, S.A. Ward, N. Pillai, J. Hill, J.J. Cottrell, F.R. Dunshea, Intestinal gas capsules: A proof-of-concept demonstration, Gastroenterology, 150(2016) 37-39.

[39] J.Z. Ou, J.J. Cottrell, N. Ha, N. Pillai, C.K. Yao, K.J. Berean, S.A. Ward, D. Grando, J.G. Muir, C.J. Harrison, Potential of in vivo real-time gastric gas profiling: a pilot evaluation of heat-stress and modulating dietary cinnamon effect in an animal model, Scientific reports, 6(2016).

[40] K. Kalantar-zadeh, N. Ha, J.Z. Ou, K.J. Berean, Ingestible sensors, ACS Sensors, 2(2017) 468-483.

[41] J.K. Nicholson, E. Holmes, J. Kinross, R. Burcelin, G. Gibson, W. Jia, S. Pettersson, Host-gut microbiota metabolic interactions, Science, 336(2012) 1262-1267.

[42] F. Carbonero, A.C. Benefiel, H.R. Gaskins, Contributions of the microbial hydrogen economy to colonic homeostasis, Nat Rev Gastroenterol Hepatol, 9(2012) 504-518.

[43] A.B. Sahakian, S.R. Jee, M. Pimentel, Methane and the gastrointestinal tract, Dig Dis Sci, 55(2010) 2135-2143.

[44] R.M. Thorn, J. Greenman, Microbial volatile compounds in health and disease conditions, J Breath Res, 6(2012) 024001.

[45] M. Medani, D. Collins, N.G. Docherty, A.W. Baird, P.R. O'Connell, D.C. Winter, Emerging role of hydrogen sulfide in colonic physiology and pathophysiology, Inflamm Bowel Dis, 17(2011) 1620-1625.

[46] R.B. Canani, P. Cirillo, E. Bruzzese, M. Graf, G. Terrin, G. Gaudiello, M. De Curtis, S. Cucchiara, A. Guarino, Nitric oxide production in rectal dialysate is a marker of disease activity and location in children with inflammatory bowel disease, Am J Gastroenterol, 97(2002) 1574-1576.

[47] S.J. Shepherd, M.C. Lomer, P.R. Gibson, Short-chain carbohydrates and functional gastrointestinal disorders, Am J Gastroenterol, 108(2013) 707-717.

[48] D.K. Ong, S.B. Mitchell, J.S. Barrett, S.J. Shepherd, P.M. Irving, J.R. Biesiekierski, S. Smith, P.R. Gibson, J.G. Muir, Manipulation of dietary short chain carbohydrates alters the pattern of gas production and genesis of symptoms in irritable bowel syndrome, J Gastroenterol Hepatol, 25(2010) 1366-1373.

[49] W. Shin, Medical applications of breath hydrogen measurements, Anal Bioanal Chem, 406(2014) 3931-3939.

[50] F.L. Suarez, M.D. Levitt, An understanding of excessive intestinal gas, Curr Gastroenterol Rep, 2(2000) 413-419.

[51] W.G. Thompson, G. Longstreth, D. Drossman, K. Heaton, E. Irvine, S. Müller-Lissner, Functional bowel disorders and functional abdominal pain, Gut, 45(1999) II43-II47.

[52] K. Triantafyllou, C. Chang, M. Pimentel, Methanogens, methane and gastrointestinal motility, J Neurogastroenterol Motil, 20(2014) 31-40.

[53] D.R. Linden, Hydrogen sulfide signaling in the gastrointestinal tract, Antioxid Redox Signal, 20(2014) 818-830.

[54] W.E. Roediger, J. Moore, W. Babidge, Colonic sulfide in pathogenesis and treatment of ulcerative colitis, Dig Dis Sci, 42(1997) 1571-1579.

[55] L.R. Rivera, D.P. Poole, M. Thacker, J.B. Furness, The involvement of nitric oxide synthase neurons in enteric neuropathies, Neurogastroenterol Motil, 23(2011) 980-988.

[56] J.O. Lundberg, P.M. Hellstrom, M.K. Fagerhol, E. Weitzberg, A.G. Roseth, Technology insight: calprotectin, lactoferrin and nitric oxide as novel markers of inflammatory bowel disease, Nat Clin Pract Gastroenterol Hepatol, 2(2005) 96-102.

[57] W.E. Roediger, Review article: nitric oxide from dysbiotic bacterial respiration of nitrate in the pathogenesis and as a target for therapy of ulcerative colitis, Aliment Pharmacol Ther, 27(2008) 531-541.

[58] B.P. de Lacy Costello, M. Ledochowski, N.M. Ratcliffe, The importance of methane breath testing: a review, J Breath Res, 7(2013) 024001.

[59] N.J. Rattray, Z. Hamrang, D.K. Trivedi, R. Goodacre, S.J. Fowler, Taking your breath away: metabolomics breathes life in to personalized medicine, Trends Biotechnol, 32(2014) 538-548.

[60] K.L. Dear, M. Elia, J.O. Hunter, Do interventions which reduce colonic bacterial fermentation improve symptoms of irritable bowel syndrome?, Dig Dis Sci, 50(2005) 758-766.

[61] T.S. King, M. Elia, J.O. Hunter, Abnormal colonic fermentation in irritable bowel syndrome, The Lancet, 352(1998) 1187-1189.

[62] B. De Lacy Costello, R. Ewen, A.K. Ewer, C.E. Garner, C.S.J. Probert, N.M. Ratcliffe, S. Smith, An analysis of volatiles in the headspace of the faeces of neonates, J Breath Res, 2(2008) 037023.

[63] E. Dixon, C. Clubb, S. Pittman, L. Ammann, Z. Rasheed, N. Kazmi, A. Keshavarzian, P. Gillevet, H. Rangwala, R.D. Couch, Solid-phase microextraction and the human fecal VOC metabolome, PLoS ONE, 6(2011) e18471.

[64] C.E. Garner, S. Smith, B. De Lacy Costello, P. White, R. Spencer, C.S.J. Probert, N.M. Ratcliffe, Volatile organic compounds from feces and their potential for diagnosis of gastrointestinal disease, FASEB J, 21(2007) 1675-1688.

[65] C.S.J. Probert, Role of faecal gas analysis for the diagnosis of IBD, Biochem Soc Trans, 39(2011) 1079-1080.

[66] C. Walton, D.P. Fowler, C. Turner, W. Jia, R.N. Whitehead, L. Griffiths, C. Dawson, R.H. Waring, D.B. Ramsden, J.A. Cole, Analysis of volatile organic compounds of bacterial origin in chronic gastrointestinal diseases, Inflamm Bowel Dis, 19(2013) 2069-2078.

[67] R.P. Arasaradnam, J.A. Covington, C. Harmston, C.U. Nwokolo, Review article: Next generation diagnostic modalities in gastroenterology - Gas phase volatile compound biomarker detection, Aliment Pharmacol Ther, 39(2014) 780-789.

[68] K.H. Kim, S.A. Jahan, E. Kabir, A review of breath analysis for diagnosis of human health, Trends Analyt Chem, 33(2012) 1-8.

[69] T.G. De Meij, I.B. Larbi, M.P. Van Der Schee, Y.E. Lentferink, T. Paff, J.S. Terhaar Sive Droste, C.J. Mulder, A.A. Van Bodegraven, N.K. De Boer, Electronic nose can discriminate colorectal carcinoma and advanced adenomas by fecal volatile biomarker analysis: Proof of principle study, Int J Cancer, 134(2014) 1132-1138.

[70] S.F. Shepherd, N.D. McGuire, B.P.J. De Lacy Costello, R.J. Ewen, D.H. Jayasena, K. Vaughan, I. Ahmed, C.S. Probert, N.M. Ratcliffe, The use of a gas chromatograph coupled to a metal oxide sensor for rapid assessment of stool samples from irritable bowel syndrome and inflammatory bowel disease patients, J Breath Res, 8(2014) 026001

[71] F. Steggerda, Gastrointestinal gas following food consumption, Ann N Y Acad Sci, 150(1968) 57-66.

[72] F. Suarez, J. Furne, J. Springfield, M. Levitt, Insights into human colonic physiology obtained from the study of flatus composition, Am J Syph Gonorrhea Vener Dis, 272(1997) G1028-G1033.

[73] A. Tangerman, Measurement and biological significance of the volatile sulfur compounds hydrogen sulfide, methanethiol and dimethyl sulfide in various biological matrices, J Chromatogr B Analyt Technol Biomed Life Sci, 877(2009) 3366-3377.

[74] F. Suarez, J. Springfield, M. Levitt, Identification of gases responsible for the odour of human flatus and evaluation of a device purported to reduce this odour, Gut, 43(1998) 100-104.

[75] J. Lundberg, J. Lundberg, K. Alving, P. Hellström, Greatly increased luminal nitric oxide in ulcerative colitis, The Lancet, 344(1994) 1673-1674.

[76] M. Herulf, T. Ljung, P. Hellström, E. Weitzberg, J. Lundberg, Increased luminal nitric oxide in inflammatory bowel disease as shown with a novel minimally invasive method, Scand J Gastroenterol, 33(1998) 164-169.

[77] T. Sobko, M. Norman, E. Norin, L. Gustafsson, J. Lundberg, Birth-related increase in intracolonic hydrogen gas and nitric oxide as indicator of host–microbial interactions, Allergy, 60(2005) 396-400.

[78] K. Decroos, S. Vanhemmens, S. Cattoir, N. Boon, W. Verstraete, Isolation and characterisation of an equol-producing mixed microbial culture from a human faecal sample and its activity under gastrointestinal conditions, Arch Microbiol, 183(2005) 45-55.

[79] H. Oike, K. Aramaki, T. TOKUNACA, H. Iino, M. Hirayama, Suppressive effect of fructooligosaccharides on the generation of volatile methanethiol in a fecal incubation method and human feces, Biosci Microflora, 19(2000) 51-59.

[80] K. Kalantar-zadeh, B. Fry, Nanotechnology-enabled sensors: Springer; 2007.

[81] G. Korotcenkov, Metal oxides for solid-state gas sensors: What determines our choice?, MAT SCI ENG B-SOLID, 139(2007) 1-23.

[82] J.R. Wilkins, Pressure transducer method for measuring gas production by microorganisms, Appl Microbiol, 27(1974) 135-140.

[83] M.K. Theodorou, B.A. Williams, M.S. Dhanoa, A.B. McAllan, J. France, A simple gas production method using a pressure transducer to determine the fermentation kinetics of ruminant feeds, Anim Feed Sci Technol, 48(1994) 185-197.

[84] M. Cattani, F. Tagliapietra, L. Maccarana, H.H. Hansen, L. Bailoni, S. Schiavon, Technical note: in-vitro total gas and methane production measurements from closed or vented rumen batch culture systems, J Dairy Sci, 97(2014) 1736-1741.

[85] M.H. Tavendale, L.P. Meagher, D. Pacheco, N. Walker, G.T. Attwood, S. Sivakumaran, Methane production from in vitro rumen incubations with Lotus pedunculatus and Medicago sativa, and effects of extractable condensed tannin fractions on methanogenesis, Anim Feed Sci Technol, 123-124(2005) 403-419.

[86] R.M. Mauricio, F.L. Mould, M.S. Dhanoa, E. Owen, K.S. Channa, M.K. Theodorou, A semi-automated in vitro gas production technique for ruminant feedstuff evaluation, Anim Feed Sci Technol, 79(1999) 321-330.

[87] J.W. Cone, A.H. van Gelder, G.J. Visscher, L. Oudshoorn, Influence of rumen fluid and substrate concentration on fermentation kinetics measured with a fully automated time related gas production apparatus, Anim Feed Sci Technol, 61(1996) 113-128.

[88] Z. Davies, D. Mason, A. Brooks, G. Griffith, R. Merry, M. Theodorou, An automated system for measuring gas production from forages inoculated with rumen fluid and its use in determining the effect of enzymes on grass silage, Anim Feed Sci Technol, 83(2000) 205-221.

[89] M. Hannah, P. Moate, P.A. Hess, V. Russo, J. Jacobs, R. Eckard, Mathematical formulae for accurate estimation of in vitro CH4 production from vented bottles, Anim Prod Sci, 56(2016) 244-251.

[90] M.Z. Atashbar, S. Singamaneni, Room temperature gas sensor based on metallic nanowires, Sens Actuator B-Chem, 111(2005) 13-21.

[91] M.Z. Atashbar, D. Banerji, S. Singamaneni, Room-temperature hydrogen sensor based on palladium nanowires, IEEE Sens J, 5(2005) 792-797.

[92] J.P. Goopy, A. Donaldson, R. Hegarty, P.E. Vercoe, F. Haynes, M. Barnett, V.H. Oddy, Low-methane yield sheep have smaller rumens and shorter rumen retention time, Br J Nutr, 111(2014) 578-585.

[93] J. Hill, C. McSweeney, A.-D.G. Wright, G. Bishop-Hurley, K. Kalantar-zadeh, Measuring methane production from ruminants, Trends Biotechnol, 34(2016) 26-35.

[94] F. Monnet, An introduction to anaerobic digestion of organic wastes, Remade Scotland, (2003) 1-48.

[95] S. Tafdrup, Viable energy production and waste recycling from anaerobic digestion of manure and other biomass materials, Biomass Bioenerg, 9(1995) 303-314.

[96] J. Mata-Alvarez, Biomethanization of the organic fraction of municipal solid wastes, London, U.K.: IWA publishing; 2002.

[97] Y.J. Chan, M.F. Chong, C.L. Law, D. Hassell, A review on anaerobic–aerobic treatment of industrial and municipal wastewater, Chem Eng J, 155(2009) 1-18.

[98] K. Boe, D.J. Batstone, J.-P. Steyer, I. Angelidaki, State indicators for monitoring the anaerobic digestion process, Water Res, 44(2010) 5973-5980.

[99] Z. Zahan, M.Z. Othman, W. Rajendram, Anaerobic Codigestion of Municipal Wastewater Treatment Plant Sludge with Food Waste: A Case Study, BioMed Res Int, 2016(2016).

[100] P.F. Pind, I. Angelidaki, B.K. Ahring, A new VFA sensor technique for anaerobic reactor systems, Biotechnol Bioeng, 82(2003) 54-61.

[101] T. Mechichi, S. Sayadi, Evaluating process imbalance of anaerobic digestion of olive mill wastewaters, Process Biochem, 40(2005) 139-145.

[102] F. Molina, M. Castellano, C. García, E. Roca, J. Lema, Selection of variables for on-line monitoring, diagnosis, and control of anaerobic digestion processes, Water Sci Technol, 60(2009) 615-622.

[103] B.K. Ahring, M. Sandberg, I. Angelidaki, Volatile fatty acids as indicators of process imbalance in anaerobic digestors, Appl Microbiol Biotechnol, 43(1995) 559-565.

[104] W. Gujer, A.J. Zehnder, Conversion processes in anaerobic digestion, Water Sci Technol, 15(1983) 127-167.

[105] M. Madsen, J.B. Holm-Nielsen, K.H. Esbensen, Monitoring of anaerobic digestion processes: A review perspective, Renew Sustainable Energy Rev, 15(2011) 3141-3155.

[106] L. Björnsson, M. Murto, B. Mattiasson, Evaluation of parameters for monitoring an anaerobic co-digestion process, Appl Microbiol Biotechnol, 54(2000) 844-849.

[107] H.F. Jacobi, C.R. Moschner, E. Hartung, Use of near infrared spectroscopy in monitoring of volatile fatty acids in anaerobic digestion, Water Sci Technol, 60(2009) 339-346.

[108] J. Lay, Y. Li, T. Noike, J. Endo, S. Ishimoto, Analysis of environmental factors affecting methane production from high-solids organic waste, Water Sci Technol, 36(1997) 493-500.

[109] D.R. Boone, L. Xun, Effects of pH, temperature, and nutrients on propionate degradation by a methanogenic enrichment culture, Appl Environ Microbiol, 53(1987) 1589-1592.

[110] I. Angelidaki, B. Ahring, Anaerobic thermophilic digestion of manure at different ammonia loads: effect of temperature, Water Res, 28(1994) 727-731.

[111] J. Liu, G. Olsson, B. Mattiasson, Monitoring of two-stage anaerobic biodegradation using a BOD biosensor, J Biotechnol, 100(2003) 261-265.

[112] J. Liu, G. Olsson, B. Mattiasson, On-line monitoring of a two-stage anaerobic digestion process using a BOD analyzer, J Biotechnol, 109(2004) 263-275.

[113] I. Angelidaki, L. Ellegaard, B. Ahring, Applications of the anaerobic digestion process, in: B. Ahring (Ed.) Biomethanation II, Springer, Berlin Heidelberg, 2003, pp. 1-33.

[114] B. Schink, Energetics of syntrophic cooperation in methanogenic degradation, Microbiol Mol Biol Rev, 61(1997) 262-280.

[115] A.J. Stams, A.J. Zehnder, Ecological impact of syntrophic alcohol and fatty acid oxidation, in: J.P. Bélaich, M. Bruschi, J.L. Garcia (Eds.), Microbiology and biochemistry of strict anaerobes involved in interspecies hydrogen transfer, Springer US, New York, 1990, pp. 87-98.

[116] F. De Bok, C. Plugge, A. Stams, Interspecies electron transfer in methanogenic propionate degrading consortia, Water Res, 38(2004) 1368-1375.

[117] A. Stams, C. Plugge, F. De Bok, B. Van Houten, P. Lens, H. Dijkman, J. Weijma, Metabolic interactions in methanogenic and sulfate-reducing bioreactors, Water Sci Technol, 52(2005) 13-20.

[118] B. Schink, Synergistic interactions in the microbial world, Antonie Leeuwenhoek, 81(2002) 257-261.

[119] D.B. Archer, M.G. Hilton, P. Adams, H. Wiecko, Hydrogen as a process control index in a pilot scale anaerobic digester, Biotechnol Lett, 8(1986) 197-202.

[120] S.R. Harper, F.G. Pohland, Recent developments in hydrogen management during anaerobic biological wastewater treatment, Biotechnol Bioeng, 28(1986) 585-602.

[121] D. Kidby, D. Nedwell, An investigation into the suitability of biogas hydrogen concentration as a performance monitor for anaerobic sewage sludge digesters, Water Res, 25(1991) 1007-1012.

[122] A. Guwy, F. Hawkes, D. Hawkes, A. Rozzi, Hydrogen production in a high rate fluidised bed anaerobic digester, Water Res, 31(1997) 1291-1298.

[123] R.K. Voolapalli, D.C. Stuckey, Hydrogen production in anaerobic reactors during shock loads—influence of formate production and H 2 kinetics, Water Res, 35(2001) 1831-1841.

[124] D. Chynoweth, S. Svoronos, G. Lyberatos, J. Harman, P. Pullammanappallil, J. Owens, M. Peck, Real-time expert system control of anaerobic digestion, Water Sci Technol, 30(1994) 21-29.

[125] J. Liu, G. Olsson, B. Mattiasson, Monitoring and control of an anaerobic upflow fixed-bed reactor for high-loading-rate operation and rejection of disturbances, Biotechnol Bioeng, 87(2004) 43-53.

[126] F. Hawkes, A. Guwy, A. Rozzi, D. Hawkes, A new instrument for on-line measurement of bicarbonate alkalinity, Water Res, 27(1993) 167-170.

[127] M. Hannsson, Å. Nordberg, I. Sundh, B. Mathisen, Early warning of disturbances in a laboratory-scale MSW biogas process, Water Sci Technol, 45(2002) 255-260.

[128] R. Moletta, Y. Escoffier, F. Ehlinger, J.-P. Coudert, J.-P. Leyris, On-line automatic control system for monitoring an anaerobic fluidized-bed reactor: response to organic overload, Water Sci Technol, 30(1994) 11-20.

[129] A. Pauss, S.R. Guiot, Hydrogen monitoring in anaerobic sludge bed reactors at various hydraulic regimes and loading rates, Water Environ Res, 65(1993) 276-280.

[130] A. Pauss, G. Andre, M. Perrier, S.R. Guiot, Liquid-to-gas mass transfer in anaerobic processes: inevitable transfer limitations of methane and hydrogen in the biomethanation process, Appl Environ Microbiol, 56(1990) 1636-1644.

[131] S. Mathiot, Y. Escoffier, F. Ehlinger, J. Couderc, J.-P. Leyris, R. Moletta, Control parameter variations in an anaerobic fluidised bed reactor subjected to organic shockloads, Water Sci Technol, 25(1992) 93-101.

[132] A. Rotbart, C. Yao, N. Ha, M.D. Chrisp, J.G. Muir, P.R. Gibson, K. Kalantar-zadeh, J.Z. Ou, Designing an in-vitro gas profiling system for human faecal samples, Sens Actuator B-Chem, 238(2017) 754-764.

[133] J.Z. Ou, W. Ge, B. Carey, T. Daeneke, A. Rotbart, W. Shan, Y. Wang, Z. Fu, A.F. Chrimes, W. Wlodarski, Physisorption-based charge transfer in two-dimensional S_nS_2 for selective and reversible NO_2 gas sensing, ACS nano, 9(2015) 10313-10323.

[134] M.A. Butler, Optical fiber hydrogen sensor, Appl Phys Lett, 45(1984) 1007-1009.

[135] H. Segawa, E. Ohnishi, Y. Arai, K. Yoshida, Sensitivity of fiber-optic carbon dioxide sensors utilizing indicator dye, Sens Actuators B Chem, 94(2003) 276-281.

[136] B. Culshaw, G. Stewart, F. Dong, C. Tandy, D. Moodie, Fibre optic techniques for remote spectroscopic methane detection—from concept to system realisation, Sens Actuators B Chem, 51(1998) 25-37.

[137] S.K. Pandey, K.-H. Kim, K.-T. Tang, A review of sensor-based methods for monitoring hydrogen sulfide, Trends Analyt Chem, 32(2012) 87-99.

[138] D. Kley, M. McFarland, Chemiluminescence detector for NO and NO_2, Atmos Technol;(United States), 12(1980).

[139] Z. Zhang, H. Jiang, Z. Xing, X. Zhang, A highly selective chemiluminescent H_2S sensor, Sens Actuators B Chem, 102(2004) 155-161.

[140] J. Hodgkinson, R.P. Tatam, Optical gas sensing: a review, Meas Sci Technol, 24(2013) 012004.

[141] S.W. Sharpe, T.J. Johnson, R.L. Sams, P.M. Chu, G.C. Rhoderick, P.A. Johnson, Gas-phase databases for quantitative infrared spectroscopy, Appl Spectrosc, 58(2004) 1452-1461.

[142] P. Jasiński, Solid-state electrochemical gas sensors, Materials Science-Poland, 24(2006) 269-278.

[143] J.R. Stetter, J. Li, Amperometric gas sensors a review, Chem Rev, 108(2008) 352-366.

[144] X. Liu, S. Cheng, H. Liu, S. Hu, D. Zhang, H. Ning, A survey on gas sensing technology, Sensors, 12(2012) 9635-9665.

[145] N.H. Park, T. Akamatsu, T. Itoh, N. Izu, W. Shin, Calorimetric thermoelectric gas sensor for the detection of hydrogen, methane and mixed gases, Sensors 14(2014) 8350-8362.

[146] S. Zhao, J. Xue, W. Kang, Gas adsorption on MoS_2 monolayer from first-principles calculations, Chemical Physics Letters, 595(2014) 35-42.

[147] G.F. Fine, L.M. Cavanagh, A. Afonja, R. Binions, Metal oxide semi-conductor gas sensors in environmental monitoring, Sensors, 10(2010) 5469-5502.

[148] A. Afzal, N. Cioffi, L. Sabbatini, L. Torsi, NO*x* sensors based on semiconducting metal oxide nanostructures: progress and perspectives, Sens Actuators B Chem, 171(2012) 25-42.

[149] N. Iqbal, A. Afzal, N. Cioffi, L. Sabbatini, L. Torsi, NO*x* sensing one-and two-dimensional carbon nanostructures and nanohybrids: Progress and perspectives, Sens Actuators B Chem, 181(2013) 9-21.

[150] H. Bai, G. Shi, Gas sensors based on conducting polymers, Sensors, 7(2007) 267-307.

[151] F. Schedin, A. Geim, S. Morozov, E. Hill, P. Blake, M. Katsnelson, K. Novoselov, Detection of individual gas molecules adsorbed on graphene, Nat Mater, 6(2007) 652-655.

[152] B. Cho, M.G. Hahm, M. Choi, J. Yoon, A.R. Kim, Y.-J. Lee, S.-G. Park, J.-D. Kwon, C.S. Kim, M. Song, Charge-transfer-based gas sensing using atomic-layer MoS_2, Sci Rep, 5(2015).

[153] D.J. Late, Y.-K. Huang, B. Liu, J. Acharya, S.N. Shirodkar, J. Luo, A. Yan, D. Charles, U.V. Waghmare, V.P. Dravid, Sensing behavior of atomically thin-layered MoS_2 transistors, Acs Nano, 7(2013) 4879-4891.

[154] M. Donarelli, S. Prezioso, F. Perrozzi, F. Bisti, M. Nardone, L. Giancaterini, C. Cantalini, L. Ottaviano, Response to NO_2 and other gases of resistive chemically exfoliated MoS_2-based gas sensors, Sens Actuators B Chem, 207(2015) 602-613.

[155] Q. He, Z. Zeng, Z. Yin, H. Li, S. Wu, X. Huang, H. Zhang, Fabrication of Flexible MoS_2 Thin-Film Transistor Arrays for Practical Gas-Sensing Applications, Small, 8(2012) 2994-2999.

[156] H. Li, Z. Yin, Q. He, H. Li, X. Huang, G. Lu, D.W.H. Fam, A.I.Y. Tok, Q. Zhang, H. Zhang, Fabrication of Single-and Multilayer MoS_2 Film-Based Field-Effect Transistors for Sensing NO at Room Temperature, small, 8(2012) 63-67.

[157] D. Reger, S. Goode, D. Ball, Chemistry: principles and practice: Cengage Learning; 2009.

[158] P.R. Gibson, S.J. Shepherd, Food Choice as a Key Management Strategy for Functional Gastrointestinal Symptoms, Am J Gastroenterol, 107(2012) 657-666.

[159] E.P. Halmos, V.A. Power, S.J. Shepherd, P.R. Gibson, J.G. Muir, A diet low in FODMAPs reduces symptoms of irritable bowel syndrome, Gastroenterology, 146(2014) 67-75 e65.

[160] H.M. Staudacher, M.C. Lomer, J.L. Anderson, J.S. Barrett, J.G. Muir, P.M. Irving, K. Whelan, Fermentable carbohydrate restriction reduces luminal bifidobacteria and gastrointestinal symptoms in patients with irritable bowel syndrome, J Nutr, 142(2012) 1510-1518.

[161] H.M. Staudacher, K. Whelan, P.M. Irving, M.C. Lomer, Comparison of symptom response following advice for a diet low in fermentable carbohydrates (FODMAPs) versus standard dietary advice in patients with irritable bowel syndrome, J Hum Nutr Diet, 24(2011) 487-495.

[162] Y. Kim, G. Lee, S. Park, B. Kim, J.-O. Park, J.-h. Cho, Pressure monitoring system in gastro-intestinal tract, Robotics and Automation, 2005 ICRA 2005 Proceedings of the 2005 IEEE International Conference on, IEEE2005, pp. 1321-1326.

[163] A. Strocchi, M.D. Levitt, Factors affecting hydrogen production and consumption by human fecal flora. The critical roles of hydrogen tension and methanogenesis, J Clin Invest, 89(1992) 1304.

[164] S. Macfarlane, G.T. Macfarlane, Regulation of short-chain fatty acid production, Proc Nutr Soc India, 62(2003) 67-72.

[165] D. Rios-Covian, B. Sánchez, N. Salazar, N. Martínez, B. Redruello, M. Gueimonde, C.G. de los Reyes-Gavilán, Different metabolic features of Bacteroides fragilis growing in the presence of glucose and exopolysaccharides of bifidobacteria, Front Microbiol, 6(2015).

[166] C. Yao, J. Muir, P. Gibson, Review article: insights into colonic protein fermentation, its modulation and potential health implications, Aliment Pharmacol Ther, 43(2016) 181-196.

[167] A. Rotbart, P.J. Moate, C. Yao, J.Z. Ou, K. Kalantar-zadeh, A novel mathematical model for the dynamic assessment of gas composition and production in closed or vented fermentation systems, Sens Actuator B-Chem, (Accepted 2017).

[168] B. Flourie, F. Etanchaud, C. Florent, P. Pellier, Y. Bouhnik, J. Rambaud, Comparative study of hydrogen and methane production in the human colon using caecal and faecal homogenates, Gut, 31(1990) 684-685.

[169] O. Yenigün, B. Demirel, Ammonia inhibition in anaerobic digestion: a review, Process Biochem, 48(2013) 901-911.

[170] K.J. Berean, E.M. Adetutu, J.Z. Ou, M. Nour, E.P. Nguyen, D. Paull, J. Mcleod, R. Ramanathan, V. Bansal, K. Latham, A unique in vivo approach for investigating antimicrobial materials utilizing fistulated animals, Sci Rep, 5(2015) 11515.

[171] M. Nour, K. Berean, A. Chrimes, A.S. Zoolfakar, K. Latham, C. McSweeney, M.R. Field, S. Sriram, K. Kalantar-zadeh, J.Z. Ou, Silver nanoparticle/PDMS nanocomposite catalytic membranes for H_2S gas removal, J Membr Sci, 470(2014) 346-355.

[172] J.G. Speight, Lange's handbook of chemistry, New York: McGraw-Hill; 2005.

[173] S. Victoria, Summary: Food waste in the garbage bin 2013, in: S. Victoria (Ed.), Sustainability Victoria2014.

[174] E.W. Rice, L. Bridgewater, A.P.H. Association, Standard Methods for the Examination of Water and Wastewater, American Public Health Association Washington, DC (2012).

[175] I. Angelidaki, M. Alves, D. Bolzonella, L. Borzacconi, J. Campos, A. Guwy, S. Kalyuzhnyi, P. Jenicek, J. Van Lier, Defining the biomethane potential (BMP) of solid organic wastes and energy crops: a proposed protocol for batch assays, Water Sci Technol, 59(2009) 927-934.

[176] T.L. Hansen, J.E. Schmidt, I. Angelidaki, E. Marca, J. la Cour Jansen, H. Mosbæk, T.H. Christensen, Method for determination of methane potentials of solid organic waste, Waste Manage, 24(2004) 393-400.

[177] G. Zhen, X. Lu, T. Kobayashi, G. Kumar, K. Xu, Anaerobic co-digestion on improving methane production from mixed microalgae (Scenedesmus sp., Chlorella sp.) and food waste: kinetic modeling and synergistic impact evaluation, Chem Eng J, 299(2016) 332-341.

[178] J. Owens, D. Chynoweth, Biochemical methane potential of municipal solid waste (MSW) components, Water Sci Technol, 27(1993) 1-14.

[179] E.H. Koupaie, M.B. Leiva, C. Eskicioglu, C. Dutil, Mesophilic batch anaerobic co-digestion of fruit-juice industrial waste and municipal waste sludge: Process and cost-benefit analysis, Bioresour Technol, 152(2014) 66-73.

[180] L. Neves, R. Oliveira, M. Alves, Influence of inoculum activity on the bio-methanization of a kitchen waste under different waste/inoculum ratios, Process Biochem, 39(2004) 2019-2024.

[181] I. Siegert, C. Banks, The effect of volatile fatty acid additions on the anaerobic digestion of cellulose and glucose in batch reactors, Process Biochem, 40(2005) 3412-3418.

[182] R. Lindeboom, F. Fermoso, J. Weijma, K. Zagt, J. Van Lier, Autogenerative high pressure digestion: anaerobic digestion and biogas upgrading in a single step reactor system, Water Sci Technol, 64(2011) 647-653.

[183] C.K. Yao, Exploring colonic fermentation and new technical applications for understanding functional & inflammatory bowel disease, In: Department of Gastroenterology, Melbourne, Australia: Monash University; 2017.

[184] W. Roediger, W. Babidge, Nitric oxide effect on coloncyte metabolism: Co-action of sulfides and peroxide, Mol Cell Biochem, 206(2000) 159-167.

[185] M. Pitcher, E. Beatty, J. Cummings, The contribution of sulphate reducing bacteria and 5-aminosalicylic acid to faecal sulphide in patients with ulcerative colitis, Gut, 46(2000) 64-72.